

Republic of Iraq  
Ministry of Higher Education and Scientific Research  
University of Kerbala  
College of Engineering  
Department of Civil Engineering



# Effect of Climate Change on the Groundwater Recharge in Dibdibba Basin, Iraq

A Thesis

Submitted to Department of Civil Engineering at University of  
Kerbala in Partial Fulfillment of the Requirements for the  
Degree of Master of Science in Civil Engineering

By

**Forqan Saad Hashim**

B.Sc. in Civil Engineering / University of Kerbala (2017)

Supervised by

**Prof. Dr. Waqed H. Hassan**

September 2020

Muharram 1442

بِسْمِ اللَّهِ الرَّحْمَنِ الرَّحِيمِ

يَرْفَعِ اللَّهُ الَّذِينَ آمَنُوا مِنْكُمْ وَالَّذِينَ أُوتُوا  
الْعِلْمَ دَرَجَاتٍ وَاللَّهُ بِمَا تَعْمَلُونَ خَبِيرٌ ﴿11﴾

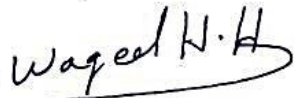
صَدَقَ اللَّهُ الْعَلِيُّ الْعَظِيمُ

سورة المجادلة - الآية 11

## **SUPERVISOR CERTIFICATE**

I certify that the thesis entitled **“Effect of Climate Change on the Groundwater Recharge in Dibdibba basin, Iraq”** prepared by **"Forqan Saad Hashim"**, has been carried out completely under our supervision at College of Engineering, University of Kerbala, in partial fulfillment of the requirements for the Degree of Master of Science in Civil Engineering.

Signature:



**Prof. Dr. Waqed H. Hassan**

(Supervisor)

Date: / / 2020

## إقرار المقوم اللغوي

أشهد اني قد اطلعت على رسالة طالب الماجستير (فهد بن محمد بن محمد) الموسومة بـ

### Effect of Climate Change on the Groundwater Recharge in Dibdibba basin, Iraq

وقد قومتها من الناحية اللغوية والاسلوبية وبذلك تكون صالحة لأغراض المناقشة مع توصيتنا بالآخذ  
بنظر الاعتبار تصحيح بعض الملاحظات اللغوية المؤشر عليها -----  
مع التقدير...



التوقيع :

أسم المقوم ونقبة العلمي : ٢٠٣. مكي محمد محمد

التخصص العام : هندسة

التخصص الدقيق : هندسة المنشآت

محل العمل : كلية الهندسة في جامعة كربلاء - القسم المعادي

رقم الهاتف النقال : 392 3181 (+969) 773

التاريخ : ٢٠٢٠/١٠/٢٧

## EXAMINATION COMMITTEE CERTIFICATION

We certify that we have read the thesis entitled “**Effect of Climate Change on the Groundwater Recharge in Dibdibba basin, Iraq**” and as an examining committee, we examined the student “**Forqan Saad Hashim**” in its content and in what is connected with it, and that in our opinion it is adequate as a thesis for the degree of Master of Science in Civil Engineering.

**Supervisor**

Signature: 

Name: Prof. Dr. Waqed H. Hassan

Date: / / 2020

**Member**

Signature: 

Name: Dr. Riyadh J.M. Al-Saadi

Date: / / 2020


**Member**

Signature: 

Name: Assist. Prof. Dr. Hussein Janna

Date: / / 2020

**Chairman**

Signature: 

Name: Prof. Dr. Basim K. Nile

Date: / / 2020

**Approval of Head of Civil Engineering**

Department

Signature: 

Name: Dr. Raid R.A. Almuhamma

Date: 3 / 12 / 2020

**Approval of Deanery of the College of**

Engineering - University of Kerbala

Signature: 

Name: Assist. Prof. Dr. Laith Sh. Rasheed

Date: 7 / 1 / 2020

## *Dedication*

*This thesis is deducted to my family. A special feeling of gratitude to my loving parents who are supported me mentally and emotionally throughout my study process. To my brother (Mustafa) for his continuous supports. To my friends (Samara, Maryam, Zahraa) who were there to listen and support me throughout my study.*

**Forqan**

## **ACKNOWLEDGEMENT**

Above all and beyond, I would like to thank Allah, who gave me the desire and ability to complete this work in spite of the constrains along the way.

Firstly, I would like to express my sincere thanks and deepest gratitude to *Prof. Dr. Waqed H. Hassan*, the supervisor of my research, who I had the excellent luck and the honor of being under his supervision, for his continuous encouragement and invaluable guidance throughout this thesis.

A special thank and gratitude are extended to my family for their support and help along the way.

Finally, I would like to express my extreme love and appreciation to everyone who has supported this work.

**Forqan Saad**

**2020**

## **Abstract**

In Iraq, groundwater is considered as an alternate water resource, essentially for areas far away from surface water. Groundwater is affected by many factors including climate change, industrial human activities, unplanned urbanization and industrialization. This study deals with the development model to generate future climate data in order to estimate future groundwater recharge. For the current study, Dibdibba unconfined aquifer in Karbala city, Iraq was chosen as a case study. It depended on rainfall recharge, which is associated to change in temperature and rainfall. The historical data for the period 1979-2018 were used to predict future climate data for two future periods 2040 and 2099 by using general circulation model (GCMs), CanESM2, based on three emission scenarios RCP2.6, RCP4.5 and RCP8.5 by using statistical downscaling model (SDSM) program. These data were divided into two groups: data from, 1979 to 2000 was used for building the downscale model and for calibration, while for validating the models use data from, 2001 to 2018. The calibration results of SDSM model gave a coefficient of determination ( $R^2$ ) ranged from (0.877 to 0.905).

After testing (SDSM) capacity to produce climatic data depended on the period 1979 to 2018, climate data (rainfall and temperature) will generated for the next periods 2040 and 2099. Following this, a Groundwater Modeling System (GMS) model is constructed in order to assess the groundwater recharge under future climate data.

The results indicate that the temperature was expected to increase between (0.5 to 0.7) °C at 2040, and between (0.5 to 1.07) °C at 2099, and the rainfall expected to decrease by 6.3%, 10.3%, and 23.8% for near future 2040, and by 13.8%, 17.5%, and 21.3% for far future 2099 for RCP2.6, RCP4.5, and RCP8.5 scenarios, respectively. Six predicted



scenarios for groundwater recharge were selected for each scenario of climate data for the two periods 2040 and 2099 after calibrated the model in GMS. The model matched the observed head of groundwater with  $R^2 = 0.99$  for steady state condition. The results show that the recharge of groundwater decreases by 6.4%, 10%, and 27.6 % for near future 2040 and decrease by 13.6%, 17.6%, and 25.3% for far future 2099 compared to the year 2018 under RCP2.6, RCP4.5, and RCP8.5 scenarios, respectively.

# Table of Contents

Abstract	I
Table of Contents	III
List of Figures	V
List of Tables	VII
List of Abbreviations	VIII

## **CHAPTER ONE: INTRODUCTION**

1.1	General	1
1.2	Problem Statement	2
1.3	Thesis Objective	3
1.4	Thesis Methodology	3
1.5	Thesis Layout	4

## **CHAPTER TWO: LITERATURE REVIEW**

2.1	Climate change	5
2.2	Climate Change Models and Scenarios	8
2.3	Groundwater Modeling	11
2.3.1	Groundwater Recharge definition	11
2.3.2	Groundwater Recharge Modeling	13
2.4	Summary	17

## **CHAPTER THREE: MODELING AND CASE STUDY**

3.1	Stage of the research	18
3.2	Generation Future Climate Data	21
3.2.1	Description of (GCM) and their scenarios	21
3.2.2	Data analysis	22
3.2.3	Statistical Downscaling Model (SDSM)	23
3.2.3.1	Monitoring and screen variables	25
3.2.3.2	Calibration and validation	25
3.2.3.3	Climatic scenarios generation	26
3.3	Groundwater Flow Modeling	27
3.3.1	Governing equation	27
3.3.2	Types of boundary conditions	30
3.3.3	Groundwater Modeling System (GMS)	31
3.3.3.1	Construction of the conceptual model	31
3.3.3.2	Data collection (Input Parameters)	34
3.3.3.3	Calibration of the steady state	34
3.3.3.3.1	Automatic calibration using PEST package	35
3.4	Study area and data	36
3.4.1	Description of the Study area	36

3.4.2 The topography	38
3.4.3 Hydrogeological data	39
3.4.4 Groundwater head	43
3.4.5 Groundwater model data	44
3.4.5.1 Grid design	44
3.4.5.2 Boundary conditions	45
3.4.5.3 Aquifer hydraulic conductivity	46
3.4.5.4 Zone division	47
3.4.6 Metrological data	48

## **CHAPTER FOUR: RESULTS AND DISCUSSION**

4.1 Topics of search results	50
4.2 SDSM model and future climate data	50
4.2.1 Temperature	50
4.2.1.1 Calibration results of downscaled model	50
4.2.1.2 Temperature analysis	54
4.2.2 Rainfall	60
4.3 Groundwater recharge model	64
4.3.1 Steady-state calibration	64
4.3.2 Prediction scenarios	72
4.3.2.1 First scenario	73
4.3.2.2 Second scenario	75
4.3.2.3 Third scenario	77
4.3.2.4 Fourth scenario	79
4.3.2.5 Fifth scenario	81
4.3.2.6 Sixth scenario	83

## **CHAPTER FIVE: CONCLUSIONS AND RECOMMENDATIONS**

5.1 Introduction	87
5.2 Conclusions	87
5.3 Recommendations	89
5.4 Recommendations for future studies	89

<b>REFERENCES</b>	<b>90</b>
-------------------	-----------

## List of Figures

Figure (2-1): General Circulation Models (GCMs) (Flato et al., 2014).	9
Figure (3-1): Flow chart of the research methodology.	20
Figure (3-2): IPCC Emissions Scenarios for CanESM2 model.	22
Figure (3-3): SDSM Version4.2 climate scenario generation (Wilby et al., 2007).	24
Figure (3-4): Elementary control volume (AlMussawy, 2013).	28
Figure (3-5): Methodology of construction of conceptual model.	33
Figure (3-6): Geographical location of the study area.	37
Figure (3-7): Topography of the study area.	38
Figure (3-8): location of the observed wells penetrating in the study area.	39
Figure (3-9): Groundwater head level data histogram.	41
Figure (3-10): Groundwater head level data normal QQPlot.	42
Figure (3-11): The contour maps of the groundwater piezometric head in the study area based on the data in Table (3-3).	43
Figure (3-12): 3D grid for conceptual model (Z-magnification=30) produced by GMS software.	44
Figure (3-13): Boundaries of flow model and grid distribution.	45
Figure (3-14): Hydraulic conductivity and recharge zones in the study area.	47
Figure (3-15): The average of monthly rainfall for period (1979-2018).	48
Figure (3-16): Average of min temperature for period (1979-2018).	49
Figure (3-17): Average of max temperature for period (1979-2018).	49
Figure (4-1): Correlation between observed and predicted data (1979-2018) for maximum temperature.	52
Figure (4-2): Correlation between observed and predicted data (1979-2018) for minimum temperature.	52
Figure (4-3): Comparison between observed and predicted data (1979-2018) for maximum temperature.	53
Figure (4-4): Comparison between observed and predicted data (1979-2018) for minimum temperature.	53
Figure (4-5): Comparison between average monthly observed (1979- 2018), and Values predicted by scenarios RCP2.6, RCP4.5 and RCP8.5 (2020 – 2099) (a) Maximum temperature (b) Minimum temperature.	55

Figure (4-6): Comparison between average annually observed (1979- 2018), and values predicted by scenarios RCP2.6, RCP4.5 and RCP8.5 for 2040 (a) Maximum temperature (b) Minimum temperature.	57
Figure (4-7): Comparison between average annually observed (1979- 2018), and values predicted by scenarios RCP2.6, RCP4.5 and RCP8.5 for 2099 (a) Maximum temperature (b) Minimum temperature.	58
Figure (4-8): Increase in temperatures under different model scenarios for 2040 and 2099.	59
Figure (4-9): Comparison between observed and predicted annual rainfall for verification period (2001–2018).	60
Figure (4-10): Comparison between observed annual rainfall (1979–2018) and predict by RCP2.6, RCP4.5and RCP8.5 scenarios for 2040 and 2099.	62
Figure (4-11): Decrease in rainfall under different model scenarios for 2040 and 2099.	63
Figure (4- 12): Target of calibration (Environmental Modeling Research Laboratory, 1999).	64
Figure (4- 13): Contour map of observed heads before calibration of Dibdibba aquifer.	65
Figure (4-14): Contour map of simulated heads after calibration of Dibdibba aquifer.	67
Figure (4- 15): Correlation between observed and computed head values for steady state condition.	68
Figure (4-16): Errors analysis for steady state calibration.	69
Figure (4-17): calibrated hydraulic conductivity for the Dibdibba aquifer (m/day).	71
Figure (4- 18): The analysis of sensitivity of parameter.	72
Figure (4-19): The predicted head distribution for the first proposed scenario RCP2.6 at 2040.	74
Figure (4- 20): The predicted head distribution for the second proposed scenario RCP4.5at 2040.	76
Figure (4- 21): The predicted head distribution for the third proposed scenario RCP8.5at 2040.	78
Figure (4- 22): The predicted head distribution for the fourth proposed scenario RCP2.6 at 2099.	80

Figure (4- 23): The predicted head distribution for the fifth proposed scenario RCP4.5 at 2099.	82
Figure (4- 24): The predicted head distribution for the sixth proposed scenario RCP8.5 at 2099.	84

## List of Tables

Table (3-1): Coordinates of the study station.	23
Table (3-2): Features of GCM as SDSM software input.	23
Table (3-3): Data of observation wells used to build a model.	40
Table (3-4): The hydraulic parameter of Dibdibba aquifer.	46
Table (4-1): Validation results for climate variables over the observation period (2001-2018).	51
Table (4-2): Comparison between observed and computed head values.	66
Table (4- 3): Errors value of the steady-state calibration.	69
Table (4-4): Calibrated hydraulic conductivity and recharge values.	70
Table (4- 5): The water budget for the study area (Dibdibba aquifer) under current condition (2018).	72
Table (4- 6): The water budget for the study area (Dibdibba aquifer) under RCP2.6 scenario at 2040.	73
Table (4-7): The water budget for the study area (Dibdibba aquifer) under RCP4.5 scenario at 2040.	75
Table (4-8): The water budget for the study area (Dibdibba aquifer) under RCP8.5 scenario at 2040.	77
Table (4- 9): The water budget for the study area (Dibdibba aquifer) under RCP2.6 scenario at 2099.	79
Table (4-10): The water budget for the study area (Dibdibba aquifer) under RCP4.5 scenario at 2099.	81
Table (4-11): The water budget for the study area (Dibdibba aquifer) under RCP8.5 scenario at 2099.	83
Table (4-12): Analysis of groundwater recharge under different scenarios of climate change at near future (2040).	85
Table (4-13): Analysis of groundwater recharge under different scenarios of climate change at far future (2099).	86

## List of Abbreviations

Abbreviation	Description
AR5	Fifth Assessment Report
CanESM2	Canadian Earth System Model Second Generation
CGCM3.1	Canadian Global Coupled Model Third Generation
DEM	Digital Elevation Model
ESDA	Exploratory Spatial Data Analysis
GCM	General Circulation Model
GHG	Green House Gases
G.A.M.S.O	General Authority for Meteorology and Seismic Observation
GMS	Groundwater Modeling System
GIS	Geographic Information System
IPCC	Intergovernmental Panel on Climate Change
ME	Mean Error
MLR	Multiple Linear Regression
M.a.s.l	Meter Above Sea Level
NCEP	National Center of Environmental Prediction
PEST	Parameter Estimation Tools
RCP	Representative Concentration Pathway
R <sup>2</sup>	Coefficient of Determination
RMSE	Root Mean Square Error
SRTM	Shuttle Radar Topography Mission
SRES	Special Report on Emissions Scenarios
SDSM	Statistical Downscaling Model
S.W.L	Static Water Level
USGS	U.S Geological Survey
UTM	Universal Transverse Mercator
WGS	World Geodetic System

# Chapter One

## INTRODUCTION

### 1.1 General

Water plays a major role in economic development and food security around the world. However, increasing water demand in recent decades resulting from population growth, economic development, and urbanization, has caused water scarcity, and has restricted economic development in many countries across the world, so that groundwater can be used as an alternative resource of water supply to compensate for shortage of surface water. In last years, the groundwater becomes one of the most important natural resources. As a well water source, groundwater has several benefits when compared with surface water; it is less exposed to seasonal effects, comparatively clear from pollution and long-term variations, and finally has a regular spread over large areas. Groundwater is commonly available in places and areas where surface water is not found. The aquifer development is likely to respond gradually to rising demands, while surface water demands many investments in building facilities and improving water technology and requirements.

Groundwater is the major source of irrigation in countries with arid and semiarid climate. Groundwater is also a major source for domestic use and drinking water supply. In some countries in the Middle East the domestic water supply is entirely dependent on groundwater (Shahid et al., 2017). It is very important to manage this source to meet the increasing water demand.



Nowadays there is a growing need for the exploitation of groundwater resources with rising population and living standards. However, due to certain anthropogenic factors such as industrial human activities, and unplanned urbanization and industrialization that lead to a climate change, the amount of groundwater supplies continues to decline.

Climate change is threatening most countries, but the Middle East region is proven to be particularly vulnerable to climate change. The Middle East already suffers from limited water resources, but climate change is threatening to reduce water availability further. The severity of the reduced availability of water resources in Iraq is growing at a fast pace due to increasing water demand caused by the high rate of growth of Iraq's population. Meanwhile, Climate Change is complicating the water issue in several forms including more frequent sand/dust storms, extreme temperature, and drought episodes, which make sustainability a real challenge. To respond to this challenge, sustainable development should be a central theme in Iraq's development plans, especially when addressing the water sector.

## **1.2 Problem Statement**

The case study (Dibdibba aquifer) located in the central part of Iraq between Karbala and Najaf .This area suffering from the chancing recharge of groundwater due to the climate change and urbanization growth. Climate change leads to increase in temperature and decrease the average rainfall. This change in climate causes decrease in recharge of groundwater. Likewise, the unfair exploitation of wells' water through large withdrawal, leads to the deterioration of the groundwater quality and quantity.

### 1.3 Thesis Objective

The aim of this thesis is to study the impact of climate change on groundwater recharge. This study is used to generate future climate data of the study area. Also, this study will be used to determine the expected recharge ratios of groundwater in future time periods (2040 and 2099) depended on future climate data generated for near future (2040) and far future (2099).

### 1.4 Thesis Methodology

The Methodology of the study can be summarized as below:

1. Using the metrological data for the study area (Karbala city) from the General Authority for Metrology and Seismic Observations (G.A.M.S.O) for period from 1979 to 2018. This data includes daily rainfall (mm), daily maximum temperature (C<sup>°</sup>), and daily minimum temperature (C<sup>°</sup>).
2. Using (CanESM2) model with its scenarios to generate future climate data for the study area for the next 20 and 79 years, and making calibration for the (CanESM2) model to generate the best data by using many statistical indicators.
3. Using statistical downscaling model (SDSM) software to generate expected future climate data.
4. The generation future climate data can be applied on the study area by using groundwater modeling system (GMS) software to estimating the recharge ratios of groundwater for future time periods (2040 and 2099).

## 1.5 Thesis Layout

This thesis consists of five chapters as follows:

- Chapter 1: illustrates introduction, statement of problem, thesis objectives, thesis methodology and thesis layout.
- Chapter 2: shows the previous studies for the various parts, the first part presents climate change. The second part presents the climate change models and their scenarios, and the final part presents groundwater recharge model.
- Chapter 3: describes generation of future climate data by use CanESM2 model, also describes GMS model, stating the study area and the properties of all data used.
- Chapter 4: displays results of future climate data model. The results of groundwater recharge model. The results of prediction scenarios of groundwater recharge under future climate data are also discussed.
- Chapter 5: contains the conclusions of the present study and recommendations.

## Chapter Two

# LITERATURE REVIEW

### 2.1 Climate change

The term of climate change indicates to the significant and long-term change in the average weather rate of a region, including major changes in temperature, rainfall, or wind speed patterns, among other effects, that occur over several decades or longer.

It is very essential to recognize the difference between climate change and climate variability, where the previous denotes to a long-term alteration in the climate, whereas the latter is the natural variation in the climate from one period to the next.

The climate change effects on resources of groundwater may be more severe because of decreased rainfall and raised potential evapotranspiration (ETP) that may result in more intense groundwater abstraction in the future (Surinaidu et al., 2013, Brouyère et al., 2004).

Other research has shown climate data like average annual temperature has risen from 0.3 to 0.6°C for the late 19th century, and expected rise from 1 to 3.5°C for next 100 years (Solomon et al., 2007).

(Sansom et al., 2007) examined the potential climate change effects, found these effects would lead to both floods and droughts. GCM was used to measure the change of climate in New Zealand; they found a rise in rainfall because of raised frequency of rainfall due to climate change.

In lands where increase in intensity of rainfall is predicted, pollutants such as pesticides, organic matter, and heavy metals are progressively being washed from soils to water bodies (Parry et al., 2007). As recharge to aquifers takes place by bodies of surface water, so the quality of groundwater is possible to decline.

(Evans, 2009) studied the potential forecast of climate change with 18 global models that can be used by Intergovernmental Panel on Climate Change IPCC in the Middle East and found that the temperature will increase about 1.4°C in the middle of the century and about 4°C at the end of the century with lower rainfall in Turkey, Northern Iraq, Northeastern Iran.

(Oude Essink et al., 2010) Studied effects of climate change on coastal groundwater systems in the Netherlands. They found that there was a potential rising in salt loads because of the rise in sea level, and this would result in salinization of shallow groundwater and a reduction in total fresh groundwater volumes.

(Liu, 2011) evaluated the change of groundwater recharge under several future climate scenarios and showed that both groundwater recharge and deep-rooted vegetation coverage increase with decreasing rainfall frequency and with increasing average rainfall depth per rainfall event.

The Intergovernmental Panel on Climate Change (IPCC) predicts a rise of temperature from 2 to 6°C by the end of this century because of the rising of greenhouse gas emissions (Pathak et al., 2012).

The average temperature for the period 1988-2007 is higher than the average temperature for the earlier twenty years by 1°C in Baghdad and 1.5°C in Nasiriya south of Baghdad. Similar trends can be seen in the recorded rainfall. For instance, rainfall in Baghdad during the past decade is less than the long-term average by about 50% (excluding the recent rainfall in Baghdad in late December 2012) (Hassan, 2013).

(Shahid et al., 2015) reported that increased evaporation under higher temperature would offset the increased rainfall benefit and therefore, no substantial improvement in recharge of groundwater in northwest of Bangladesh.

(Samper et al., 2015) studied the climate change effect on average recharge of the aquifer Plana de La Galera in Spain, reporting that it would reduce about 23% for the period 2020 to 2050, and about 27% for the period 2069 to 2099, compared to the period 1960–1990.

Climate change can directly and indirectly impact on groundwater supplies. Changing in patterns of rainfall and rising temperatures can directly effect on groundwater discharge, storage, recharge and water levels. Moreover, rising sea levels, increased water demand for irrigation, and vegetation cover changes, can indirectly impact on groundwater quality and quantity. Higher temperatures can lead to raise evaporation and plant transpiration rates that lead to drier soil, higher soil moisture losses, and reduce recharge of groundwater (Shahid et al, 2017).

Both thermal and chemical properties of groundwater may be affected by climate change. Groundwater temperatures in shallow aquifers may increase due to the increase of air temperatures. In arid and semiarid areas increased evapotranspiration may lead to groundwater salinization (Shahid et al, 2017).

Increasing rainfall because of changes in the intensity and distribution of rainfall may minimize the recharge of groundwater. The increased rainfall due to increase of rainfall intensity will increase runoff peak, but not the total amount of recharge. Also the total annual groundwater recharge may decline in the area where annual rainfall is expected to raise only because of increase intensity of rainfall. In the same way, changes the distribution of rainfall will effect on recharge of groundwater(Shahid et al., 2017).

(Osman et al., 2017) studied the climate change impact on rainfall in the dry lands in Iraq by using 7 GCMs for three durations: 2011-2030, 2046-2065, and 2080-2099. The results indicated that average annual rainfall in most regions would reduce at the end of century.

## 2.2 Climate Change Models and Scenarios

About 16 General Circulation Models (GCMs) with greenhouse gas (GHG) emission scenarios were used to evaluate the differences in the projections of precipitation and temperature by use several of General Circulation Models (GCMs), as shown in Figure (2-1).

The output produced by GCMs will help in understanding climate change future impacts. (Lemke et al., 2007) find that the global temperatures will rise from 2°C to 4.5°C for next 80 years by using these models.

(Abbaspour et al., 2009) studied climate change impacts on resources of water in Iran for two durations: first for period (2010–2040), and second for period (2070–2100). The suggested scenarios A2, A1B and B1 developed by the Canadian global coupled model (CGCM 3.1) were used to expect future climate data and to downscale the climate data for study area.

The predictions of the General Circulation Models (GCMs) used by the Intergovernmental Panel on Climate Change (IPCC) present a pessimistic picture of the flows in the Tigris and Euphrates rivers. Rainfall in the highlands of Turkey is predicted to be reduced by 10-60%, which in turn translates into a similar decline in the flow of the Tigris and Euphrates rivers. One recent study predicted that the Euphrates river flow will be reduced by 29% to 73% and the entire Fertile Crescent may disappear by the end of the century (Hassan, 2013).

(Hashemi et al., 2015) studied climate change effects on recharge of groundwater in arid areas by using the CGCM 3.1 model with various scenarios for the downscaling using the delta-change method. For all studied scenarios the results showed no substantial difference between current and future recharge of groundwater.

Model name
ACCESS1.0, ACCESS1.3
BCC-CSM1.1, BCC-CSM1.1(m)
BNU-ESM
CanCM4
CanESM2
CCSM4
CESM1 (BGC)
CESM1 (WACCM)
CESM1 (FASTCHEM)
CESM1 (CAM5)
CESM1 (CAM5.1-FV2)
CMCC-CM, CMCC-CMS
CMCC-CESM
CNRM-CM5
CSIRO-Mk3.6.0
EC-EARTH
FGOALS-g2
FGOALS-s2
FIO-ESM v1.0
GFDL-ESM2M, GFDL-ESM2G
GFDL-CM2.1
GFDL-CM3
GISS-E2-R, GISS-E2-H
GISS-E2-R-CC, GISS-E2-H-CC
HadGEM2-ES
HadGEM2-CC
HadCM3

Figure (2-1): General Circulation Models (GCMs) (Flato et al., 2014).



(Abbasnia et al., 2016) studied changes in future maximum temperatures by using CGCM3 model with emission scenarios A2, B1 and A1B using the statistical downscaling model (SDSM) for seven stations in Iran for the periods 2041 to 2070 and 2071 to 2099. At all stations, they expected the average maximum temperature rise from 0.3 to 3.5°C.

(Kahsay et al., 2018) studied the climate change effect on recharge of groundwater and surface flow in the Ethiopian Tekeze sub catchment. To find future climate data, they used the representative concentration pathway scenarios RCP 2.6 and RCP 4.5 in the analysis. Also the WetSpass model was used to simulate future components of the water balance. The results showed that groundwater recharge may be reduced by about 3.4% for the RCP 2.6 scenarios and about 1.3% for the RCP 4.5 scenarios.

(Hassan, 2020) studied the climate change impact (temperature and rainfall) on the recharge of groundwater in the aquifer of Umm er Radhuma in Iraq Western Desert. .WetSpass is used as modeling method. Climate data were produced by using HadCM3 model with emission scenarios A2 and B2 for the duration 2020 to 2099. The results showed rising in average annual temperature between 0.51°C and 1.01°C, in rainfall by about 5.4% and 3.19% for A2 and B2 respectively. For the two scenarios, average annual recharge of groundwater is predicted to be reduced by about 16% at the year 2100.

## 2.3 Groundwater Modeling

### 2.3.1 Groundwater Recharge definition

Groundwater is the main source of water supply in several countries across the world, so it should be well recharged. Groundwater recharge can be defined as water added to the aquifer through the unsaturated zone after infiltration and percolation following any storm rainfall event. There are several factors affected on groundwater recharge such as infiltration capacity, climate change, land use change, human activities, and natural processes.

The recharge of groundwater can be also impact because of the following events:

- Changes in rainfall, evaporation, and runoff are predicted to impact on the recharge. It is likely that rising of the intensity of rainfall will lead to raise the runoff and reduce the recharge.
- Rising in sea level can lead to raise saline intrusion of coastal and island aquifers, depending on the relative position of sea level to the groundwater table level.
- Changes in rainfall include changes in concentrations of  $CO_2$  that can affect the dissolution of carbonate rocks and, thus, the formation and growth of groundwater aquifers.
- Natural vegetation and crop patterns changes are reflected in the climate change influencing recharge.
- Increasing flood events contributes to the drainage of unconfined aquifers in arid and semi-arid regions, thereby impacting the quality of groundwater in alluvial Wadi aquifers.
- Changes in organic soil carbon can impact the infiltration properties of shallow aquifers, and consequently, the recharge of groundwater. (Şen, 2015)

A study in northwest Bangladesh showed that annual groundwater recharge will substantially increase due to the increase of annual rainfall. However, there will be a wide variation in the groundwater level. During the pre-monsoon season, the groundwater levels may go down further, when groundwater is required for irrigation. On the other hand, during post-monsoon months, climate change would bring the groundwater level closer to the surface and make it more vulnerable to pollution in the study region. Dropping the groundwater levels in dry months can lead to more frequent and severe droughts in groundwater in several lands of the world (Shahid et al., 2017).

### **2.3.2 Groundwater Recharge Modeling**

Groundwater Modeling System (GMS) utilized for groundwater simulation. GMS is a mathematical model to assess natural discharges and recharges of the aquifer. Since this model has suitable compatibility with GIS software, data layers production were implemented in the GIS software environment.

The GMS is a simulation method used to simulate groundwater. It includes a graphical interface and numerous of different analytics codes like MODFLOW 2000. MODFLOW is 3D, finite difference, and saturated flow model developed by the United States of Geological Survey. (McDonald and Harbaugh, 1988).

(Al-Kharabsheh, 2000) has used MODFLOW to simulate the flow of groundwater and the effect of five pumping scenarios depending on the groundwater balance analysis to estimate the safe yield of future abstraction in the upper aquifer of the Azraq basin in Jordan.

Another application of MODFLOW was executed in Kuwait to make a calibrated model for simulating the drawdown and field operation in discontinuous layering and multiple screens. The application of

MODFLOW gave good information about the hydraulic impact on the historical and future groundwater abstractions (Székely et al., 2000).

(Al-Tae and Al-Sadiq, 2003) developed 3D numerical groundwater flow model by using (GMS) program to study the movement of groundwater, direction, and estimated quantity for the Sulaivaney plain, Mosul Governorate, Iraq. The study area flow map was created to find the direction of water, groundwater and its non-confined paths, and their estimated quantities. Moving of groundwater with the Sulaivaney plain attained about  $579.655 \text{ m}^3 / \text{day}$ , while groundwater which feeds the Mosul dam reservoir from the study area was  $533695 \text{ m}^3 / \text{day}$  corresponding to the results of previous regional studies.

(Gurwin and Lubczynski, 2005) used MODFLOW to develop a conceptual model under (GMS) based on data from several hundred boreholes and to calibrate a numerical multi-aquifer model. Historical natural groundwater table (quasi-natural simulation) data and transmissivity test data for pumping were used to perform a steady state calibration. The recharge of calibration was first spread spatially depending on surface lithology, and then modified till a good match was obtained between determined and observed heads. The quasi-natural simulation budget input of  $\sim 165,000 \text{ m}^3 / \text{day}$  consists of 40.5 % of the lateral inflow from the SW model boundary, 34.5 % of the total net precipitation recharge, 13 % of the Mietkowskie Lake infiltration and 12% of river infiltration. The budget output (same as input) consists of  $\sim 88 \%$  river drainage and  $\sim 12 \%$  lateral outflow. Also, it shows that complex multi-aquifer structures can be well and efficiently modeled by setting up a conceptual model within the numerical model context and by applying a quasi-3D solution.

(Hussain,2008) used two models of numerical finite difference to determine the different potential groundwater recharge sources for the region around the sacred shrines of Imam AL-Hussein and Imam AL-Abbas, Karbala, Iraq. The first model was built by using the Modflow software under the GMS application, while the second model was a mathematical model built and applied by using the Quick Basic language. The results showed that the amount of groundwater recharge of upper layer was of about (760.71 and 3256.758) m<sup>3</sup> / day due to the leakage of the drinking pipe network, sanitary and septic tanks.

(Marnani et al., 2010) prepared the three dimensional groundwater modeling of Firozabad plain (Iran). It is a mathematical representation of groundwater flow generated by (GMS) software using code MODFLOW 2000 (Marnani et al., 2010).The results for the various scenarios including predicting the status of water level in next 5 years was analyzed in the study area.

(Al-Hassoun et al., 2011) predicted the water level fluctuations and estimated the annual change of water table in an alluvial aquifer at Wadi Hada Al Sham near Makkah, Saudi Arabia. The methodology was obtained using the groundwater numerical model (MODFLOW). The model was calibrated and then used to predict the elevations of the water table because of the 5-year pumping. The model's performance was found to be in agreement with the previous records. In addition, the results of simulation show a significant decline of the elevations of the water table in the area of research during the study period.

(AL-Fatlawi, 2011) developed a mathematical model by using modflow software to determine the availability of groundwater and levels of groundwater in reply to the pumping in aquifer of Umm Er Radhuma, Western Desert, Iraq. The results showed that the aquifer receives an average rainfall recharge of about 0.0578 mm / day.

(Al-Muqdadi and Merkel, 2012) used Visual Modflow software to examine and model the flow of groundwater into Iraq western desert. The model was built with five main aquifers representing the Tayarat aquifer, second aquiclude, Um Er Duhmma aquifer, first aquiclude and Dammam aquifer. The average recharge calculated was 0.0479 mm / day based on the water balance for 30 years continued from 1980 to 2008.

GMS and integrated data layers in GIS (Geographic Information System) have been used for plain modeling in the steady and unsteady states. Finally, using calibrated model, effect of an artificial-recharge project on eastern part of the Gouharkouh aquifer has been surveyed and amount of rise in groundwater level during 1 year has been predicted. According to the modeling results, artificial-recharge project will lead to the groundwater level rise by about 1.7 m around the areas near the implementation of the project (Aidi and Hassani, 2013).

(Al-Mussawy and Khalaf, 2013) used the GMS software with Modflow package to create optimum 3D model for groundwater management in the desert of Karbala, Iraq, to simulate the ground flow of the confined aquifer of Dammam. The findings showed that the rate of vertical recharge ranged from about  $2.74 \times 10^{-9}$  to  $8.49 \times 10^{-8}$  mm / day.

(Ramadhan et al., 2013) studied the recharge of groundwater in arid and semi-arid lands using 4 methods; one of these methods was numerical modeling by using Modflow software and applied this study on Dibdibba aquifer in plateau of Karbala-Najaf, Iraq. The findings showed that the recharge of groundwater was 0.0619 mm / day by using numerical model depended on Modflow software.

(Kareem, 2018) used Visual MODFLOW software to evaluate the present system of groundwater resources as well as future water resource threats in Al-Najaf province, Iraq mid-west. The calibration was carried out with value of recharge of about 0.045 mm / day and the findings

showed that the best correspondence was in a good agreement with observations of the field.

(Al-Kubaisi et al., 2018) used Modflow package with GMS software to simulate the flow of the Dibdibba aquifer. The calibrated models were used to test three scenarios to show the response of the aquifer to applied stress for the period 2018-2023. The first scenario assumed that the current number of operating wells (650) with a total discharge of 18306000 m<sup>3</sup>/year. The predicted maximum decline in the hydraulic head reached (1 m) compared with observed values. In the second scenario, it assumed increasing of pumping rates to 23996225 m<sup>3</sup>/year from 875 pumping wells. The hydraulic head declined more than the first scenario to reach (1.5 m) in the observation well No. 3 and (1m) in the observation Well, No. 4 during five years of the simulation period. The third scenario assumed increasing pumping rates to 61398000 m<sup>3</sup>/year (annual discharge of 1150 productive wells, i.e., 80 % of the present estimation discharge) to increase agricultural land to reach (28750 donums) to cover all of the study areas. The hydraulic head in the third scenario reached 1.5m in the observation well, No. 4 which declined more than the first and second scenarios during the simulation period of the groundwater system for five years.

## 2.4 Summary

Groundwater is an important major resource of water. It needs to be more active interest in this topic with regard to its vulnerability to overuse, pollution and particularly climate change. Climate change was become a main threat to environmental, especially in dry areas. Identifying and assessing future climate change is therefore of paramount importance for suitable environmental planning to adapt and to decrease its impact.

Problems of groundwater have taken scientist's attention in various parts of the world and for tens of years, and thousands of studies have been performed to study and model groundwater flow behavior and the effect of conditions and parameters on it. In Iraq, Dibdibba aquifer has several experiments have been carried out to model groundwater flow, but under climate change no tries to model groundwater flow. GMS software with Modflow demonstrated their efficiency in coping with various problems of groundwater and in generality previous studies these programs achieved a high degree of accuracy in findings by comparing them with observed data collected.



## Chapter Three

### MODELING AND CASE STUDY

#### 3.1 Stages of the research

This chapter involves three main stages. In each stage, all required data, parameters, and characteristics will be discussed in the next subsections.

The first stage involves the generation of future climate data for the next periods, Global Climate Models (GCMs) description with their scenarios and their work methodology, and characteristics of the input parameters. The future climate data will be generated by use the statistical downscaling model (SDSM) program. The SDSM program was used to downscale output of GCM. Downscaling includes building relationships between climate data on a regional scale, and atmospheric data on a global scale. The base of the SDSM model is multivariate regression. To predict climate data for any period (annually, seasonally or monthly), a multivariate linear regression model is built between the dependent and independent variables, global-scale predictors represent the independent variables while predicted climatic parameters at a local scale (daily rainfall, min. and max. temperature) represent dependent variables. The outcome of this stage will include climate data for future periods.

While the second stage, include steps of applying the resulted of generation future climate data on the studied area. The selected area shape has been taken as a GIS Arc Map shape file. The data of study area (top elevation and groundwater head) have been smoothed and refined using the same program. The output data of GIS and SDSM programs have been input to the Groundwater Modeling System (GMS) program to

present the final results of groundwater recharge under different scenarios of climate change.

The third stage will consist of properties of the case study like location, topography, groundwater head, boundary condition, and hydraulic conductivity of study area. In addition, the collected data shall be presented in this stage. The description of the case study area and all data is generated with the help of GIS ARC Map program. The methodology of the research plan can be shown in Figure (3 -1).

The research includes two main programs: Statistical downscaling model (SDSM) and Groundwater Modeling System (GMS). So, the climate data analyze by SDSM program and built a model to generated future climate data to enter it to GMS then made simulation and prediction for groundwater recharge of the study area under different scenarios of climate change.

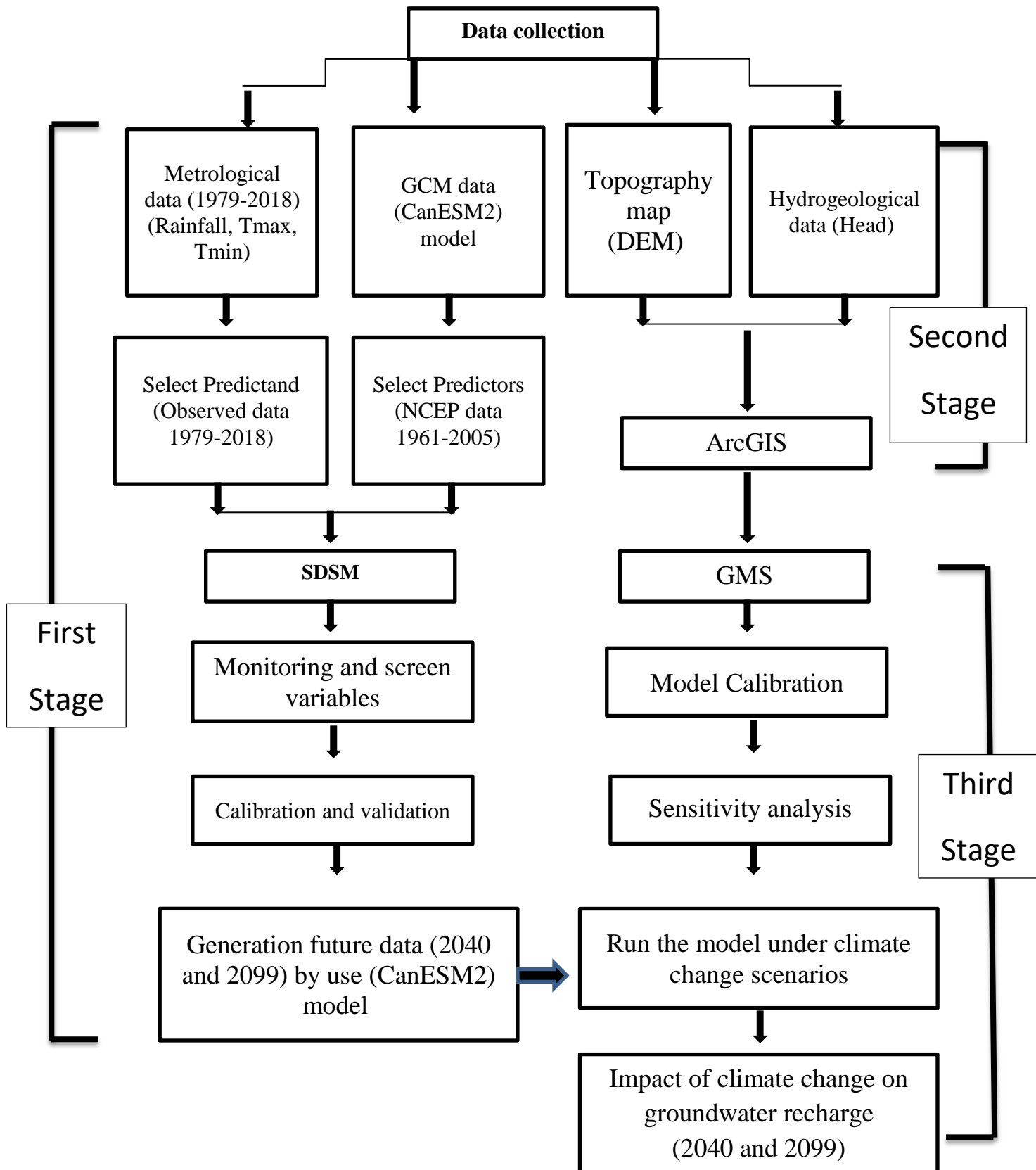


Figure (3-1): Flow chart of the research methodology.

## 3.2 Generation Future Climate Data

### 3.2.1 Description of (GCM) and their scenarios

Global Climate Models (GCMs) used to generate climate data in the future. In this study, Canadian Earth System Model Second Generation (CanESM2) was the model which used to predict future climate data. Three commonly-used, daily climate change scenarios, RCP 2.6, RCP 4.5 and RCP 8.5 were used to generate the climate data for the years 2020–2099.

A Representative Concentration Pathway (RCP) is a concentration of greenhouse gas trajectory depended by the IPCC for its fifth Assessment Report (AR5) in 2014. It replaces the Special Report on Emissions Scenarios (SRES) projections reported in 2000.

For climate modeling and research, there are four pathways were selected. They describe various climate futures, all of which are considered depending on the greenhouse gases (GHG) volume released in future. The four RCPs, was RCP2.6, RCP4.5, RCP6, and RCP8.5, are classified after a possible range of radiative forcing values in the year 2100 (2.6, 4.5, 6.0, and 8.5 W/m<sup>2</sup>, respectively).

The RCPs are regular with a wide range of possible changes in future anthropogenic (i.e., human) GHG emissions, and goal to act their atmospheric concentrations. RCP 2.6 assumes that global annual GHG emissions (measured in CO<sub>2</sub> -equivalents) peak between 2010–2020, with emissions reducing basically thereafter. In RCP4.5, emissions will be peak at 2040, after that they will reduce. In RCP6, emissions will be peak at 2060, after that they will reduce. In RCP 8.5, emissions keep on increase during 21<sup>st</sup> century as shown in Figure (3-2).

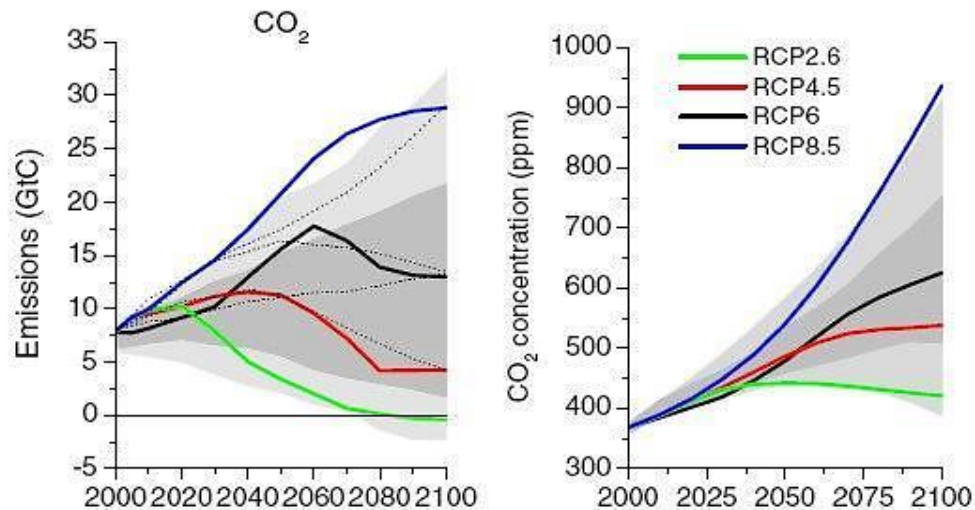


Figure (3-2): IPCC Emissions Scenarios for CanESM2 model.(Wayne, 2013)

### 3.2.2 Data analysis

To generate future climate data in the coming decades, the SDSM was used to downscale GCMs output. Downscaling includes determining relationships between global-scale atmospheric data as predictors with regional-scale climate data to be predicted (Wilby and Dawson, 2013). Two data sets are used to generate future climate data (rainfall, maximum, and minimum temperature) at a selected station:

1. Daily data (rainfall, minimum and maximum temperature) was provided by the Organization for Meteorology and Seismology in Iraq, for Karbala station during the period 1979 to 2018.
2. Daily global climatic data, as predictors, were taken from the Canadian Climate Change Scenarios Network. These data include National Center of Environmental Predictions (NCEP) collected for the observation period, also output from CanESM2 for both current and future periods (2040 and 2099) under existing scenarios. GCM data sets were used (CanESM2) model to downscale by using SDSM software (Wilby et al., 2007). Table (3-1) shows the

GCM data sets were used (CanESM2) model to downscale by using SDSM software (Wilby et al., 2007). Table (3-1) shows the coordinate of the meteorological station used to obtain meteorological data for the study area. Table (3-2) shows the features of GCM used as SDSM model input (Lemke et al., 2007).

Table (3-1): Coordinates of the study station.

Station	Coordinates	
Karbala	Longitude	43°25'33"
	latitude	32°38'58"

Table (3-2): Features of GCM as SDSM software input.

GCM	IPCC	SRES	Resolution
CanESM2	IPCC4	RCP2.6,RCP4.5,RCP8.5	2.79° × 2.81°

### 3.2.3 Statistical Downscaling Model (SDSM)

The SDSM (Wilby et al., 2002) ,was used to downscale output of GCM and to predict climate data through multiple linear regression (MLR). The structure of SDSM is shown in Figure (3-3). To generate climate data for any duration (monthly, seasonally or annually), a multivariate linear regression model is built between independent variables (global-scale predictors) and a dependent variable (local-scale predicted climatic data) (daily rainfall, min. and max. temperature) over many stages.

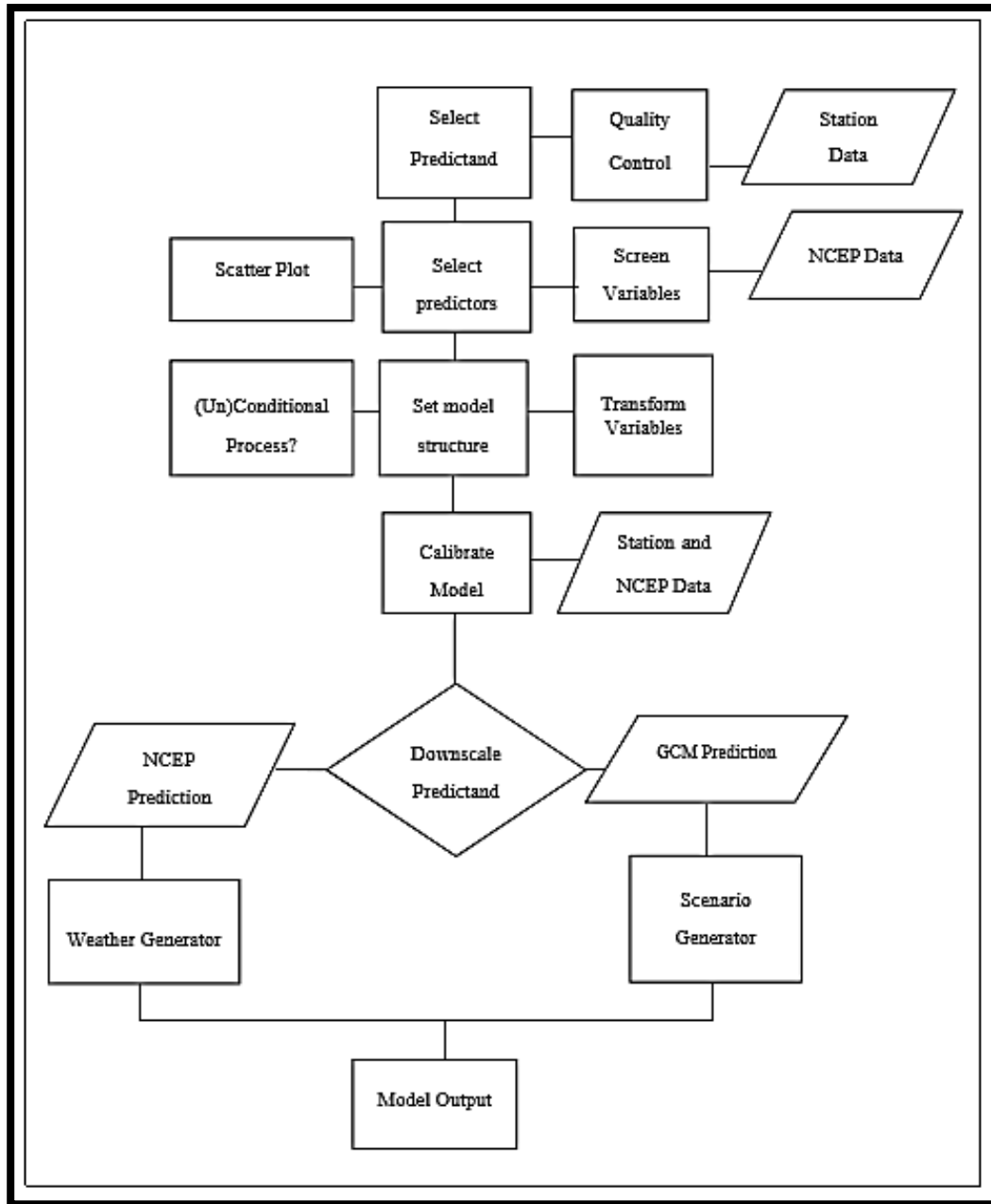


Figure (3-3): SDSM Version4.2 climate scenario generation (Wilby et al., 2007).

### 3.2.3.1 Monitoring and screen variables

In this step the major aim is to help in chosen of the suitable downscaling predictor parameters. For this step, climate data is normally distributed, so it can be looked an unconditional variable. Thus, to choose the multivariate regression model in SDSM, direct relationship is built between the observed data (rainfall, min. and max. temperature) as predicted variables and the global predictors as independent variables. So, to identify and chose proper predictors with greatest correlation with the observed data at study station, the analysis of correlation was used between the predictors and the predicted variables that is involve the analysis of correlation matrix, the correlation of partial, the scatter plot, and also the percentage of variance clarified between variables. So, for this study, the best predictors were chosen depending on the correlation analysis results for selecting the best multiple regression models at selected station.

### 3.2.3.2 Calibration and validation

Data for the period from 1979 to 2018 were divided into two parts. The data for the first part from 1979 to 2000 were used to calibrate the model and the data for the second part from 2001 to 2018 were used to validate the model. Various statistical tests have been used to determine the validity performance within the SDSM. The results of the multivariate regression model at baseline were compared with the observed data of the selected station. The prediction model has been validated by using the coefficient of determination ( $R^2$ ), the root mean square error (RMSE) and mean bias error (MBE).  $R^2$  is a relativity factor, its best value is “1” (Equation3- 1). RMSE is the standard deviation of the residuals (prediction errors) and is equal to zero if the model predictions fit very well with the observations (Equation3-2).The MBE represents



the error estimation of modeling. It can be negative or positive, but zero is the best value (Equation 3-3).

$$R^2 = \frac{(n(\sum p_i o_i) - (\sum p_i)(\sum o_i))^2}{(n(\sum p_i^2) - (\sum p_i)^2)(n(\sum o_i^2) - (\sum o_i)^2)} \quad \dots (3-1)$$

$$RMSE = \sqrt{\frac{\sum_1^n (P_i - O_i)^2}{n}} \quad \dots (3-2)$$

$$MBE = \frac{\sum_1^n (P_i - O_i)}{n} \quad \dots (3-3)$$

Where,  $P_i$  is the predicted daily value;  $O_i$  the observed daily value; and  $n$  is total number of data.

### 3.2.3.3 Climatic scenarios generation

The GCMs have been designed using various scenarios of potential emissions for the future. This was to offset changes in human behavior that could influence climate change. In the Special Report on Emission Scenarios (SRES) by IPCC, there are more than 40 scenarios related to emissions that examine the quantity of greenhouse gas emissions, the technology growth, the land use, the land cover and other human activities. On this basis, an SDSM has been developed with future climate scenarios to obtain functions of alterations of local variables. At this point, and taking into account statistical calibration and regression equations among many global-scale predictor parameters, e.g. Rainfall, maximum temperature, and minimum temperature at the station over the baseline period (1979–2018), the GCM output (CanESM2) was statistically downscaled under the different emissions scenarios. A Time-

-series of daily rainfall, temperature maxima, and temperature minima at local station were then modeled.

### 3.3 Groundwater Flow Modeling

#### 3.3.1 Governing equation

The governing equation can be derived by collecting the continuity equation with the constituent relation Darcy's law (Anderson et al., 1992).

The equation of continuity can be obtained by applying the concept of the elemental Cartesian fixed control volume as shown in Figure (3-4), and the assumption that the fluid properties are considered to be uniform in time and space (White, 2009). In the y-direction, the area of the sides is denoted as  $\Delta x \Delta z$ , inflow as  $q_{y,in}$  and the outflow  $q_{y,out}$ .

The flow through the left side can be expressed as

$$q_{y,in} = v_{in} \rho \Delta x \Delta z \quad \dots (3-4)$$

And the flow through the right side as

$$q_{y,out} = (v_{in} + \frac{\partial v}{\partial y} \Delta y) \rho \Delta x \Delta z \quad \dots (3-5)$$

Where

$v$  is the fluid velocity in the y-direction (L/T) and

$\rho$  is the density of the fluid (assumed constant) (M/L<sup>3</sup>).

The change in flow between the left and right faces can be written as

$$q_{y,in} - q_{y,out} = \frac{\partial v}{\partial y} \rho \Delta x \Delta y \Delta z \quad \dots (3-6)$$

Equations for the remaining directions could be formulated in a similar way (White, 2009). According to the conservation of mass principle, a

change in inflow and outflow should be equal to the change in storage within the control volume.

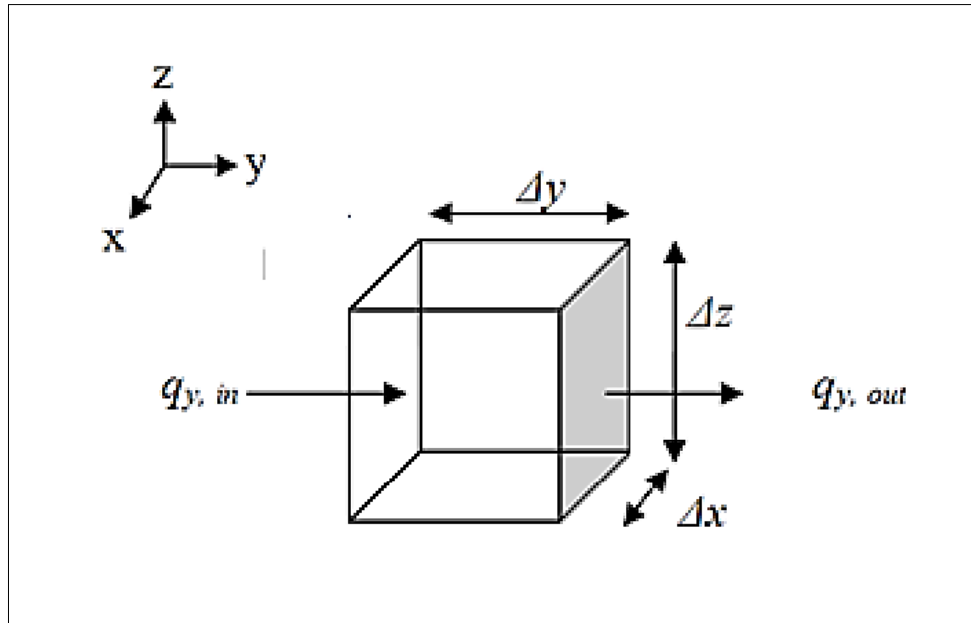


Figure (3-4): Elementary control volume (AlMussawy, 2013).

The change in storage per unit change in head can be written as

$$S_s = \frac{\Delta V_{fluid}}{\Delta h \Delta V_{storage}} \quad \dots (3-7)$$

Where

$$V_{storage} = \Delta x \Delta y \Delta z \quad \dots (3-8)$$

A change in storage during a time,  $\Delta t$ , could be written as

$$\frac{\Delta V}{\Delta t} = S_s \frac{\Delta h}{\Delta t} \Delta x \Delta y \Delta z \quad \dots (3-9)$$

Accounting for the remaining directions yields

$$\frac{\partial u}{\partial x} \rho \Delta x \Delta y \Delta z + \frac{\partial v}{\partial y} \rho \Delta x \Delta y \Delta z + \frac{\partial w}{\partial z} \rho \Delta x \Delta y \Delta z = - S_s \frac{\Delta h}{\Delta t} \rho \Delta x \Delta y \Delta z \quad \dots (3-10)$$

This can be simplified to

$$\frac{\partial u}{\partial x} + \frac{\partial v}{\partial y} + \frac{\partial w}{\partial z} = - S_s \frac{\Delta h}{\Delta t} \quad \dots (3-11)$$

This equation is represented water balance equation (Anderson & Woessner, 1992). Darcy's law can be applied and the resultant equation will be:

$$\frac{\partial}{\partial x} \left( k_x \frac{\partial h}{\partial x} \right) + \frac{\partial}{\partial y} \left( k_y \frac{\partial h}{\partial y} \right) + \frac{\partial}{\partial z} \left( k_z \frac{\partial h}{\partial z} \right) + w = - S_s \frac{\partial h}{\partial t} \dots (3-12)$$

Where

$K_x$ ,  $K_y$ , and  $K_z$ : represents hydraulic conductivity values for the x, y, and z coordinate axes, that supposed to be parallel to the directions of principal coordinate with unite of (L/T).

$h$ : represents water head with units of (L).

$W$ : represents volumetric flux per unit volume. For flow withdrawal from groundwater, the value sign will be negative while for flow adding to groundwater the, value sign will be positive.

$S_s$ : represents specific storage coefficient with units ( $L^{-1}$ ).

$t$ : represents the time with units of (T).

The governing equation was the groundwater flow equation for 3-D fluid movement in a heterogeneous and anisotropic porous media under conditions of non-equilibrium (unsteady state conditions). Under conditions of equilibrium (steady state conditions) the storage term in above equation is equal to zero (Kresic, 2006).

Governing equation explains how the hydraulic head and flow movement distributed over a continuous field. This equation cannot be analytically solved for practical applications involving complex systems (Anderson and Woessner, 1992).

Therefore, numerical methods were used to find approximate solutions. Where, the finite-difference method considers the most commonly method used to find approximate solutions by convert the differential equations to linear equations.

### **3.3.2 Types of boundary conditions**

Boundary conditions refer to hydraulic conditions along the perimeter of the problem domain (Anderson et al., 2015) and can be mathematically classified into three types:

1. Type 1 (Specified head boundary). This type of boundary condition is also named as Dirichlet conditions. The head along this boundary is set to be known value. With space, the heads of this type may vary. A special case of this boundary is a constant head boundary in which the heads along the boundary are a constant value.
2. Type 2 (Specified flow boundary). This type of boundary is also called the Neumann conditions in which the derivative of the head along the boundary is specified. The particular case of this boundary is no flow boundary in which the flow across the boundary is set at zero value.
3. Type 3 (Head- dependent boundary). In this type of boundary which is also named as Cauchy conditions, the flow across the boundary is calculated from Darcy's law using a gradient calculated as the difference between a specified head outside the boundary and the head computed by the model at the node located on or near the boundary (Anderson et al., 2015).

### **3.3.3 Groundwater Modeling System (GMS)**

The Groundwater Modeling System (GMS) is a modeling environment used for groundwater simulations. It contains a graphical interface and a number of different analysis codes, including MODFLOW 2000. MODFLOW is a 3-D, cell-centered, finite difference, saturated flow model developed by the United States Geological Survey (McDonald and Harbaugh, 1988). MODFLOW can perform both steady state and transient simulations and has a wide variety of boundary conditions and input options. GMS supports MODFLOW as a pre- and post-processor. The input data for MODFLOW are generated by GMS and saved to a set of files. These files are read by MODFLOW when MODFLOW is launched from the GMS menu. The output from MODFLOW is then imported for post-processing in GMS. GMS feature objects were used for automated mesh creation and for generating all MODFLOW packages inputs.

#### **3.3.3.1 Construction of the conceptual model**

The conceptual model is a synthesis of what is known about the site being studied (Kresic and Mikszewski, 2012). To perform this crucial step of model development, the hydro geologists assemble and analyze all relevant data and articulate necessary aspects of the groundwater system (Anderson et al., 2015). As the conceptual model approximates the true situation of the aquifer, the numerical model is expected to give reasonable predictions. Based on the relevant gathered data about the Dibdibba aquifer in the study area, the conceptual model is built. The Dibdibba aquifer is treated as a single unconfined aquifer. Data pre- and post-processing was carried out in the “map module” of the groundwater modeling system (GMS) environment.

There are two approaches can be using to build a MODFLOW model in GMS: Grid approach and conceptual model approach.

1. The grid approach includes applying sources/sinks with the 3-D grid and other model parameters on a cell-by-cell basis.
2. The conceptual model approach includes applying GIS tools in the Map module to build a conceptual model. The construction methodology of conceptual model can be shown in Figure (3-5). The sources/sinks location, parameters of layer like hydraulic conductivity, boundaries of model, and any required data for simulation can be defined at this level of conceptual model (coverage).

When complete the model, the grid is created, and conceptual model is transformed to the grid model, and all of the cell-by-cell assignments are automatically performed. For automatic mesh creation, GMS feature objects were used to create all MODFLOW package inputs, and the maps of GIS input were pre-processed using software of GIS.

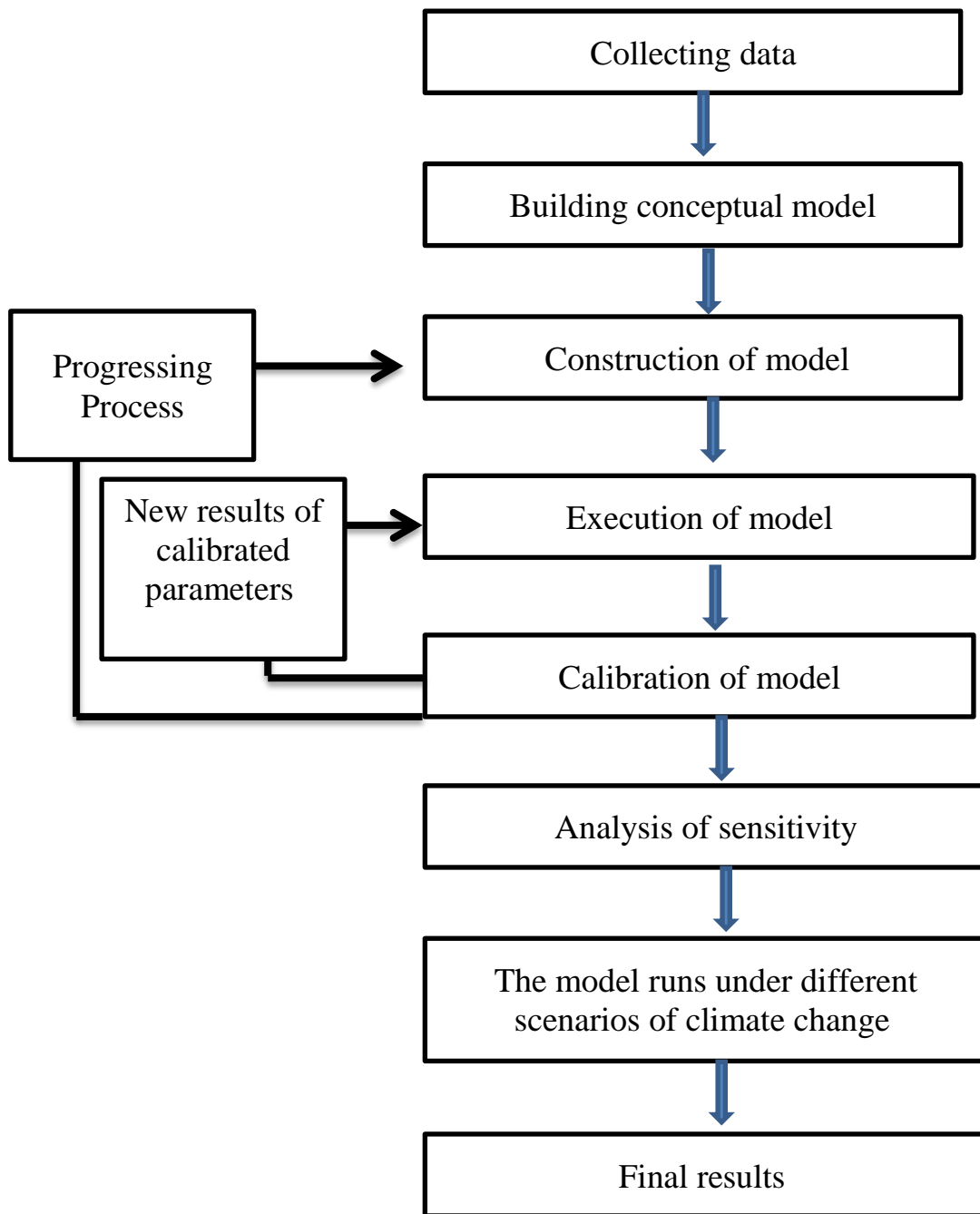


Figure (3-5): Methodology of construction of conceptual model.



### 3.3.3.2 Collection of Data (Input Parameters)

Building a conceptual model of groundwater will require adequate, reliable, and full hydrogeological data covering the entire field of study. This data involve a grid size of model and spacing, elevations of layer, boundary conditions, hydraulic conductivity, recharge and any additional model input. The data required for any study area are given below (all input parameters discussed with details in the next section in this chapter):

- Geographical data (Location of the study area).
- Topographical data (Contour Map of elevation).
- Geological data (Distribution of aquifers).
- Hydrogeological data (Hydraulic conductivity, and heads).
- Data of observation wells.
- Climate change data (current and future temperature and rainfall).

### 3.3.3.3 Calibration of the steady state

At any process of groundwater modeling, the calibration of model considers an essential part. It must be developed to make the model effective in replicating the observed aquifer behavior, in order to incorporate a groundwater model in any management role. Calibration is a method in which model certain parameters like the recharge and the hydraulic conductivity are automatically varied, and the model can be repeatedly run till computed values match with observed values at an acceptable level of accuracy.

### 3.3.3.3.1 Automatic calibration using PEST package

PEST, a nonlinear, least-squares inverse modeling program developed by Doherty (1998) to automatically calibrate a model by traditional trial and error procedure. PEST runs the MODFLOW model thousands of times, through calibration, comparing model-predicted outcomes with observations. The objective function is evaluated after each model runs to decide if the model run was an improvement over the preceding run. PEST tests each modified parameter after each model runs, to decide the next best change to that parameter. PEST then prepares the input data set with the modified parameters for the next model run, executes the experiment, and re-evaluates the output. The target is a weighted, least-square fit approximation between the values expected from the models and the observations values.

The first step in testing the inverse model is to "parameterize" the participation. This involves characterizing which parts of the input model should optimize the advantage of the inverse model. There are two parameterization approaches: zonal and pilot stage. The zonal method will be used in that analysis. This includes characterizing hydraulic conductivity and recharge polygonal zones, coding the zones as parameters, and deciding a starting value for each zone. The hydraulic conductivity (HK) or recharge values assigned to the zones will then be identified by PEST as it attempts to reduce the residual error between measured and observed heads and flows.

One range of parameter zones should be defined for the first trail at parameter estimation. Ideally suited for this purpose is the conceptual model approach used in GMS because the conceptual model consists of polygon-defined recharge and K zones. Code the polygons as parameter zones to each polygon by defining a "primary value" .The key value

should be a value not foreseen to occur elsewhere in the MODFLOW input code. Usually, a negative meaning works perfect. Using nine parameter zones that consist of eight hydraulic conductivity zones and one recharge zone.

### **3.4 Study area and data**

In this subsection, a description of location of the study area, topography of the case study, groundwater head, boundary condition, hydraulic conductivity of study area, and metrological data are presented with details. In addition, the description of case study area and all data is generated with the help of GIS ARC Map program.

#### **3.4.1 Description of the Study area**

Geographically, the study area (Dibdibba aquifer) is located in the central part of Iraq between Karbala and Najaf cities, between ( $31^{\circ} 55' N - 32^{\circ} 45' N$ ) latitude and ( $43^{\circ} 50' E - 44^{\circ} 30' E$ ) longitude, as shown in Figure (3-6). The Dibdibba aquifer represents unconfined aquifer so that it's more exposed to climate change because it is near to the surface and covers an area of 1100 km<sup>2</sup>. The aquifer is bounded by two cliffs; at the northwest by a Tar AlSayed and at the south and southwest by Tar Al-Najaf. The Razzaza Lake which is considered an open surface reservoir is located at the northern part of the aquifer, while at the east; the quaternary sediments bounded the aquifer. Dibdibba aquifer is considered a most important aquifer in Iraq, extending from its center to its far south. Al-Dibdibba depends on the rainfall recharge which is affected by the temperature changes (Al-Mussawi, 2008). The topography elevation ranges from 10 m to 90 m above sea level.

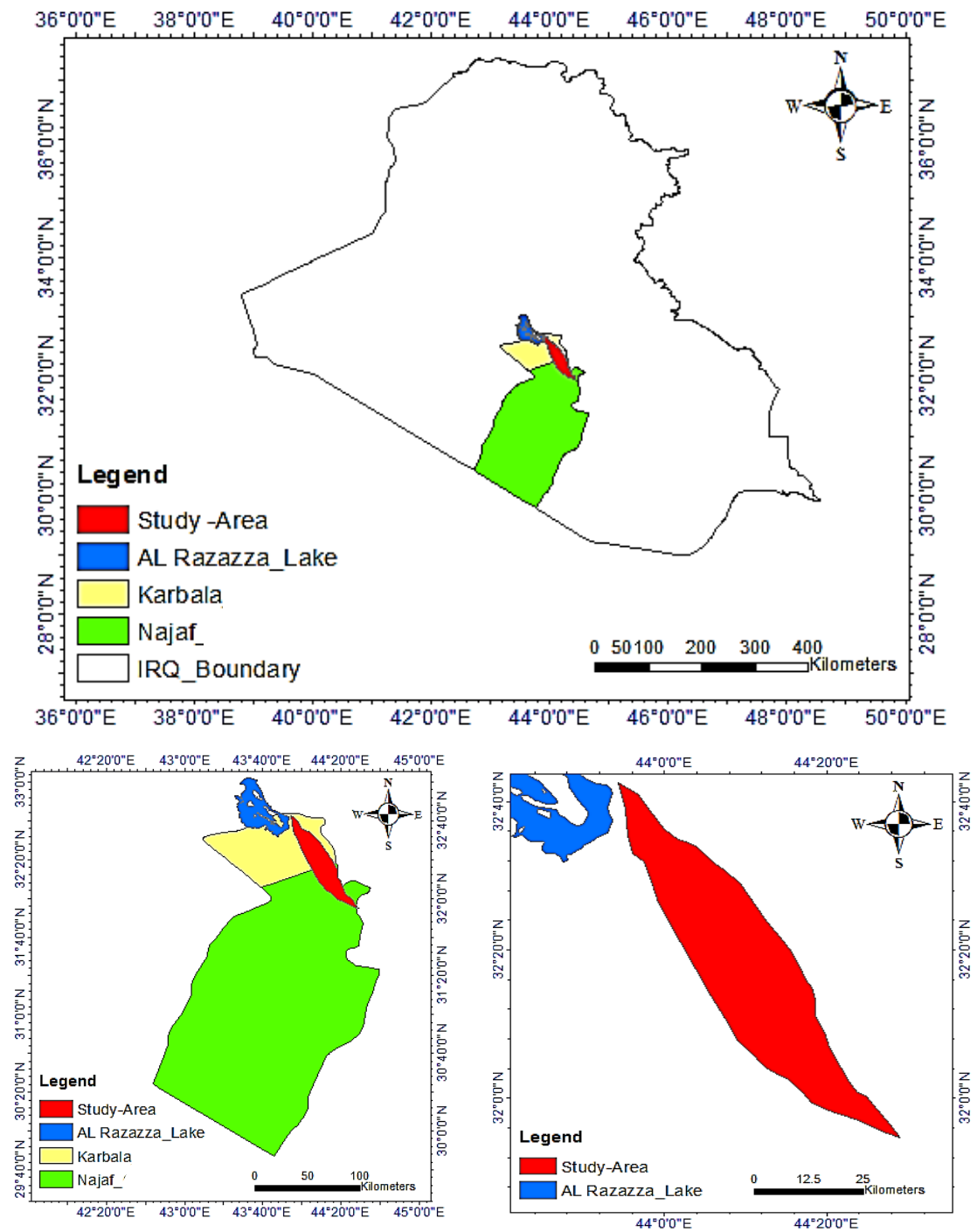


Figure (3-6): Geographical location of the study area.

### 3.4.2 The topography

The topography map of the study area has been generated by using GIS (geographic information system) software. The ground surface map was prepared using digital elevation model (DEM) of type Shuttle Radar Topography Mission (SRTM) with a spatial resolution of 30 m provided from the USGS (U.S Geological survey). The original DEM tiles were first merged to create new mosaic raster, fill sinks and reproject to UTM (WGS 1984 38N projected coordinate system). The topography elevation ranges from 10 to 90 m above sea level and decreases from west to east as shown in Figure (3-7).

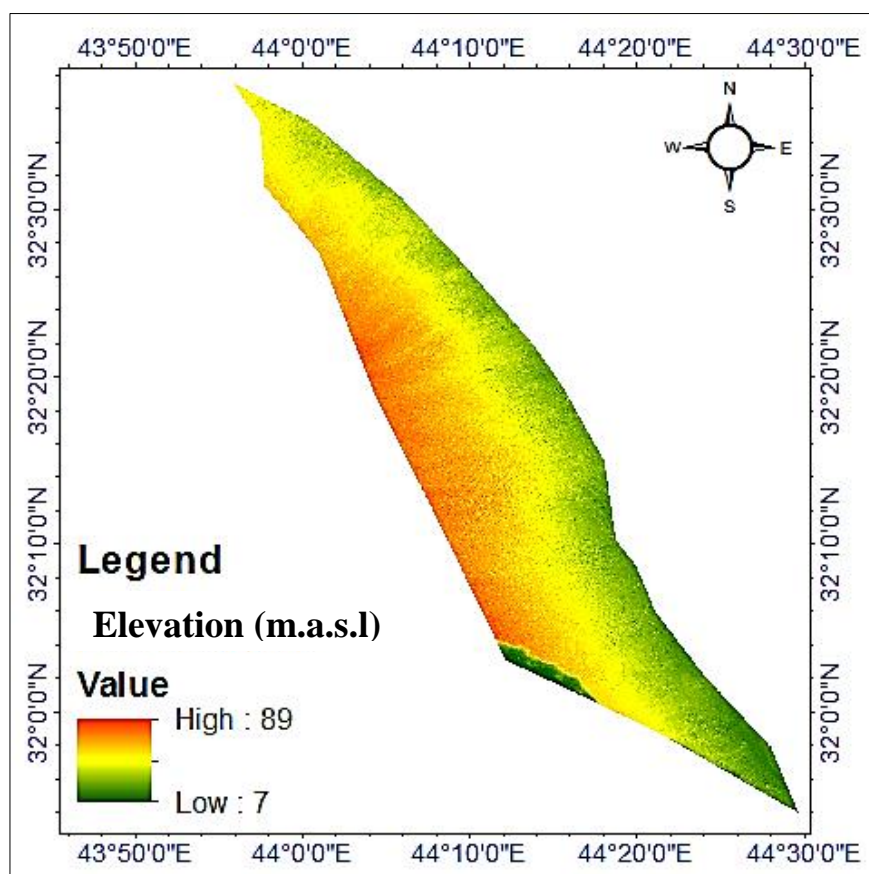


Figure (3-7): Topography of the study area.

### 3.4.3 Hydrogeological data

To build and develop any model, it must collect and process the necessary data for the construction of the nearest match to the natural conditions. The available hydrogeological data for the study area like the aquifer parameters are taken from selected wells distributed in the study area. Table (3-3) is used as an observation data to build the model using Geostatistical Analyst integrated into ArcGIS software. Figure (3-8) shows the location of the selected wells used to estimate the aquifer parameters needed to run the model. All of these wells were dug in the Dibdibba unconfined aquifer (Well drilling department).

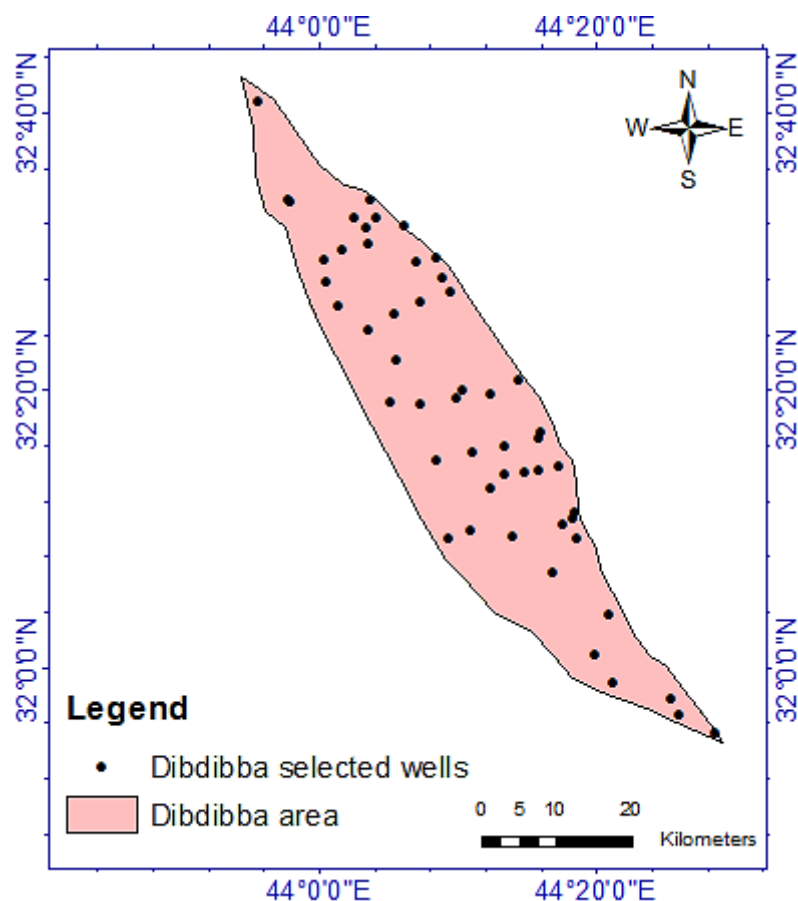


Figure (3-8): Location of the observed wells penetrating the Dibdibba aquifer in the study area (Well drilling department).

Table (3-3): Data of observation wells used to build a model  
(Well drilling department).

well ID	Lat.	Long.	Head (m)	well ID	Lat.	Long.	Head (m)
NO.4	32.564083	43.96358	27	NO.31	32.25006	44.142	29
NO.5	32.4905	44.00683	27	NO.32	32.34706	44.24047	13
NO.6	32.502861	44.02931	24.5	NO.33	32.51033	44.06058	22
NO.7	32.529167	44.05892	20	NO.34	32.18761	44.30781	4
NO.8	32.540778	44.07081	17	NO.35	32.17942	44.30511	10
NO.9	32.487778	44.11789	17	NO.36	32.17344	44.29317	11
NO.10	32.531639	44.10436	16.4	NO.37	32.15964	44.23383	20
NO.11	32.492889	44.14303	15.7	NO.38	32.16514	44.18272	30
NO.12	32.451889	44.15869	15	NO.40	32.15567	44.30963	10
NO.13	32.44175	44.12378	18	NO.41	32.24236	44.28842	10.5
NO.14	32.426444	44.09233	25	NO.42	32.23831	44.26603	14
NO.15	32.408056	44.06072	30	NO.43	32.23564	44.24806	16
NO.16	32.319972	44.08594	33	NO.44	32.23333	44.22294	18
NO.17	32.317806	44.12342	27	NO.45	32.21708	44.20717	19
NO.18	32.324556	44.16636	21	NO.50	31.9635	44.4235	23
NO.19	32.333611	44.17325	21	NO.51	31.94303	44.43428	16.5
NO.20	32.562917	44.06197	17	NO.52	32.37175	44.09308	30
NO.21	32.54075	44.0445	20	NO.55	32.15708	44.157	34.5
NO.22	32.470111	44.14847	17	NO.58	31.92164	44.47639	6
NO.24	32.328944	44.20647	16	NO.59	31.98347	44.35469	24
NO.25	32.680889	43.92728	21	NO.60	32.11479	44.28201	22.5
NO.26	32.562311	43.96612	23.1	NO.61	32.064	44.34855	19
NO.27	32.284361	44.26644	10.5	NO.62	32.01736	44.33302	28.5
NO.28	32.277056	44.26428	16	NO.63	32.43487	44.02372	28
NO.29	32.267139	44.22394	18.5	NO.64	32.46441	44.00946	31
NO.30	32.259778	44.18622	18				

Before building different models for the groundwater level data set, Exploratory Spatial Data Analysis (ESDA) is performed.

The technique of Kriging interpolation gives the best results if the data are normally distributed (bell-shaped curve). Two analytical approaches were used to determine whether the groundwater level data followed a normal distribution or not. First, as shown in Figure (3-9), histograms of the groundwater head levels were plotted with a standard data distribution curve. For quick test, the mean and the median is approximately the same value. The skewness value is also close to zero; this means that the parameter for the hydraulic head is normally distributed.

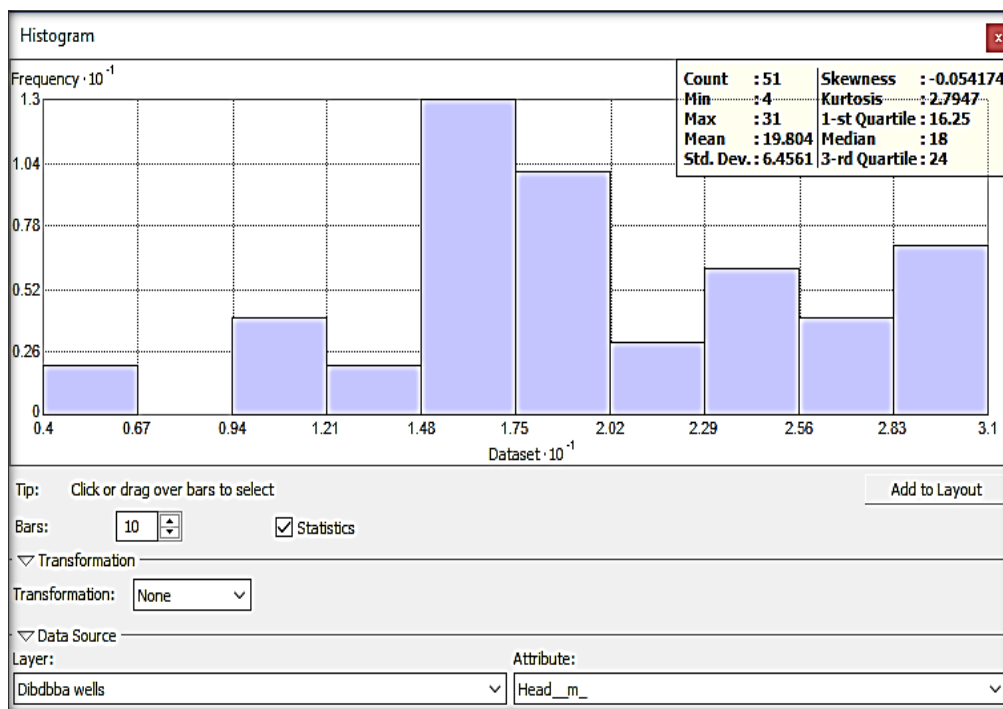


Figure (3-9): Groundwater head level data histogram.



Second, The quantile-quantile QQ Plot is a graphical technique to finding if two data sets come from populations with a common distribution. In this plot, a 45-degree reference line is plotted in the center of the graph. If the two sets fall almost over the reference line, that means, the data is almost normal and vice versa. Moreover, investigation of the normality of head data indicated that the head parameter has normal distribution as shown in Figure (3-10). This figure shows that most of the head data fall on the reference line or close to it.

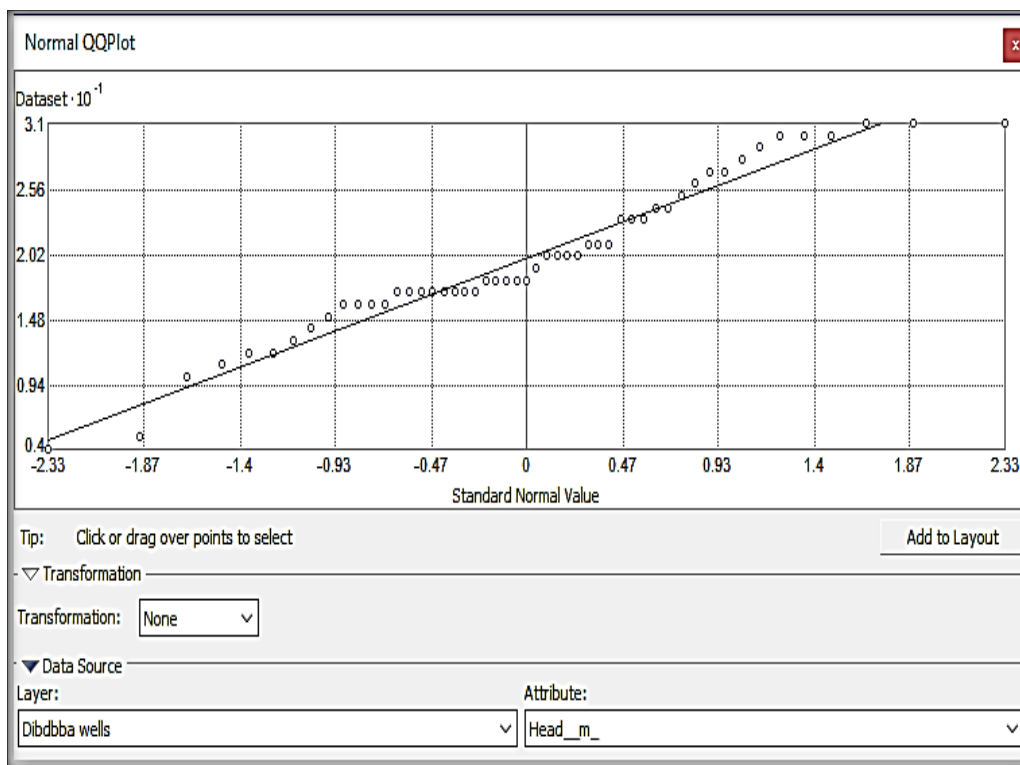


Figure (3-10): Groundwater head level data normal QQPlot .

### 3.4.4 Groundwater head

The movement of groundwater depends on the parameters of hydraulic, layout of stratification, and the hydraulic gradient. The contour map of the groundwater piezometric head in the study area based on the data in Table (3-3) and depended on 51 wells is shown in Figure (3-11) by using Kriging interpolation. The contour map of water head shows the groundwater head ranges from 35 m above sea level at the south-west to 5 m above sea level at the northeast.

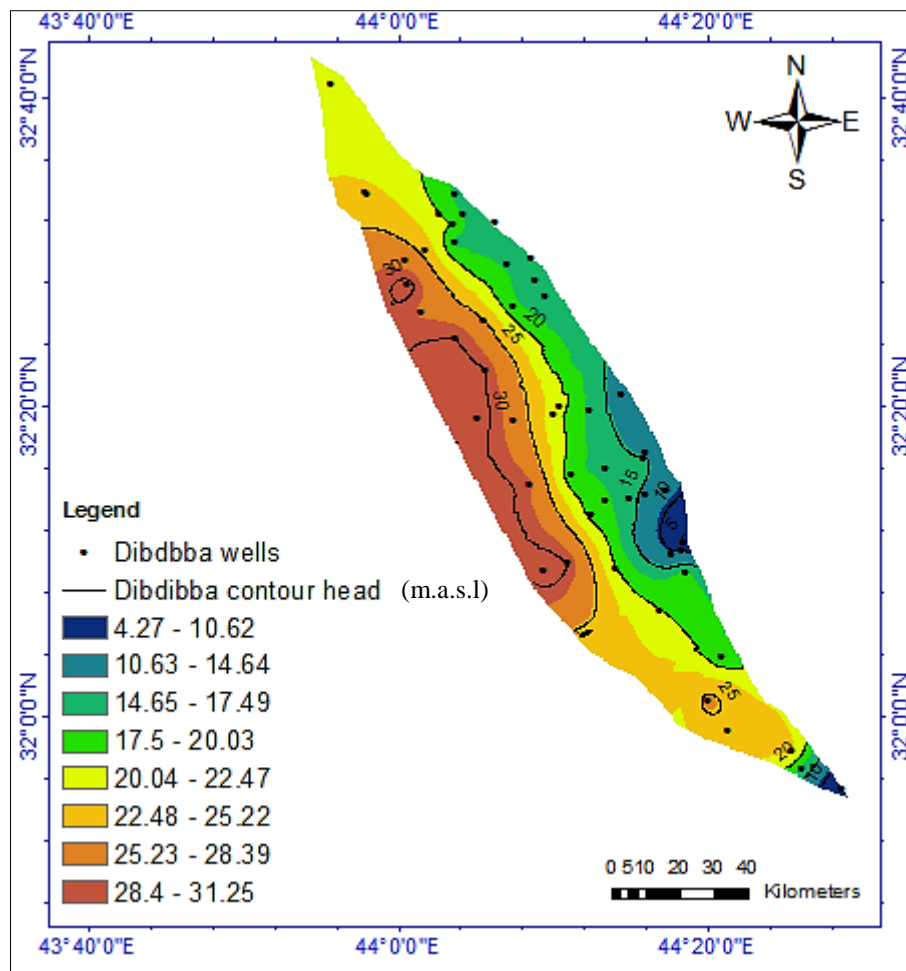


Figure (3-11): The contour map of the groundwater piezometric head in the study area based on the data in Table (3-3).

### 3.4.5 Groundwater model data

The design of modeling involves all data that was used to calibrate the model. For steady-state modeling, the input data involve the model grid size and spacing, elevations of the layer, the boundary conditions, the hydraulic conductivity, and recharging and any additional model data.

#### 3.4.5.1 Grid design

The domain of the model was chosen to cover 1100 km<sup>2</sup>. The grid of the model is composed of 3600 active cells. As shown in Figure (3-12), the cell width along rows and columns (x and y directions) is set at 500 meters. The model region was horizontally acted on a two-dimensional grid and vertically as a single unconfined layer. The values for the top elevations of the aquifer were taken from the topographic map's contour lines (Figure 3-8) of the region, and the aquifer's low elevation is the top elevations minus the depth of formation, where the average depth of formation was 40m.

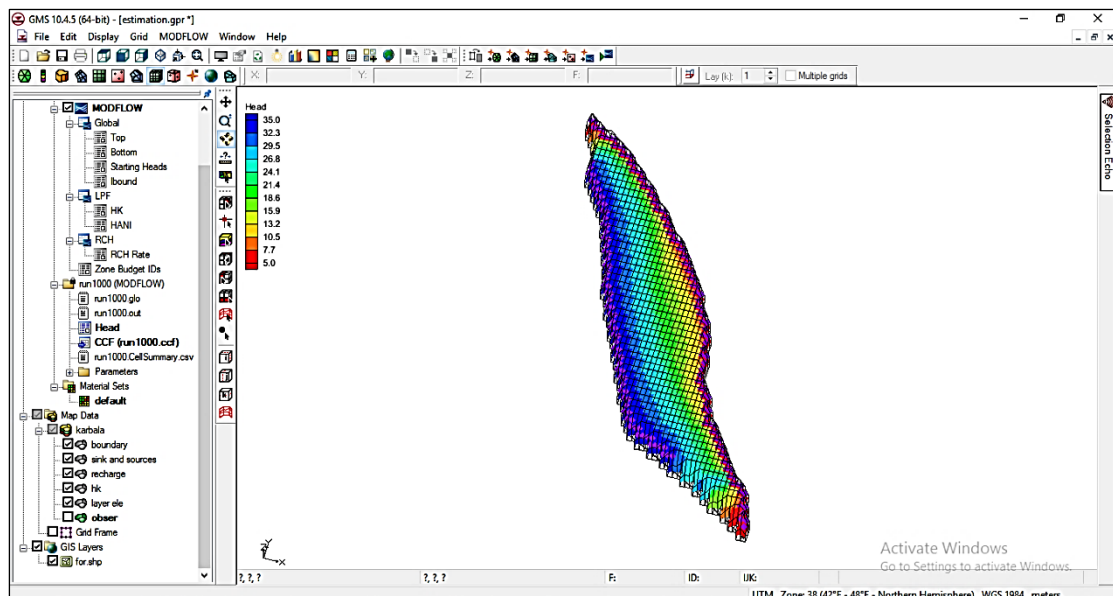


Figure (3-12): 3D grid for conceptual model (Z-magnification=30) produced by GMS software.

### 3.4.5.2 Boundary conditions

Boundary conditions were determined depending on the flow pattern of groundwater of the Dibdibba aquifer as shown in Figure (3-12) and the observed groundwater head of the wells as shown in Table (3-3). The constant-head boundary was applied on the eastern and western of the study area, these head values were 5 m and 35 m assigned from the measurements of some observation wells as shown in Figure (3-13) for eastern and western boundary of the study area, respectively. Moreover, the two features in the study area ( i.e., Tar Al Sayyed and Tar Al Najaf) are defined as a no-flow boundary on the study area 's northwest and southwest edges.

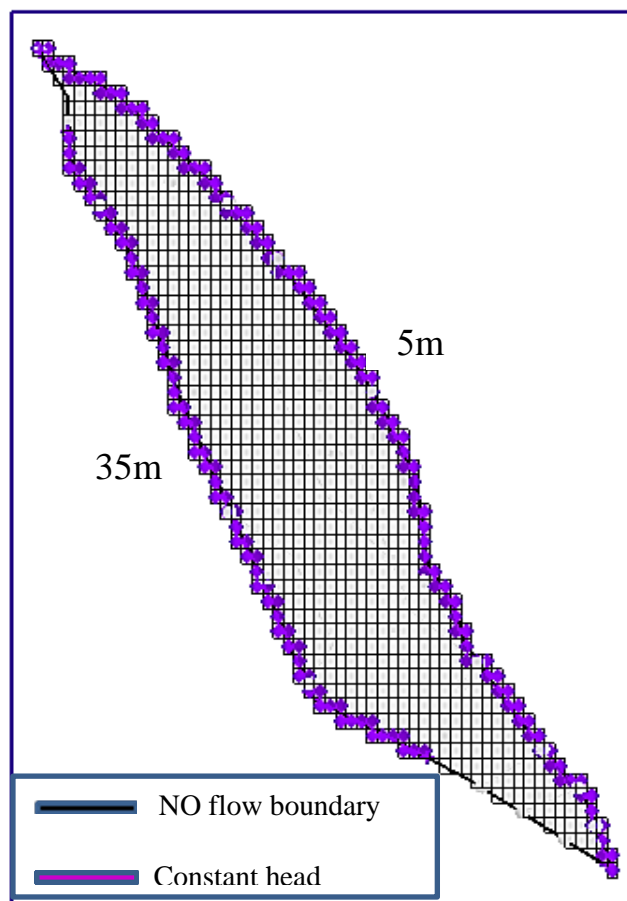


Figure (3-13): Boundaries of flow model and grid distribution.

### 3.4.5.3 Aquifer hydraulic conductivity

The hydraulic conductivity values obtained from the analysis of pumping test of groundwater system to get a suitable value for every point in the system. The hydraulic parameter of Dibdibba aquifer can be shown in table (3-4).

Table (3-4): The hydraulic parameter of Dibdibba aquifer.

Well ID	Elev. (m)	S.W.L (m)	Head (m)	K m/day
N0.4	41.5	14.5	27	18.15
N0.16	71	37.5	33	13.58
N0.24	35	19	16	16.56
NO.27	27	16.5	10.5	19.53
N0.29	50	31.5	18.5	16.67
N0.33	40	18	22	18.92
NO.40	25	15	10	17.46
N0.41	35	24.5	10.5	18.39
NO.50	38	15	23	0.68
NO.51	27	10.5	16.5	2.03
N0.55	67	32.5	34.5	0.195
NO.58	20	14	6	2.67
N0.60	42	19.5	22.5	13.71
N0.61	22	3	19	14
N0.62	33	4.5	28.5	10.43

### 3.4.5.4 Zone division

The hydraulic conductivity and the recharge for every homogeneous zone should be separately measured; the spatially changing values are of course important for the studies of groundwater modeling (Doherty et al., 2010). Therefore, the study area is divided into eight hydraulic conductivity zones depending on the results of the pumping tests on 15 wells and one recharge zone based on the geology and aquifer properties, this zones and names are explain as shown in Figure (3-14).

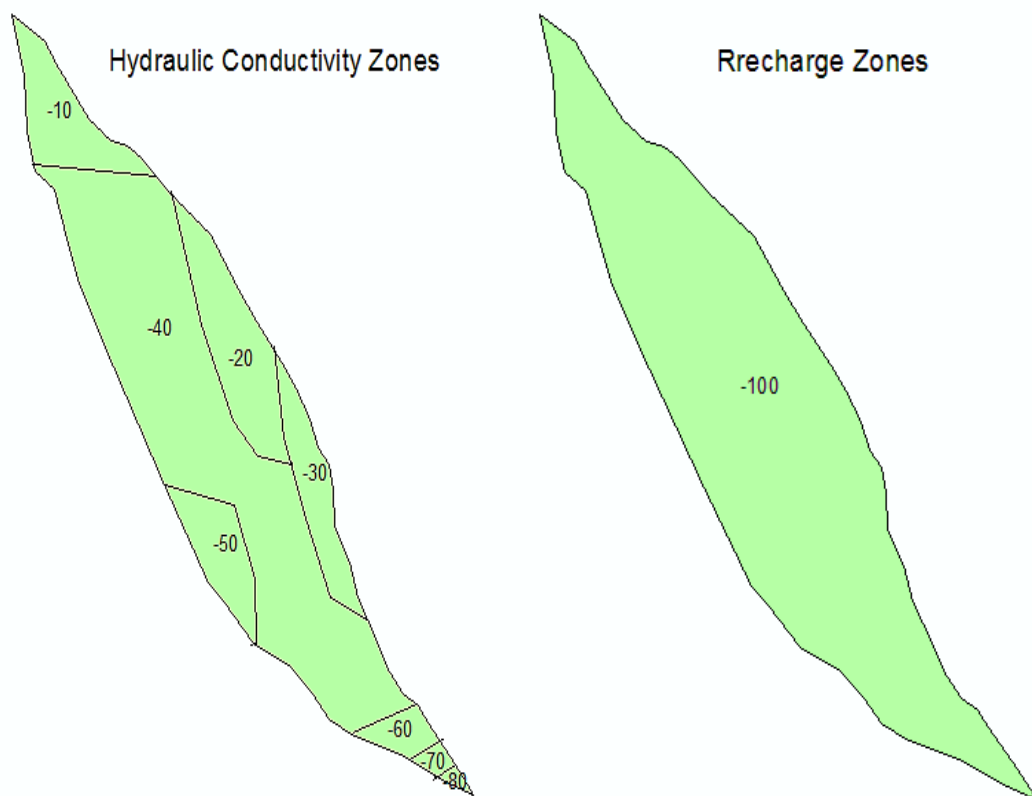


Figure (3-14): Hydraulic conductivity and recharge zones of Dibdibba aquifer in the study area.

### 3.4.6 Metrological data

Metrological data has been collected from the (G.A.M.S.O) for the period from 1979 to 2018 including; daily rainfall (mm), daily maximum temperature (°C), and daily minimum temperature (°C) of Karbala station. This data was used in SDSM program and GMS program. Figures (3-15) to (3-17) show the observed average of (monthly rainfall, mean min. temperature, and mean max. temperature) for 40 years.

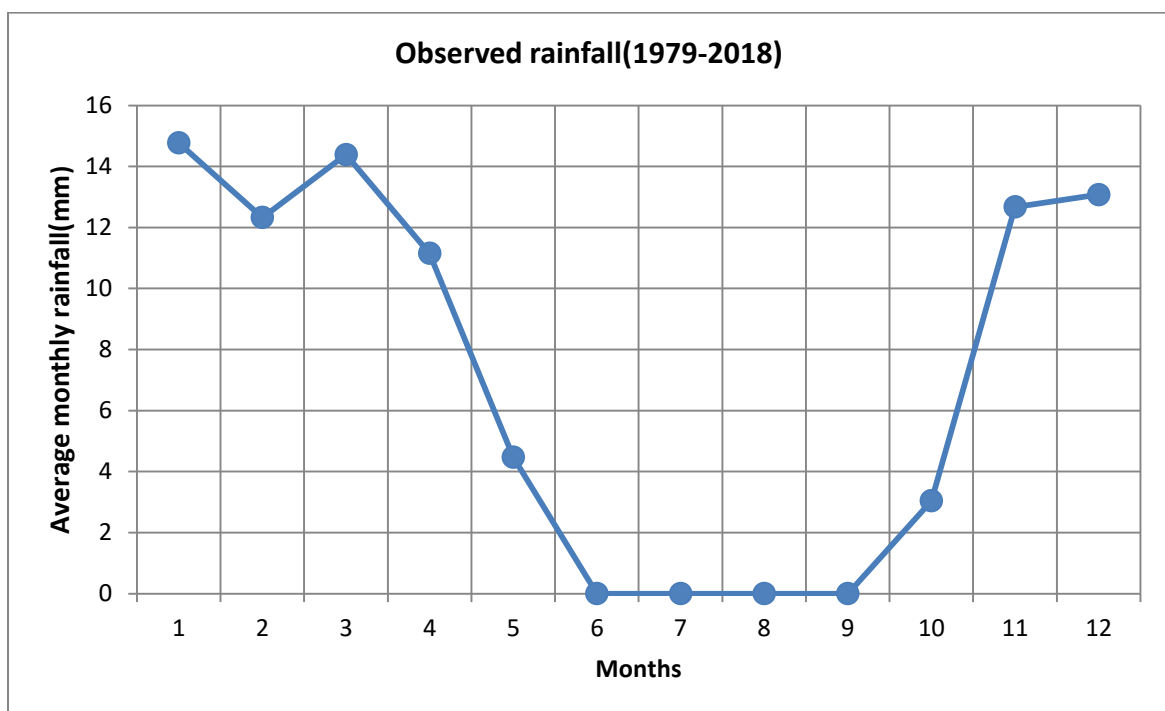


Figure (3-15): The average of monthly rainfall for period (1979-2018).

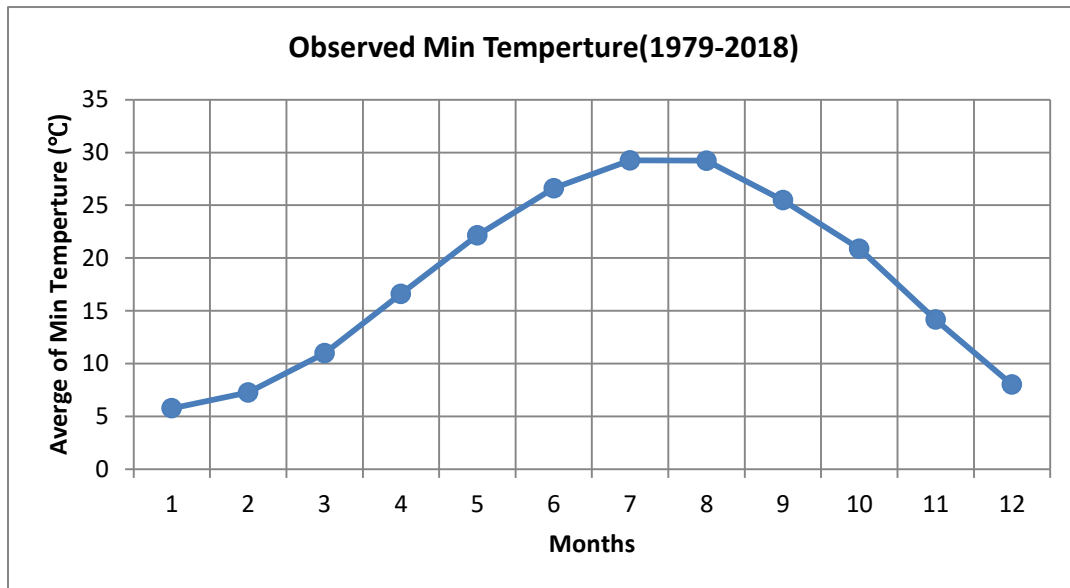


Figure (3-16): Average of min. temperature for period (1979-2018).

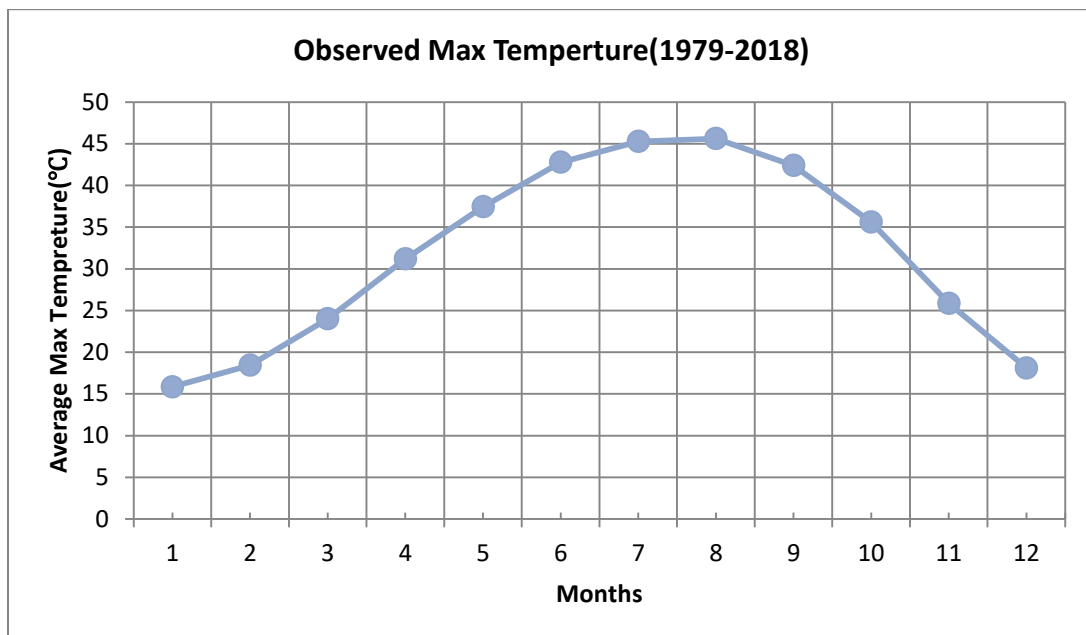


Figure (3-17): Average of max. temperature for period (1979-2018).



## Chapter Four

# RESULTS AND DISCUSSION

### 4.1 Topics of the research results

The discussion of the research results divided into three parts: the first part displays the results of future climate data for two future periods (2040 and 2099) and its calibration, the second part displays the results of groundwater recharge and its calibration, and the third part displays predicted scenarios of the groundwater flow heads and recharge for the next 20 years (2020-2040) and 79 years (2040-2099) under expected future climate change conditions.

### 4.2 SDSM model and future climate data

This part displays the calibration of SDSM model and the future climate data (rainfall, maximum temperature, and minimum temperature) for future periods (2040 and 2099).

#### 4.2.1 Temperature

##### 4.2.1.1 Calibration results of downscaled model

After testing SDSM capability, the (CanESM2) model, was used to downscale the daily (minimum, and maximum) temperatures for future periods. Calibration and validation for the appropriate model were executed by dividing observed data, for the period 1979 to 2018 in two groups. Data from 1979 to 2000 were used to calibrate and build downscale model, while data from 2001 to 2018 were used for validation. Table (4-1) shows the validation results for the climate variables, using  $R^2$ , RMSE and MBE, the ranges for which were 0.877 to 0.905, 3.12 to 3.45 and 0.0027 to 0.0106, respectively for CanESM2 model. Figures (4-1 and 4-2) show correlation between the observed and the predicted maximum and minimum temperature data for CanESM2 models respectively. Figures (4-3 and 4-4) show comparison between the observed and the predicted maximum and minimum

temperature data for CanESM2 models, respectively. The validation results confirm that the consistency of the final forms of the regression models is acceptable and they can predict expected temperatures (maximum and minimum) in the next period by using independent predictors (global climatic parameters).

Table (4-1): Validation results for climate variables over the observation period (2001-2018).

Climate variable	MBE	RMSE	R <sup>2</sup>
Maximum Temp.	0.0106	3.45	0.905
Minimum Temp.	0.0027	3.12	0.877

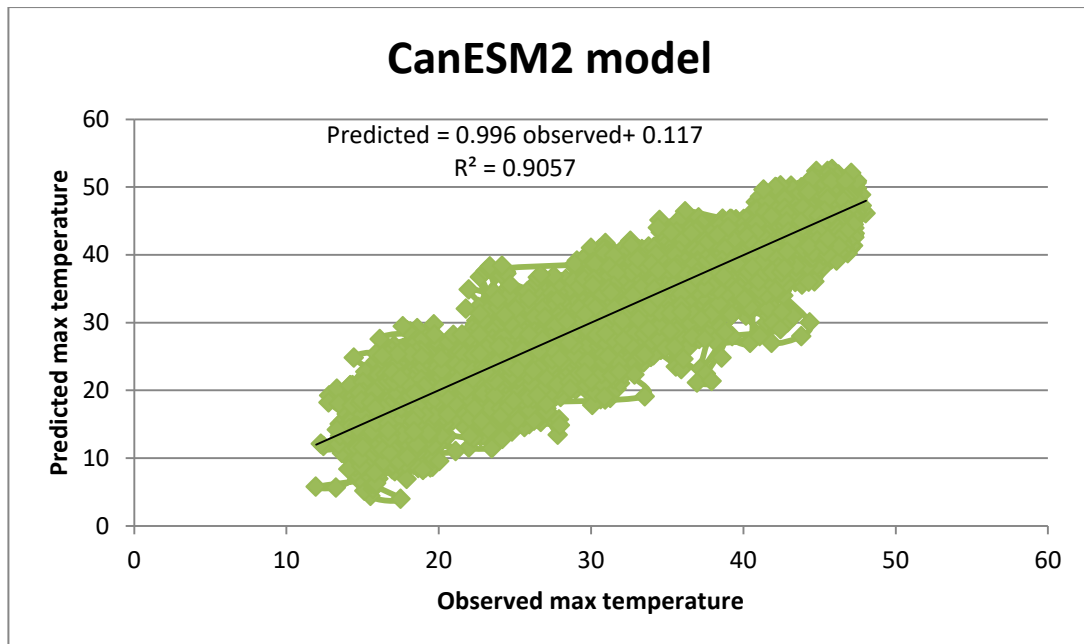


Figure (4-1): Correlation between daily observed and predicted data (2001-2018) for maximum temperature using CanESM2 model.

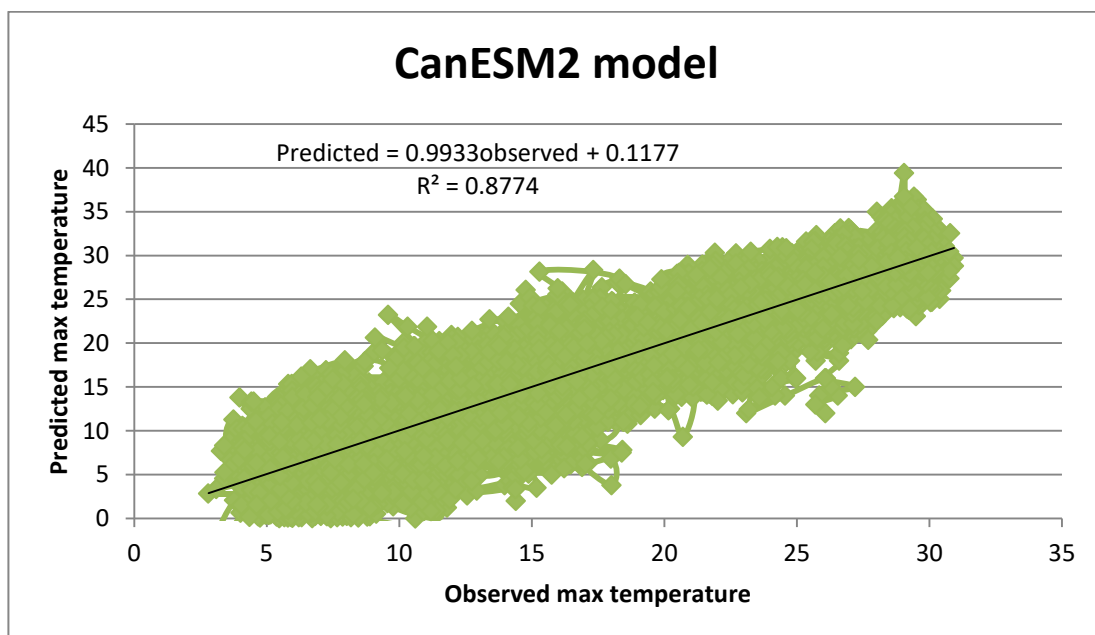


Figure (4-2): Correlation between daily observed and predicted data (2001-2018) for minimum temperature using CanESM2 model.

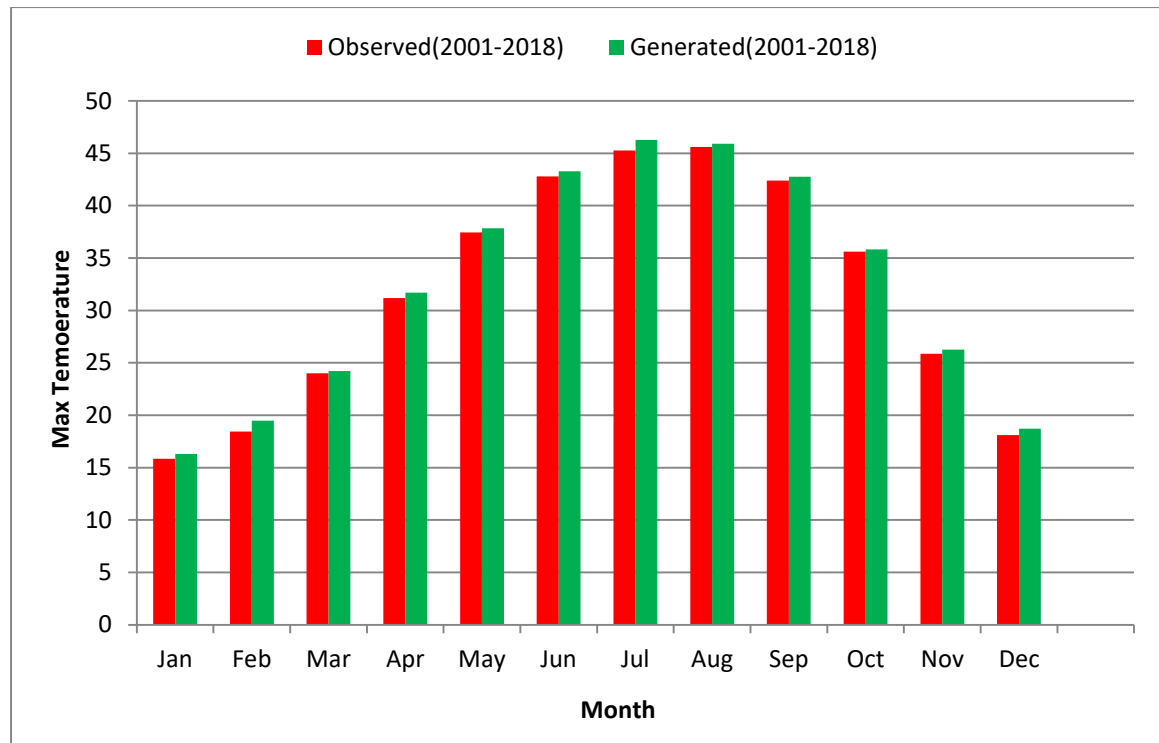


Figure (4-3): Comparison between observed and predicted data (2001-2018) for maximum temperature using CanESM2 model.

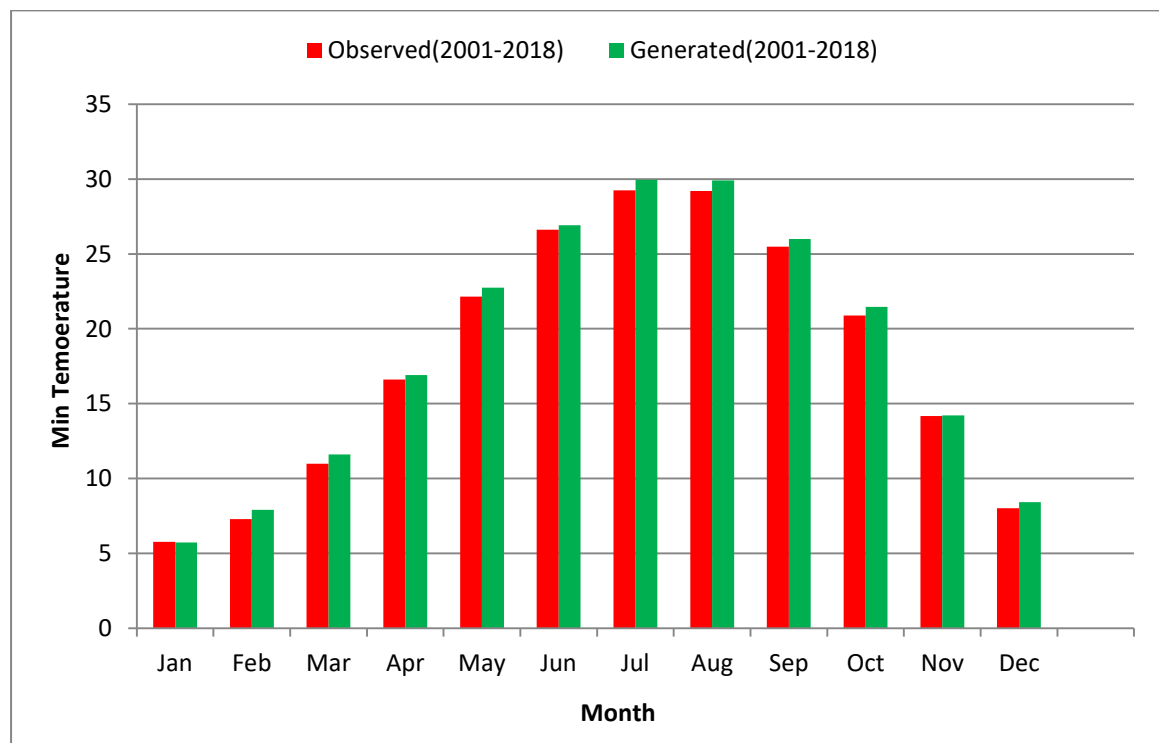
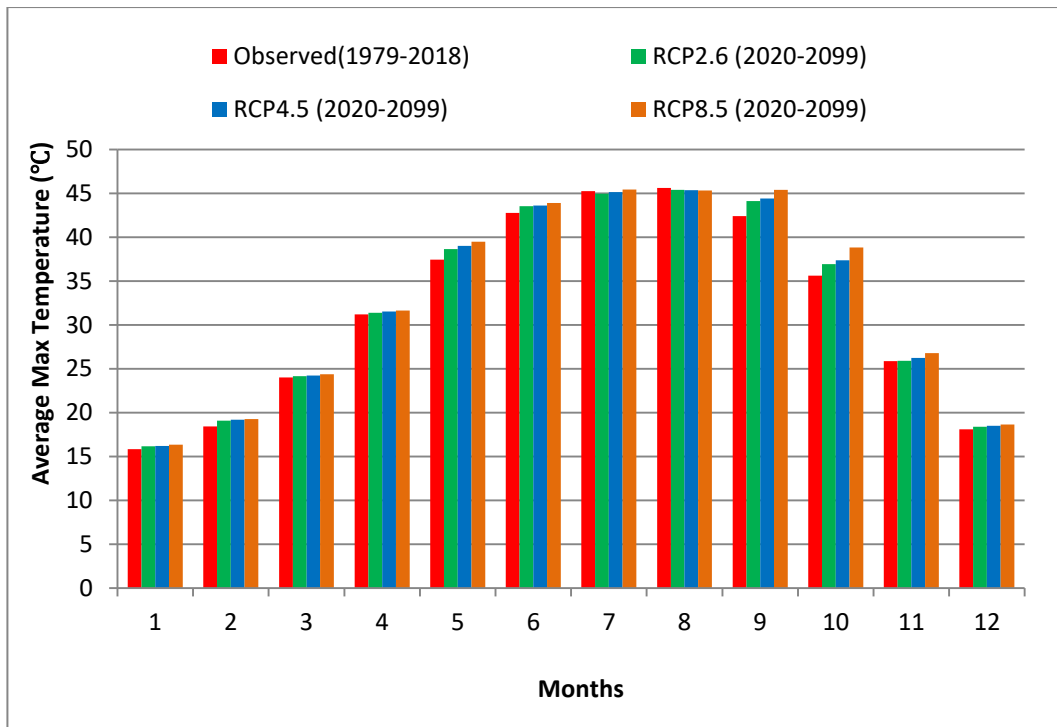


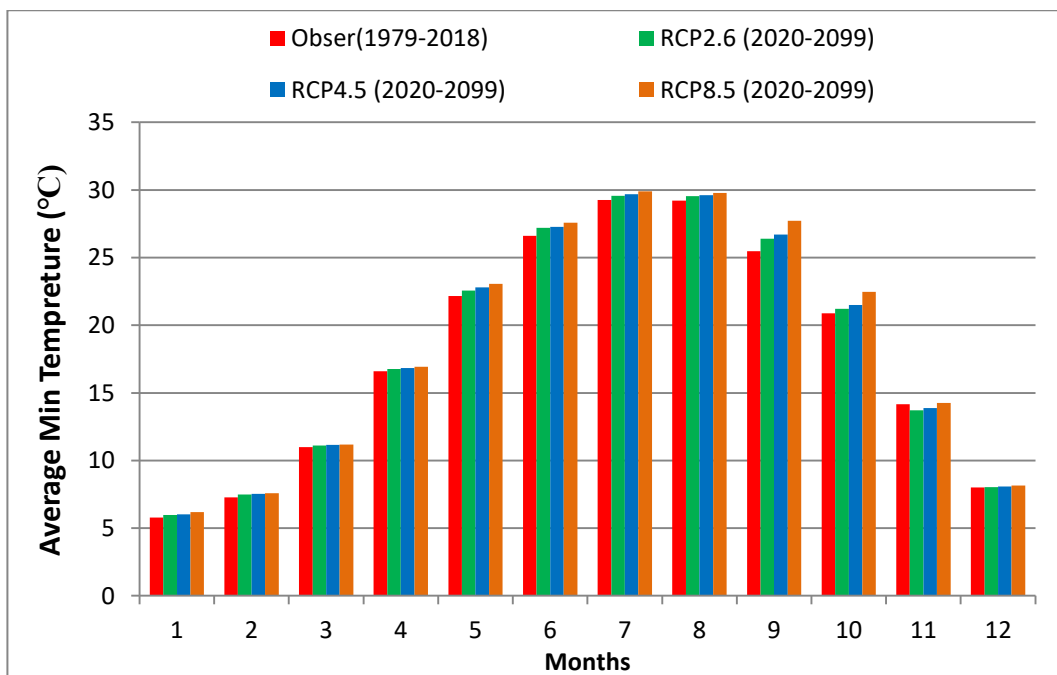
Figure (4-4): Comparison between observed and predicted data (2001-2018) for minimum temperature using CanESM2 model.

### 4.2.1.2 Temperature analysis

A comparison of average monthly maximum temperature, and minimum temperature, observed during the period 1979 to 2018, and values predicted by scenarios RCP2.6, RCP4.5 and RCP8.5 (for CanESM2), for 2020 to 2099 can be shown in Figure (4-5). The greatest increase in monthly average temperature (maximum and minimum) was predicted for July, August, and September, the summer season. The smallest increases were predicted for January, and December, the winter season. The greatest increases was predicted to be 45°C (for maximum temperature) and 30°C (for minimum temperature). While, the smallest increases were predicted to be between 15°C to 20°C (for maximum temperature) and between 5°C to 10°C (for minimum temperature).



(a) Maximum temperature



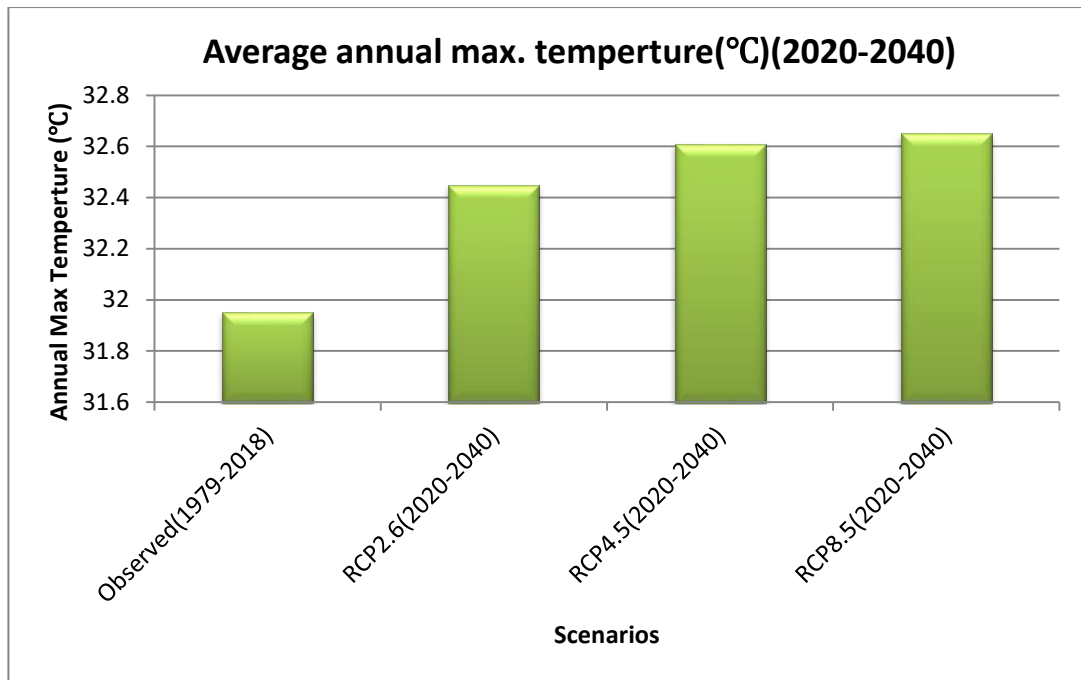
(b) Minimum temperature

Figure (4-5): Comparison between average monthly observed (1979- 2018), and values predicted by RCP2.6, RCP4.5 and RCP8.5 scenarios (2020 to 2099) (a) Maximum temperature (b) Minimum temperature.

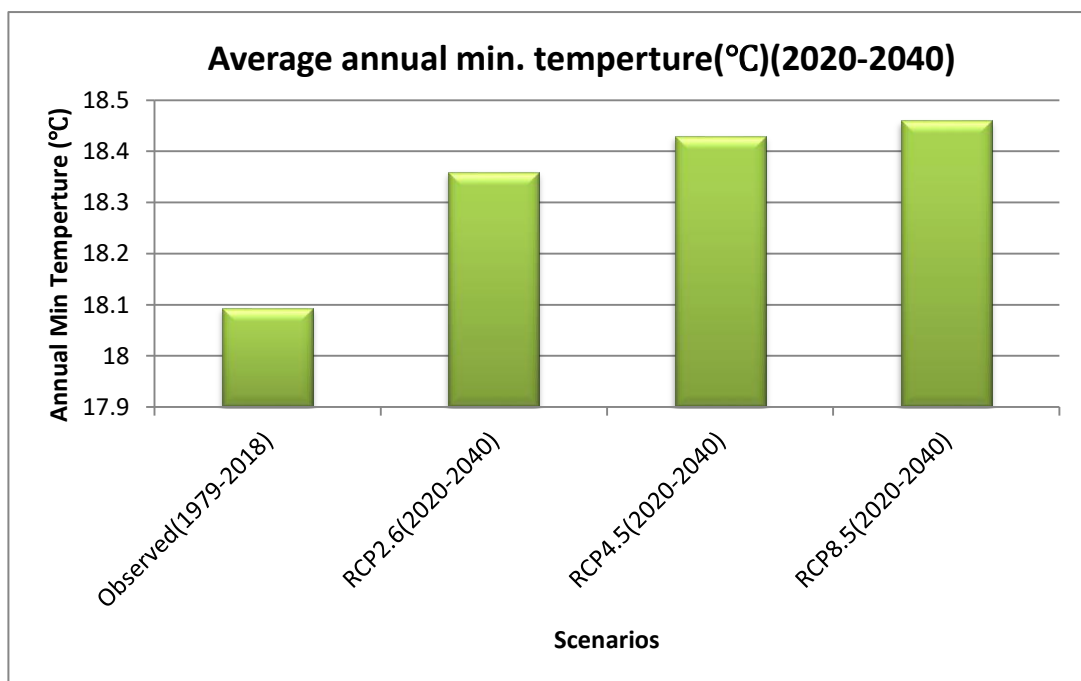
comparison of average annual maximum temperature, and minimum temperature observed during the period 1979 to 2018, and values predicted by scenarios RCP2.6, RCP4.5 and RCP8.5 (for CanESM2), for near future (2040) and far future (2099) can be shown in Figure (4-6) and Figure (4-7). For near future (2040), The scenario RCP8.5 predicted the greatest increase in the average annual maximum temperature of about 32.7°C and the scenario RCP8.5 predicted the greatest increase in average annual minimum temperature of about 18.5°C. While, The scenario RCP2.6 predicted the smallest increase in the average annual maximum and minimum temperature about 32.4°C (for max. temperature) and 18.3°C (for min. temperature).

For far future (2099), the scenario RCP8.5 predicted the greatest increase in average annual maximum and minimum temperature of about 33°C (for max. temperature) and 18.8°C (for min. temperature). While, the scenario RCP2.6 predicted the smallest increase in average annual maximum and minimum temperature of about 32.4°C (for max. temperature) and 18.3°C (for min. temperature).

Figure (4-8) shows the amount of increase in the maximum and minimum temperature under scenarios RCP2.6, RCP4.5 and RCP8.5 (for CanESM2), for years 2040 and 2099. The results shows an increase between 0.5°C and 0.7°C (for max. temperature) and between 0.2°C and 0.4°C (for min. temperature) for year 2040, while an increase between 0.5°C and 1.07 °C (for max. temperature) and between 0.2°C to 0.7°C (for min. temperature) for year 2099.



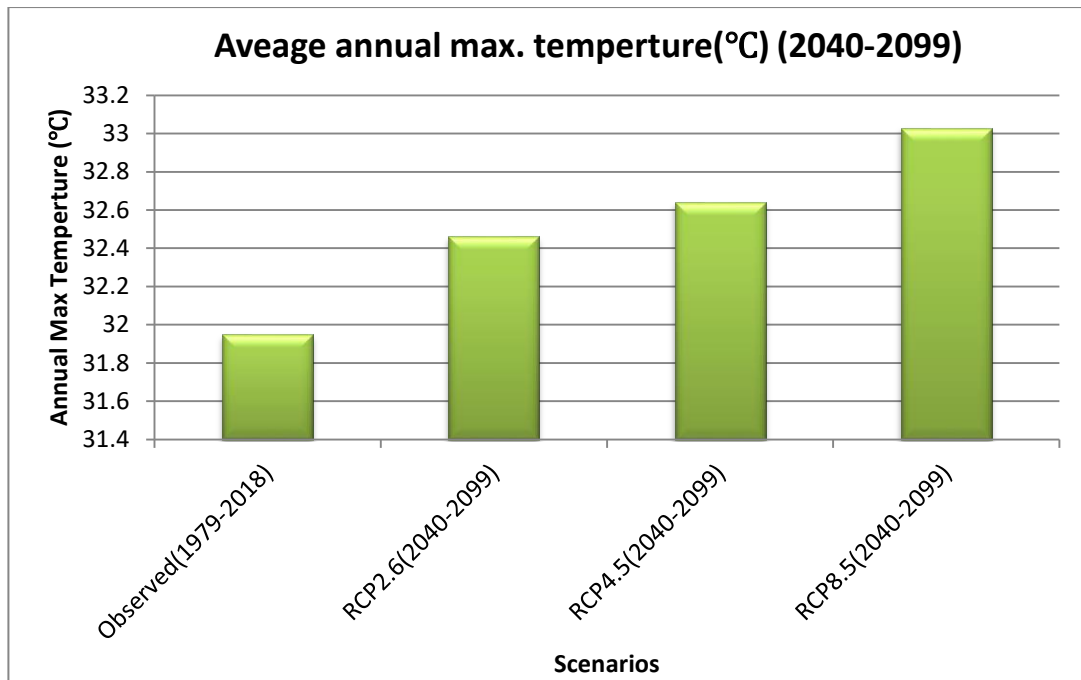
(a)Maximum temperature



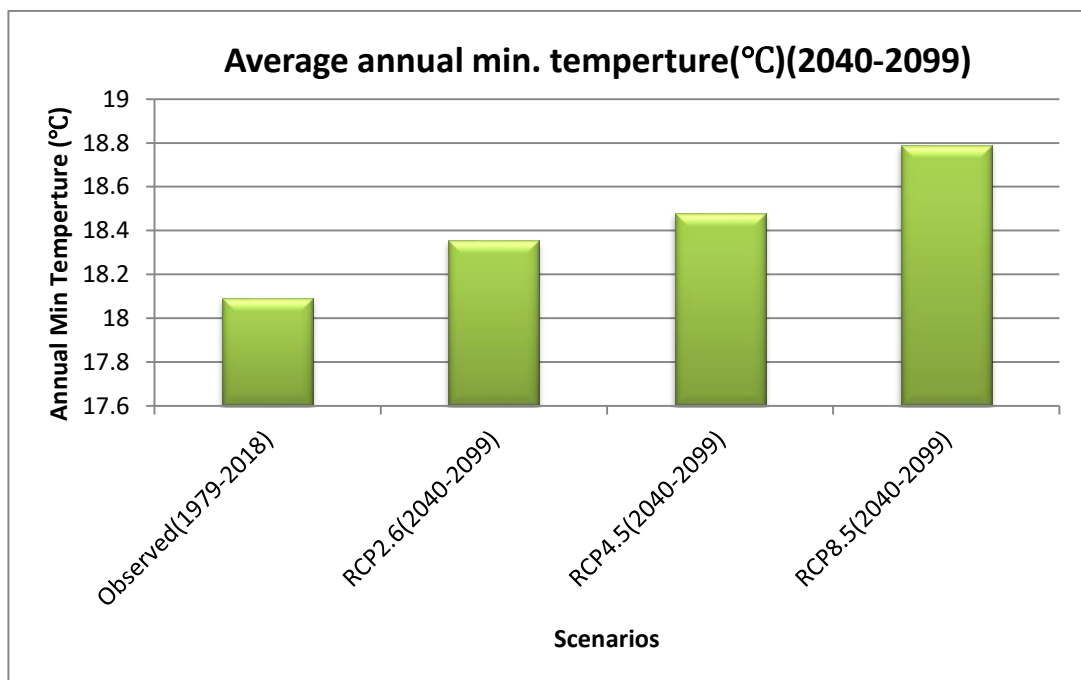
(b)Minimum temperature

Figure (4-6): Comparison between observed average annually (1979- 2018), and the values predicted by scenarios RCP2.6, RCP4.5 and RCP8.5 for 2040  
(a) Maximum temperature (b) Minimum temperature.





(a)Maximum temperature



(b)Minimum temperature

Figure (4-7): Comparison between observed average annually (1979- 2018), and the values predicted by scenarios RCP2.6, RCP4.5 and RCP8.5 for 2099  
(a) Maximum temperature (b) Minimum temperature.

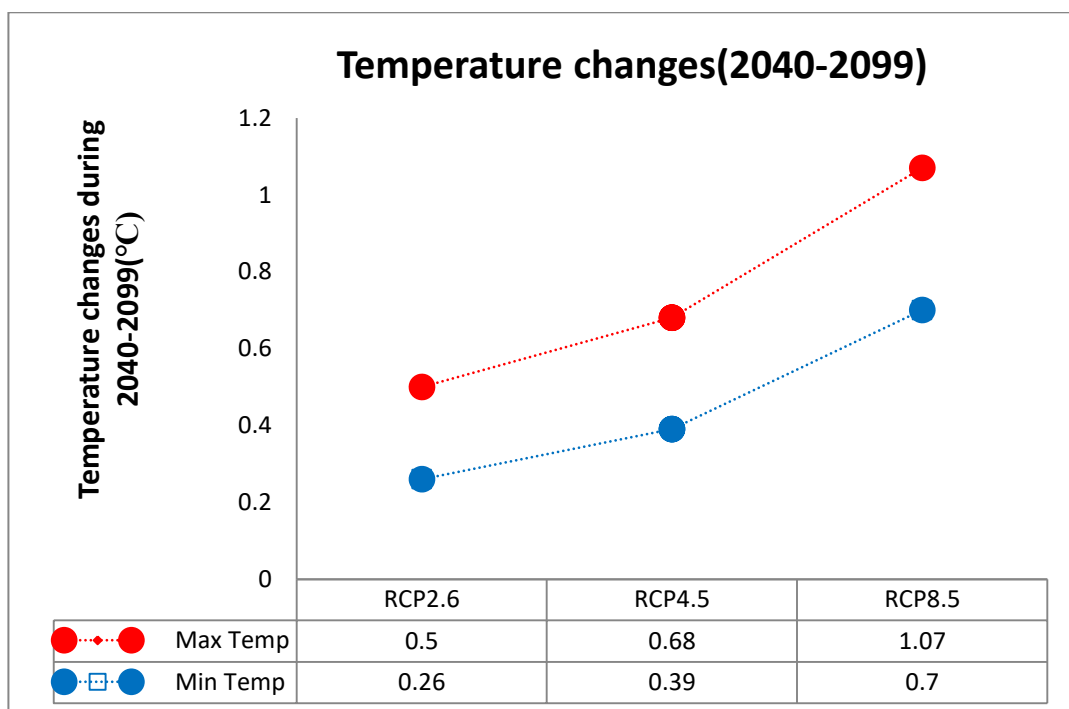
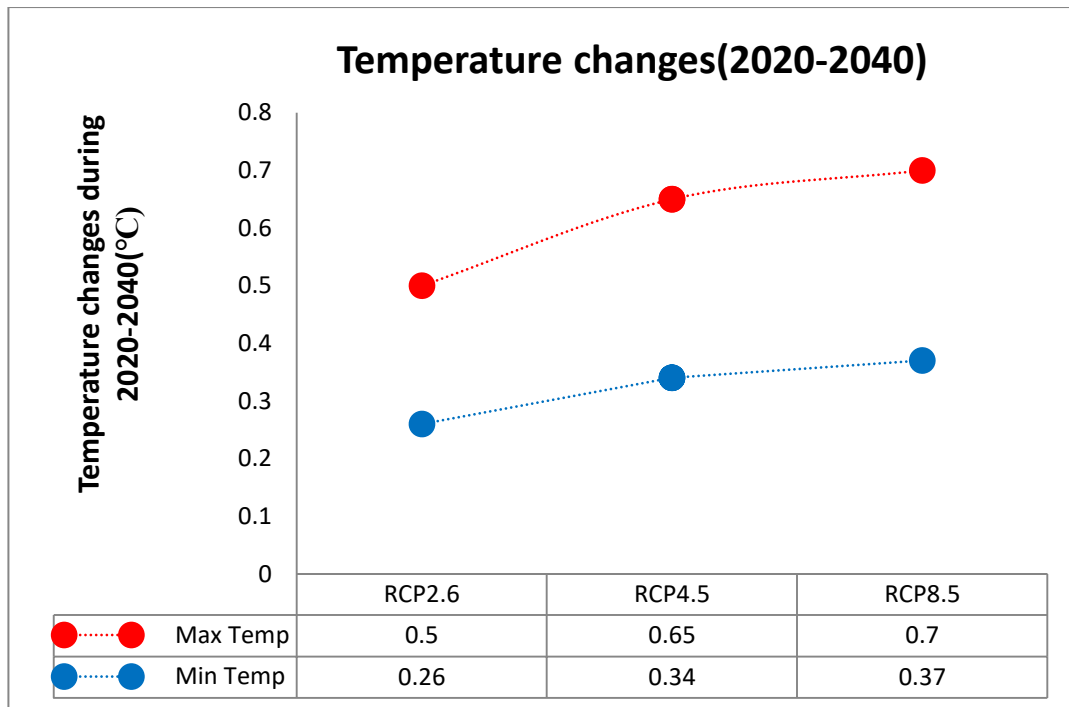


Figure (4-8): Increase in temperatures under different model scenarios for 2040 and 2099.

## 4.2.2 Rainfall

The rainfall downscaling is more complicated than other climate data like temperature, because amount of daily rainfall was relatively poor at individual places. Where, it can be determined by use the predictors of regional scale. Each quantities and events operations of rainfall must specify, as a process of conditional. Unconditional models assume a direct relationship between the local and the global scale predictors for example; local wind speed may be a function of gridded airflow indices such as the zonal or meridional velocity components. Conditional models, like daily rainfall depend on an intermediate parameter, e.g., the probability of a wet-day (Wilby and Dawson, 2013). Figure (4-9) shows the comparison between averages observed and predicted annual rainfall by using the CanESM2 model for verification period (2001–2018).

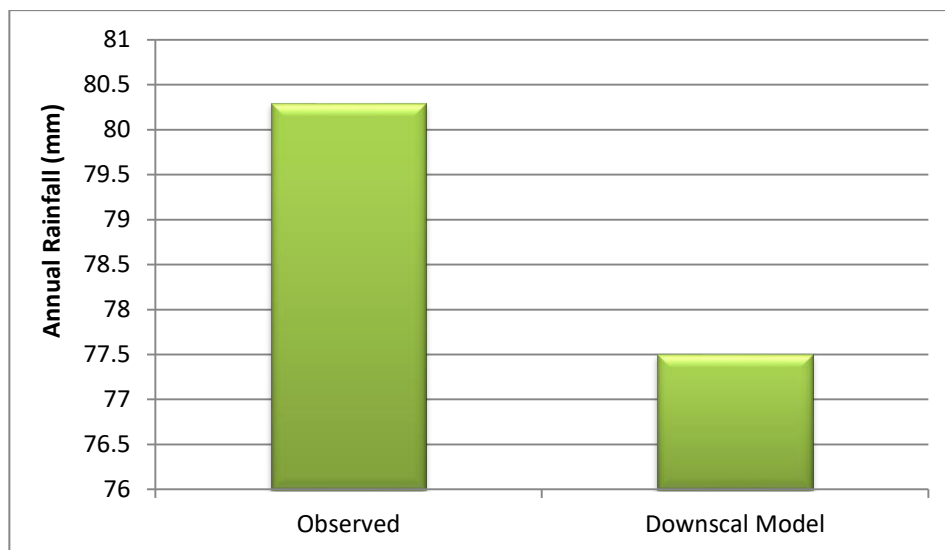


Figure (4-9): Comparison between observed and predicted annual rainfall for verification period (2001–2018).

After verification analysis, the future rainfall can be obtained, in spite of the value of predicted annual rainfall was lower than the observed value. The difference between these value may be due to the various conditional models used to execute the processes of downscale (Wilby et al., 2007). The comparison between the average observed annual rainfall over the period 1979–2018 and the average predicted annual rainfall by scenarios RCP2.6, RCP4.5 and RCP8.5 for near future (2040) and far future (2099) can be shown in Figure (4-10). It can be seen in Figure (4-9) the CanESM2 model under (RCP2.6, RCP4.5 and RCP8.5 scenario) expected a decrease in the annual rainfall rates in both future decades (2040 and 2099). Where, the RCP scenarios focus on greenhouse gas volumes.

The results show that the annual rainfall is expected to be decreased by approximately 6.3%, 10.3% and 23.8% for near future (2040) and decrease by approximately 13.8%, 17.5% and 21.3% for far future (2099) for RCP2.6, RCP4.5 and RCP8.5 scenarios, respectively at future periods (2040 and 2099) when compared to the observed value at 2018. RCP8.5 expected greatest decrease, while RCP2.6 expected smallest decrease.

Figure (4-11) shows the amount of decrease in the rainfall under scenarios RCP2.6, RCP4.5 and RCP8.5 (for CanESM2), for years 2040 and 2099. The results show a decrease between 5mm and 20mm for year 2040, while a decrease between 10mm and 18mm for year 2099.

Climate changes include many parameters, but in this study take only temperature and rainfall because they have greatest effect on groundwater recharge.

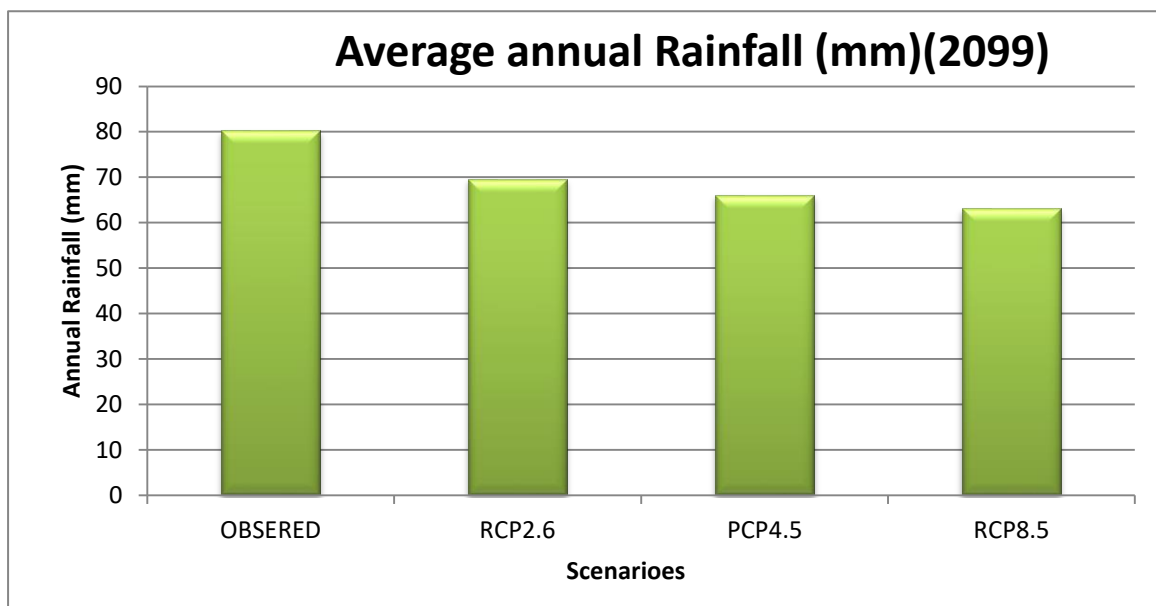
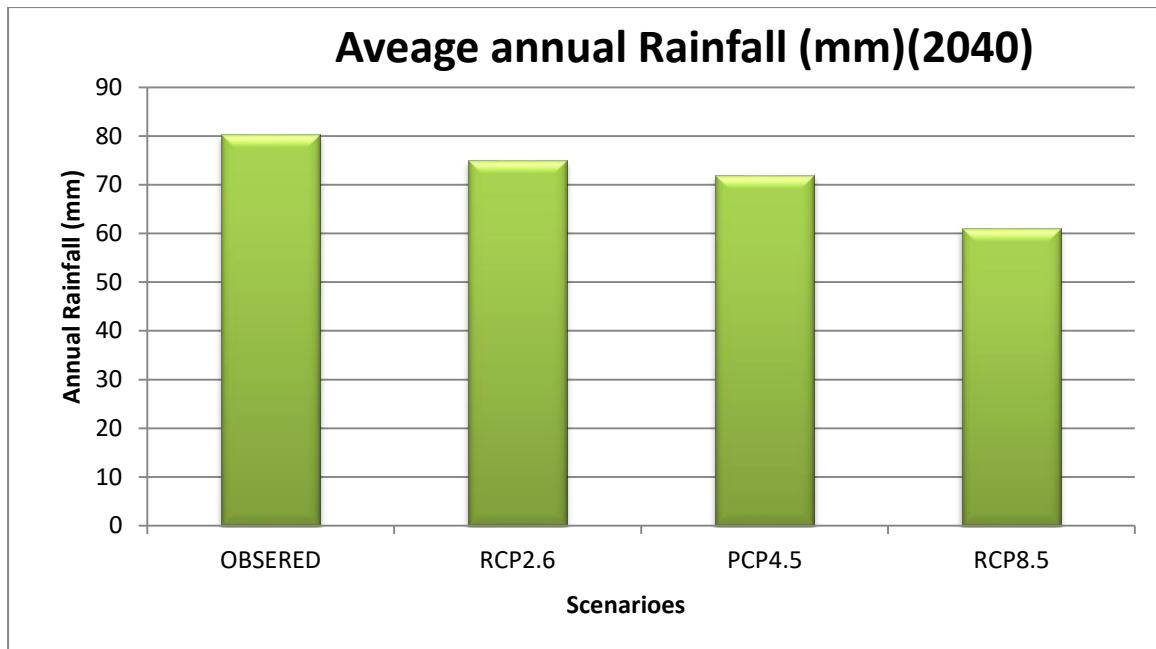


Figure (4-10): Comparison between averages observed annual rainfall (1979–2018) and predict by RCP2.6, RCP4.5 and RCP8.5 scenarios for the years 2040 and 2099.

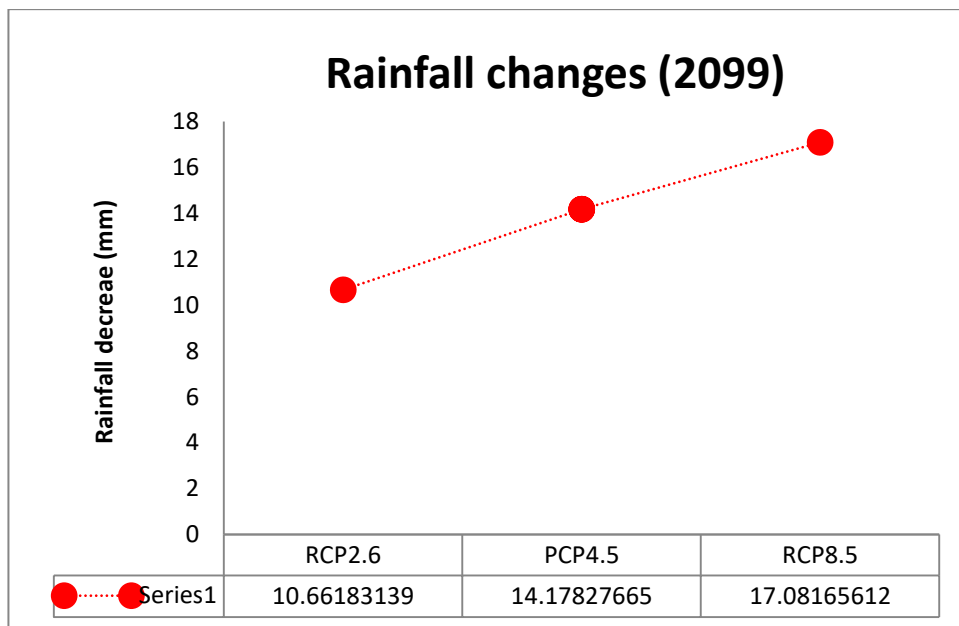
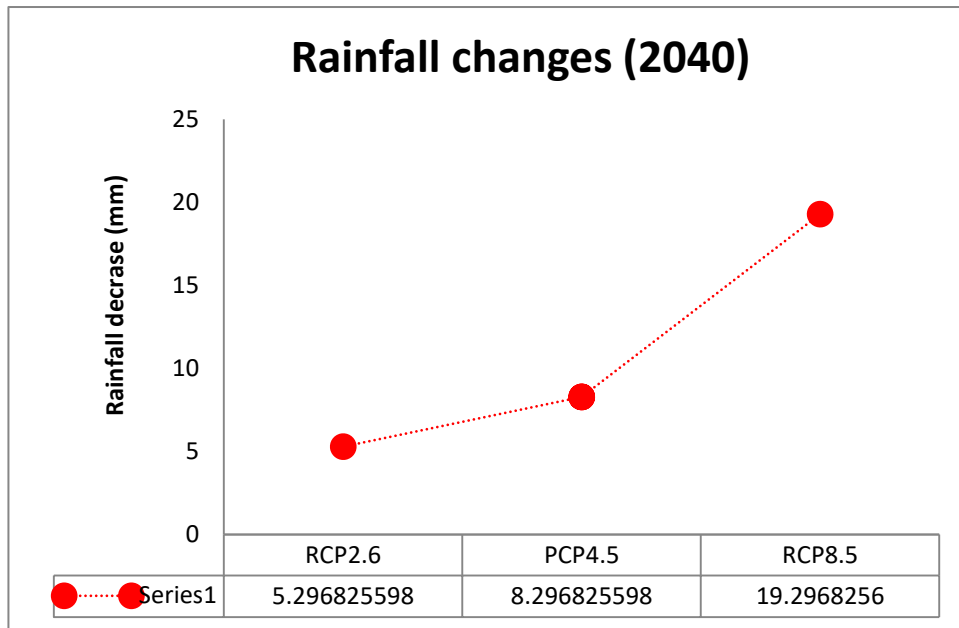


Figure (4-11): Decrease in rainfall under different model scenarios for 2040 and 2099.

## 4.3 Groundwater recharge model

### 4.3.1 Steady-state calibration

The calibration of groundwater steady state was getting by reducing the difference between the observed headwaters and the simulated headwaters. The observed heads were automatically compared with the heads computed by the model. The measured values of headwaters were registered, under interval of confidence (95%) and the observation head interval of 0.5m was selected. The calibration results are displayed as calibration targets as shown in Figure (4-12). Figure (4-13) shows contour map of observed heads before calibration for Dibdibba aquifer.

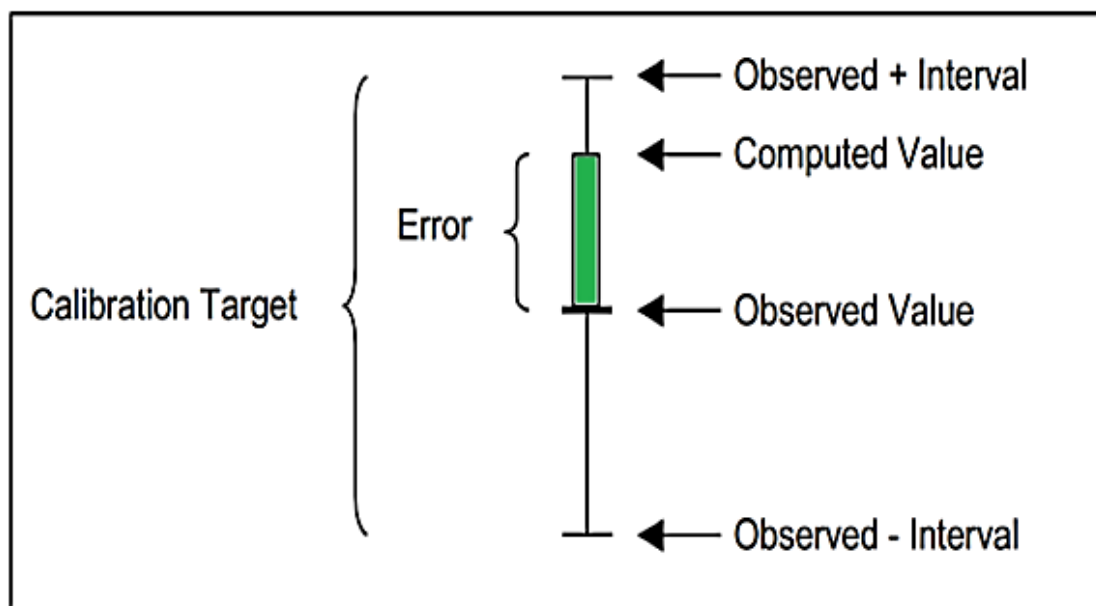


Figure (4- 12): Target of Calibration (Environmental Modeling Research Laboratory, 1999).

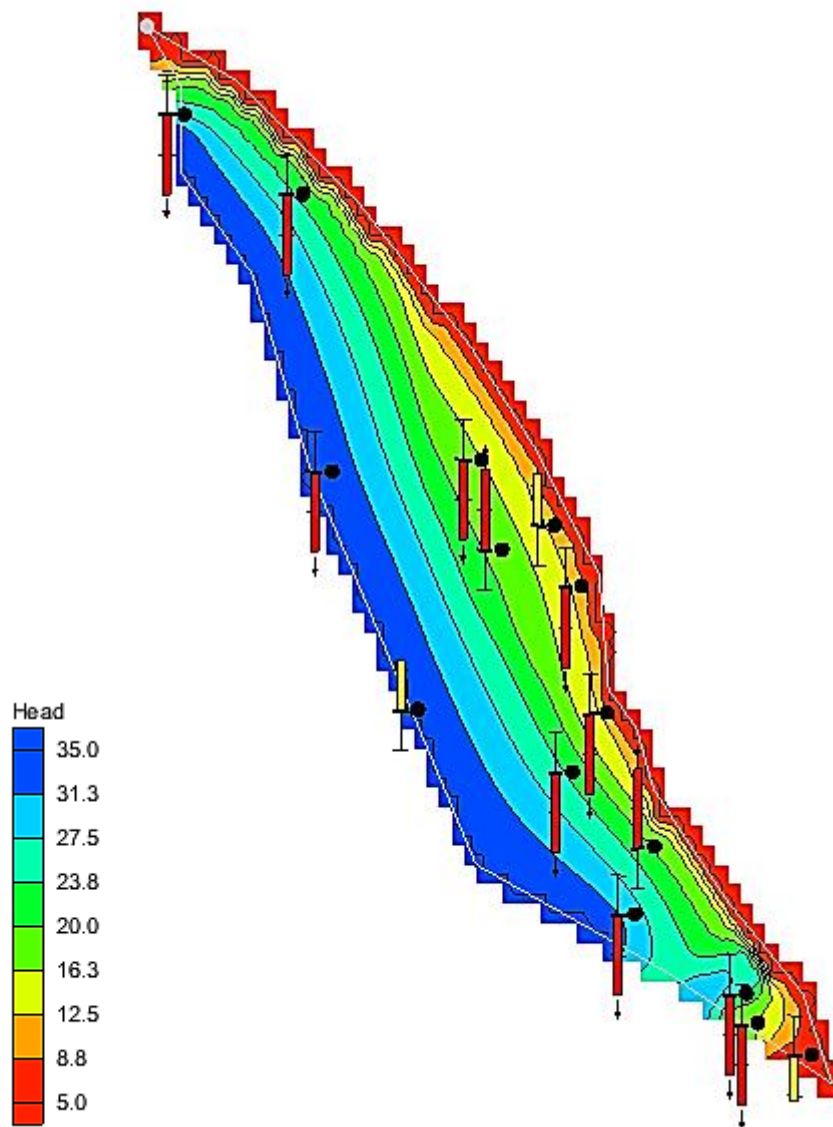


Figure (4- 13): Contour map of observed heads before calibration of Dibdibba aquifer.



The calibration target bottom and top represents value of observed less and plus the interval, respectively. The error can be displayed as full bar; the green color is referring to the error within the specified interval (0.5m or less). The yellow color is referring to the error ranged from 0.5 to 1 m while the red color is referring to the error was greater than 1 m. The aim of the process of calibration was decreasing the error or colored bar.

The results of the calibrated model under the condition of steady state can be abstracted as follows:

1- The computed water heads contour map is shown in Figure (4-14). About 15 of calibration targets were used to represent the water head in the model, 14 bars have green color, and one value exactly likes observed value, indicating that the computed values match with the observed values at an acceptable level of accuracy. Table (4-2) shows the comparison between the observed and computed head values.

Table (4-2): Comparison between observed and computed head values.

No.well	Observed Value (m.a.s.l)	Computed Value (m.a.s.l)	No.well	Observed Value (m.a.s.l)	Computed Value (m.a.s.l)
NO.4	27	27.08	NO.50	23	22.88
NO.16	33	33.48	NO.51	16.5	16.58
NO.24	16	16.17	NO.55	34.5	34.62
NO.27	10.5	10.66	NO.58	6	6.12
NO.29	18.5	18.43	NO.60	22.5	22.64
NO.33	22	21.91	NO.61	19	19.3
NO.40	10	9.65	NO.62	28.5	28.73
NO.41	10.5	10.27			

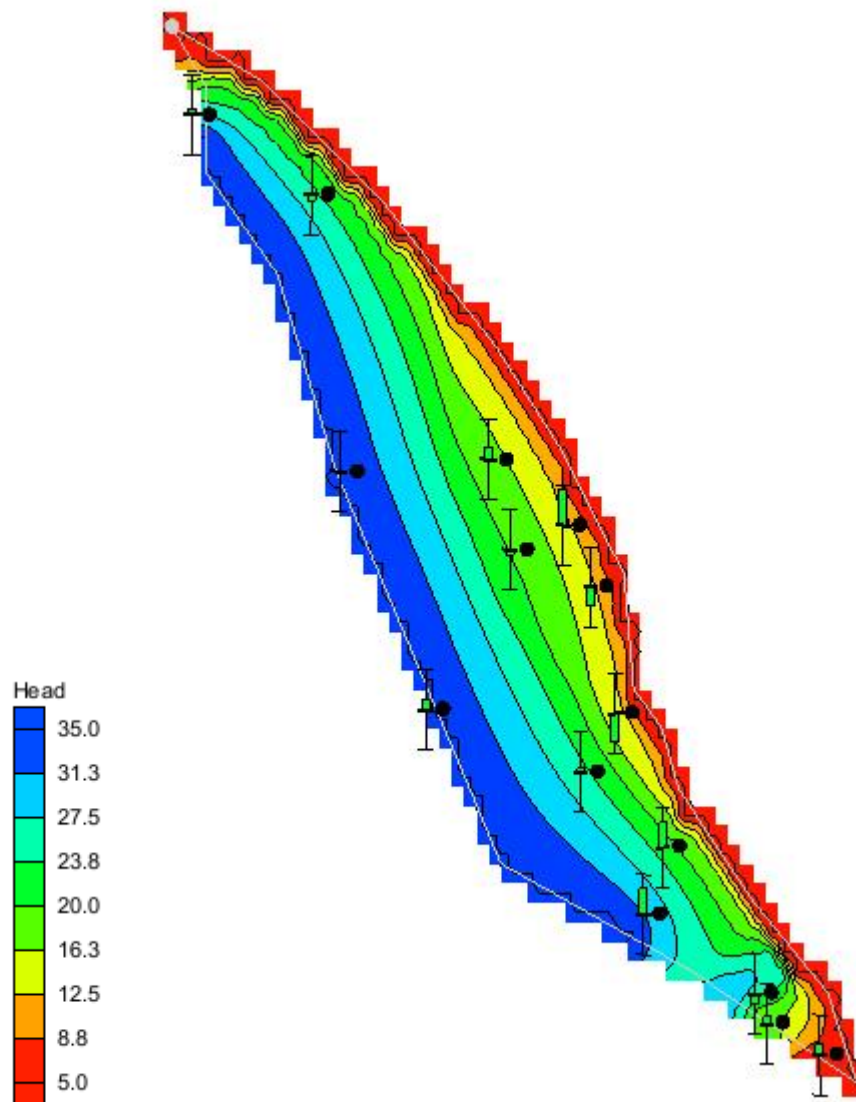


Figure (4-14): Contour map of simulated heads after calibration of Dibdibba aquifer.

2. The correlation between the observed and computed water heads was shown in Figure (4-15). The value of determination coefficient ( $R^2$ ) was found equal to 0.99 that is meaning that there was an excellent fit between the observed and computed values.

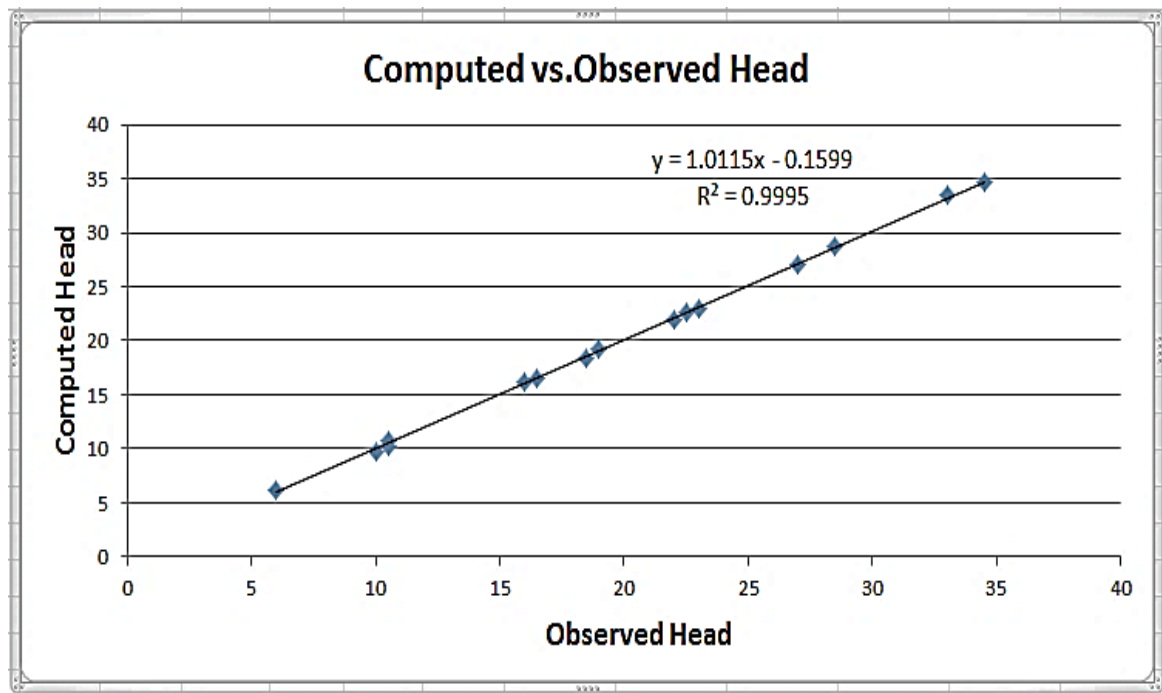


Figure (4- 15): The correlation between the observed and computed water head values.

3. Additionally, an error analysis was shown in Figure (4-16) and table (4-3). The mean error (ME) between observed and computed head was found close to zero (-0.2). Values of the root mean squared error (RMSE) and the mean absolute error (MAE) were low, this means that the model of conceptual and all data used to build the model are acceptable, and can be used to predict the flow of groundwater.

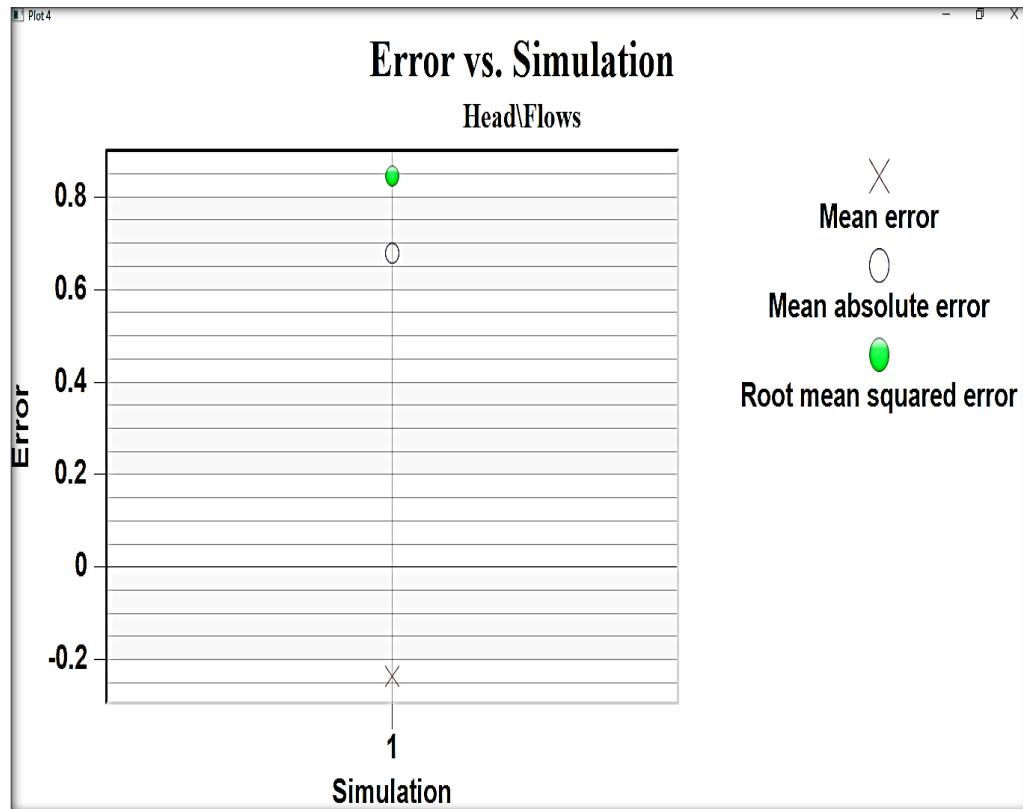


Figure (4-16): Errors analysis for the steady state calibration.

Table (4- 3): Errors value for the steady state calibration.

Criteria of Evaluation	Symbol	Value of error
Mean error (m)	ME	<b>-0.2</b>
Mean absolute error(m)	MAE	<b>0.7</b>
Root mean square error (m)	RMSE	<b>0.85</b>

Depended on calibration model, recharge rate and hydraulic conductivity optimal values were obtained as shown in (Table 4-4). The value of the calibrated hydraulic conductivity for the Dibdibba aquifer is shown in Figure (4-17). The hydraulic conductivity high values were found in the center of the study area in zone HK-20 and HK-30, while the lower value was found in the bottom of the study area in zone HK-60. In the same way, the estimated recharge rate value was 0.00000718 m/d in the identified recharge zone (RCH-100).

Table (4-4): The calibrated hydraulic conductivity and recharge values.

Zone name	HK_10 m/day	HK_20 m/day	HK_30 m/day	HK_40 m/day	HK_50 m/day	HK_60 m/day	HK_70 m/day	HK_80 m/day	RCH_100 m/day
Computed value	10	30	26.96	13.01	10.64	0.1	1.51	15	$7.18 \times 10^{-6}$

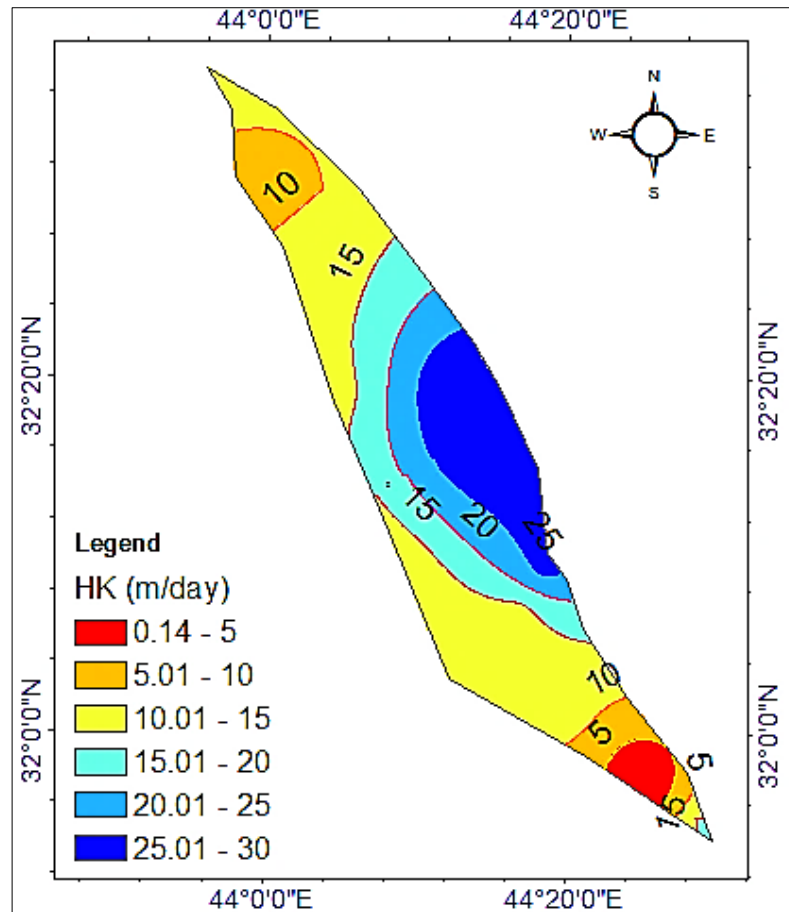


Figure (4-17): Calibrated hydraulic conductivity for the Dibdibba aquifer (m/day).

As well as calculating the optimum values of parameter, PEST also, computes the sensitivities for each parameter as shown in Figure (4-18). The information of sensitivity of parameter is beneficial to determine which the parameters have most significant effect and which have a slightly or no effect on the model. The results show that the model of the study area is sensitive to both recharge and hydraulic conductivity parameters. But the recharge parameter has more significant effect on the model than the hydraulic conductivity parameters.

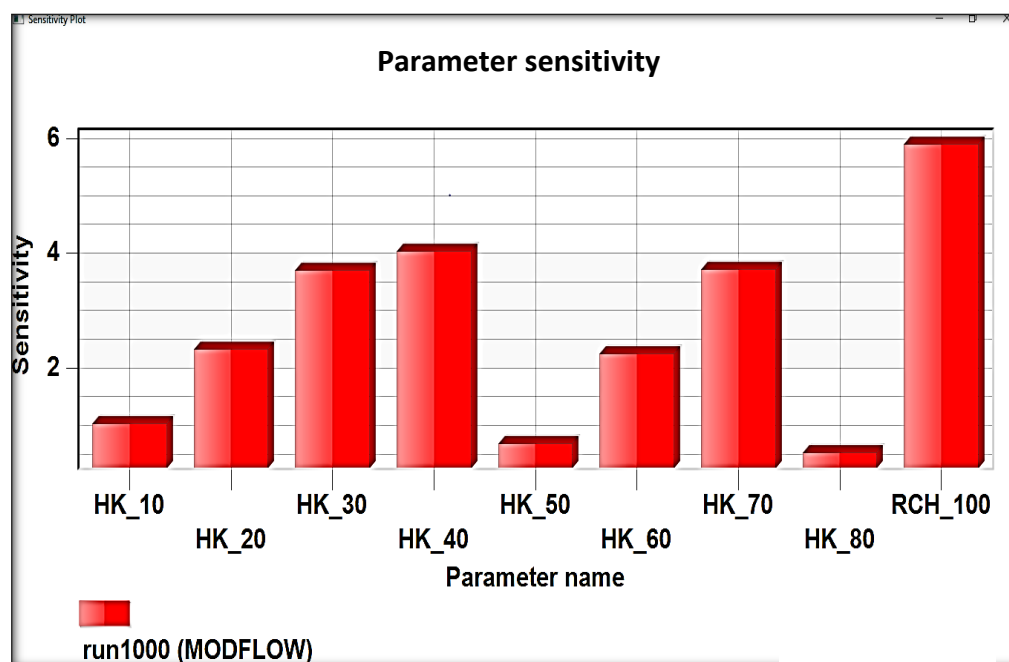


Figure (4- 18): The analysis of sensitivity of parameter.

### 4.3.2 Prediction scenarios

To predict the response of the Dibdibba aquifer system under climate change in the study area, the calibrated model was used to predict future changes in the head under different scenarios. Six scenarios were proposed to investigate the effect of climate change on the study area for the near future 2040 and far future 2099. Before run the model under different scenarios of climate change, the model was run under current observed data in order to show the difference in recharge and heads between the current and future periods (2040 and 2099). Table (4-5) shows the flow budget for current periods (2018).

Table (4- 5): The water budget for the study area (Dibdibba aquifer) under the condition of the year (2018).

Sources/Sinks	Flow In m <sup>3</sup> /day	Flow Out m <sup>3</sup> /day
CONSTANT HEAD	38,929.920	-49,285.840
RECHARGE	41,423.663	0.0
TOTAL FLOW	49,285.836	-49,285.840

### 4.3.2.1 First scenario

The first scenario was RCP2.6 under CanESM2 model which predicted an increase in maximum temperature by about 0.5°C and a decrease in rainfall by about 6.3 % at near future (2040). This change in climate data was applied on Dibdibba aquifer to determine the groundwater recharge. Table (4-6) shows the flow budget predicted at 2040 .The predicted recharge declines by 6.4 % when compared to the current recharge for the study area. This decrease could be due to decreasing in rainfall and increasing in the average temperatures that lead to increase in evaporation that can effect on amount of recharge, also increasing in temperatures may lead to increase groundwater temperatures in aquifers that may also lead to increase the evapotranspiration and the groundwater salinization which effects on quality of groundwater. Figures (4-19) shows the predicted hydraulic head at 2040. The maximum decline in the head when compared with observed values reached more than (1 m) in 14 of obs. Wells. The decreasing of the head reaches between (0.08 to 0.3m) at 2040 when compared with current head.

Table (4- 6): The water budget for the study area (Dibdibba aquifer) under RCP2.6 scenario at 2040.

Sources/Sinks	Flow In m <sup>3</sup> /day	Flow Out m <sup>3</sup> /day
CONSTANT HEAD	39,211.747	-48,952.931
RECHARGE	38,775.577	0.0
Total Source/Sink	48,952.928	-48,952.931
TOTAL FLOW	48,952.928	-48,952.931



Side view

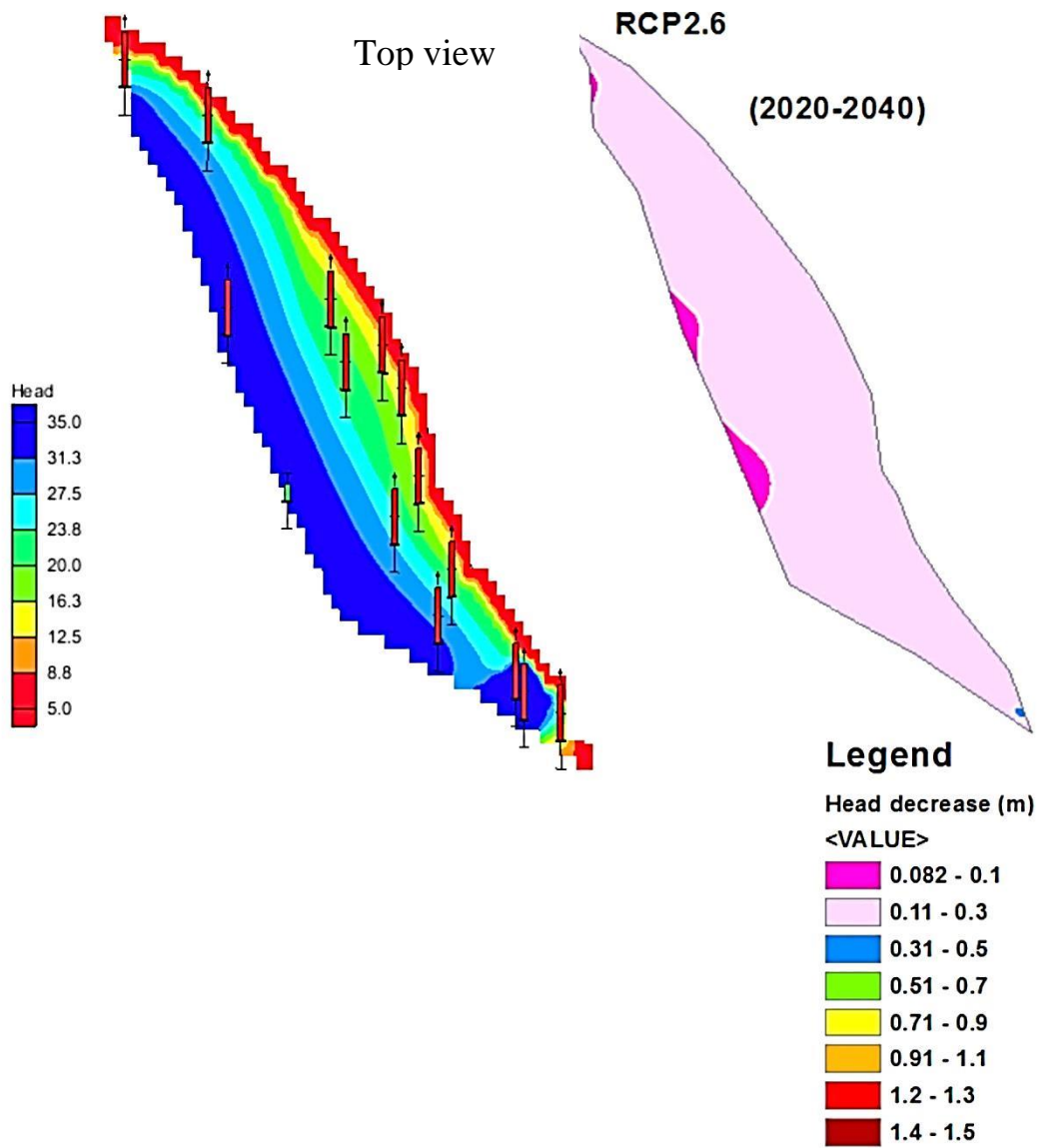
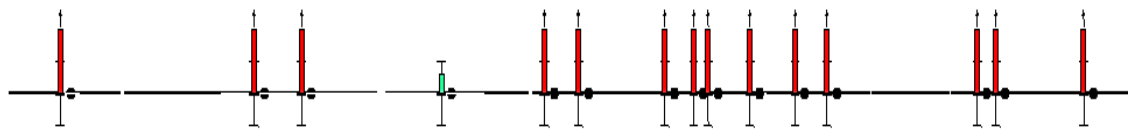


Figure (4-19): The predicted head distribution for the first proposed scenario RCP2.6 at 2040.

### 4.3.2.2 Second scenario

The second scenario was RCP4.5 under CanESM2 model which predicted an increase in maximum temperature by about 0.7°C and a decrease in rainfall by about 10.3 % at near future (2040). This change in climate data applied on Dibdibba aquifer to determine groundwater recharge. Table (4-7) showed the flow budget predicted at 2040 .The predicted recharge decline by 10 % when compared to the current recharge for the study area. This decrease could be due to decreasing in rainfall and increasing in average temperatures that lead to increase in evaporation that can effects on amount of recharge, also increasing in temperatures may lead to increase groundwater temperatures in aquifers that may also lead to increase evapotranspiration and groundwater salinization which effects on quality of groundwater. Figures (4-20) shows the predicted hydraulic head at 2040. The maximum decline in head when compared with observed values reached more than (1 m) in 13 of obs. Wells. The decreasing of the head reaches between (0.1 to 0.5m) at 2040 when compared with the current head.

Table (4-7): The water budget for the study area (Dibdibba aquifer) under RCP4.5 scenario at 2040.

Sources/Sinks	Flow In m <sup>3</sup> /day	Flow Out m <sup>3</sup> /day
CONSTANT HEAD	39,402.442	-48,727.498
RECHARGE	37,262.383	0.0
Total Source/Sink	48,727.495	-48,727.498
TOTAL FLOW	48,727.495	-48,727.498

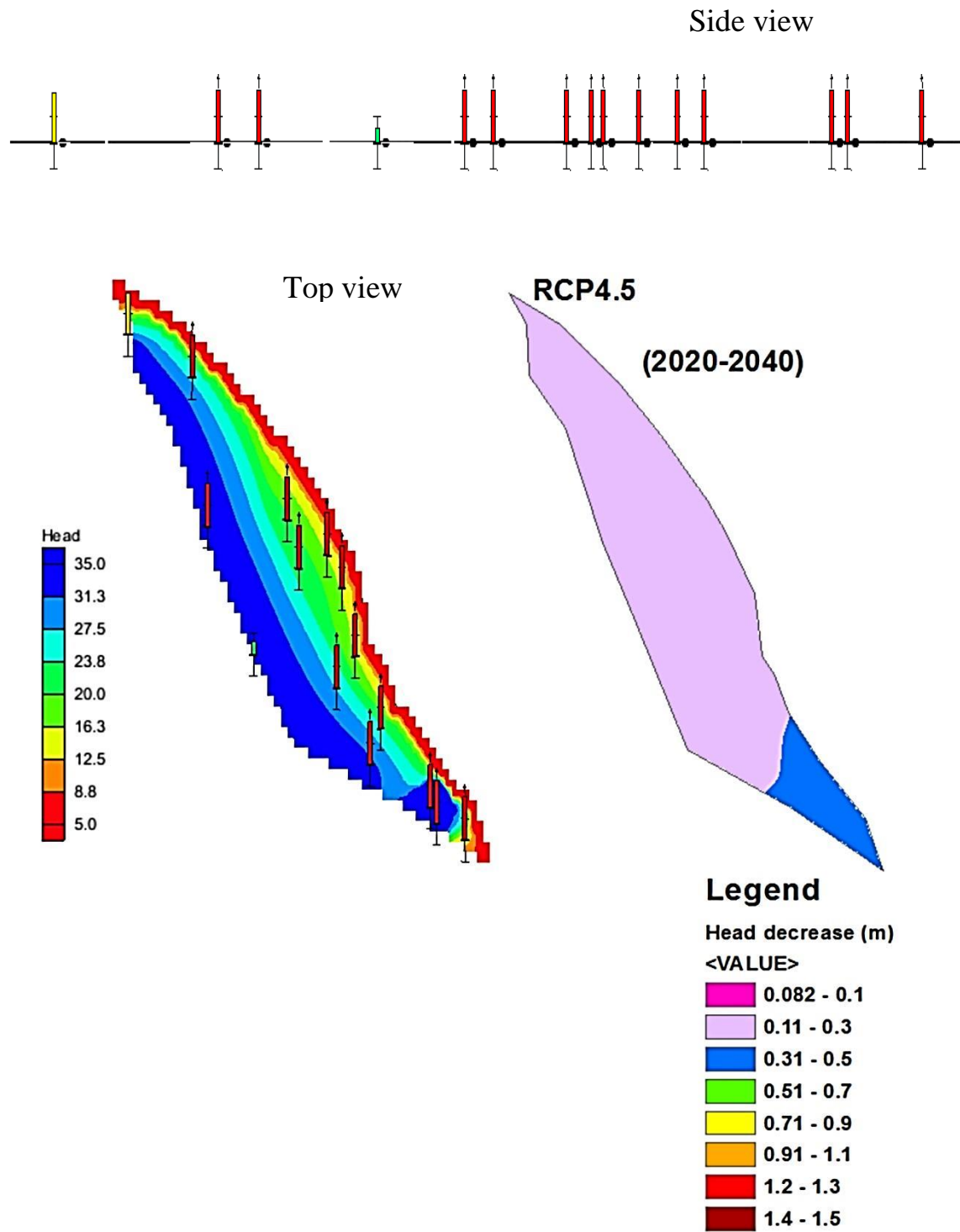


Figure (4- 20): The predicted head distribution for the second proposed scenario RCP4.5at 2040.

### 4.3.2.3 Third scenario

The third scenario was RCP8.5 under CanESM2 model which predicted an increase in maximum temperature by about 0.65°C and a decrease in rainfall by about 23.8 % at near future (2040). This change in climate data applied on Dibdibba aquifer to determine groundwater recharge. Table (4-8) showed the flow budget predicted at 2040 .The predicted recharge decline by 27.6 % when compared with current recharge for the study area. This decrease could be due to decreasing in rainfall and increasing in average temperatures that lead to increase in evaporation that can effects on amount of recharge, also increasing in temperatures may lead to groundwater temperatures in aquifers increase that may also lead to increase evapotranspiration and groundwater salinization which effects on quality of groundwater. Figures (4-21) shows the predicted hydraulic head at 2040. The maximum decline in head when compared with observed values reached more than (1 m) in 11 of obs. Wells. The decreasing of the head reaches between (0.3 to 1.3m) at 2040 when compared to the current head. RCP8.5 expected greatest decrease in head because this scenario predicted greatest increase in temperature and greatest decrease in rainfall at 2040.

Table (4-8): The water budget for the study area (Dibdibba aquifer) under RCP8.5 scenario at 2040.

Sources/Sinks	Flow In m <sup>3</sup> /day	Flow Out m <sup>3</sup> /day
CONSTANT HEAD	40,777.034	-47,098.420
RECHARGE	29,980.143	0.0
Total Source/Sink	47,098.399	-47,098.420
TOTAL FLOW	47,098.399	-47,098.420

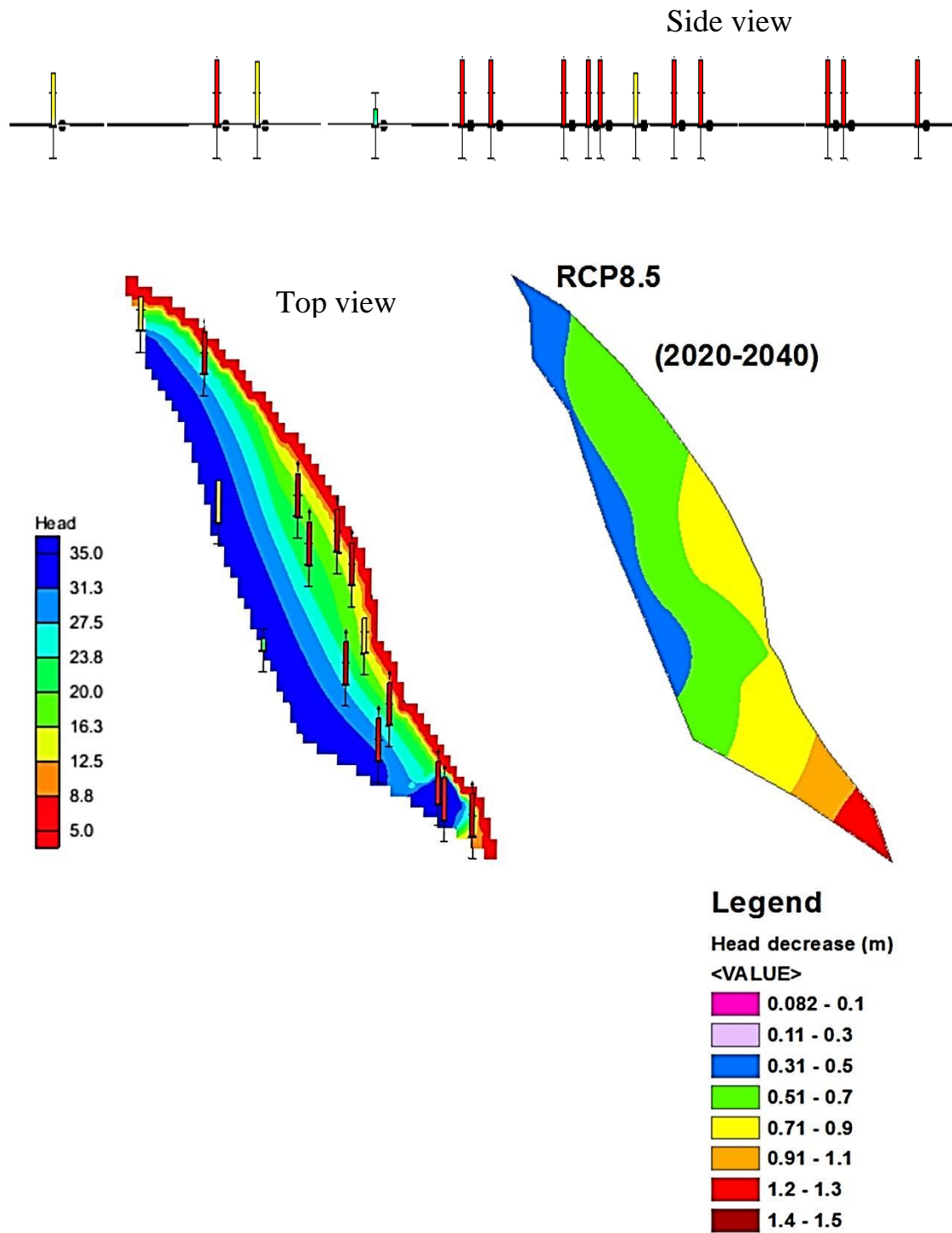


Figure (4- 21): The predicted head distribution for the third proposed scenario RCP8.5 at 2040.

#### 4.3.2.4 Fourth scenario

The fourth scenario was RCP2.6 under CanESM2 model which predicted an increase in maximum temperature by about 0.5 °C and a decrease in rainfall by about 13.8% at far future (2099). This change in climate data applied on Dibdibba aquifer to determine groundwater recharge. Table (4-9) showed the flow budget predicted at 2099 .The predicted recharge decline by 13.6% when compared with current recharge for the study area. This decrease could be due to decreasing in rainfall and increasing in average temperatures that lead to increase in evaporation that can effects on amount of recharge, also increasing in temperatures may lead to groundwater temperatures in aquifers increase that may also lead to increase evapotranspiration and groundwater salinization which effects on quality of groundwater. Figures (4-22) shows the predicted hydraulic head at 2099. The maximum decline in head when compared with observed values reached more than (1 m) in 13 of obs. Wells. The decreasing of the head reaches between (0.1 to 0.7m) at 2099 when compared to the current head.

Table (4- 9): The water budget for the study area (Dibdibba aquifer) under RCP2.6 scenario at 2099.

Sources/Sinks	Flow In m <sup>3</sup> /day	Flow Out m <sup>3</sup> /day
CONSTANT HEAD	39,541.090	-48,563.505
RECHARGE	35,749.1915	0.0
Total Source/Sink	48,563.504	-48,563.505
TOTAL FLOW	48,563.504	-48,563.505

Side view

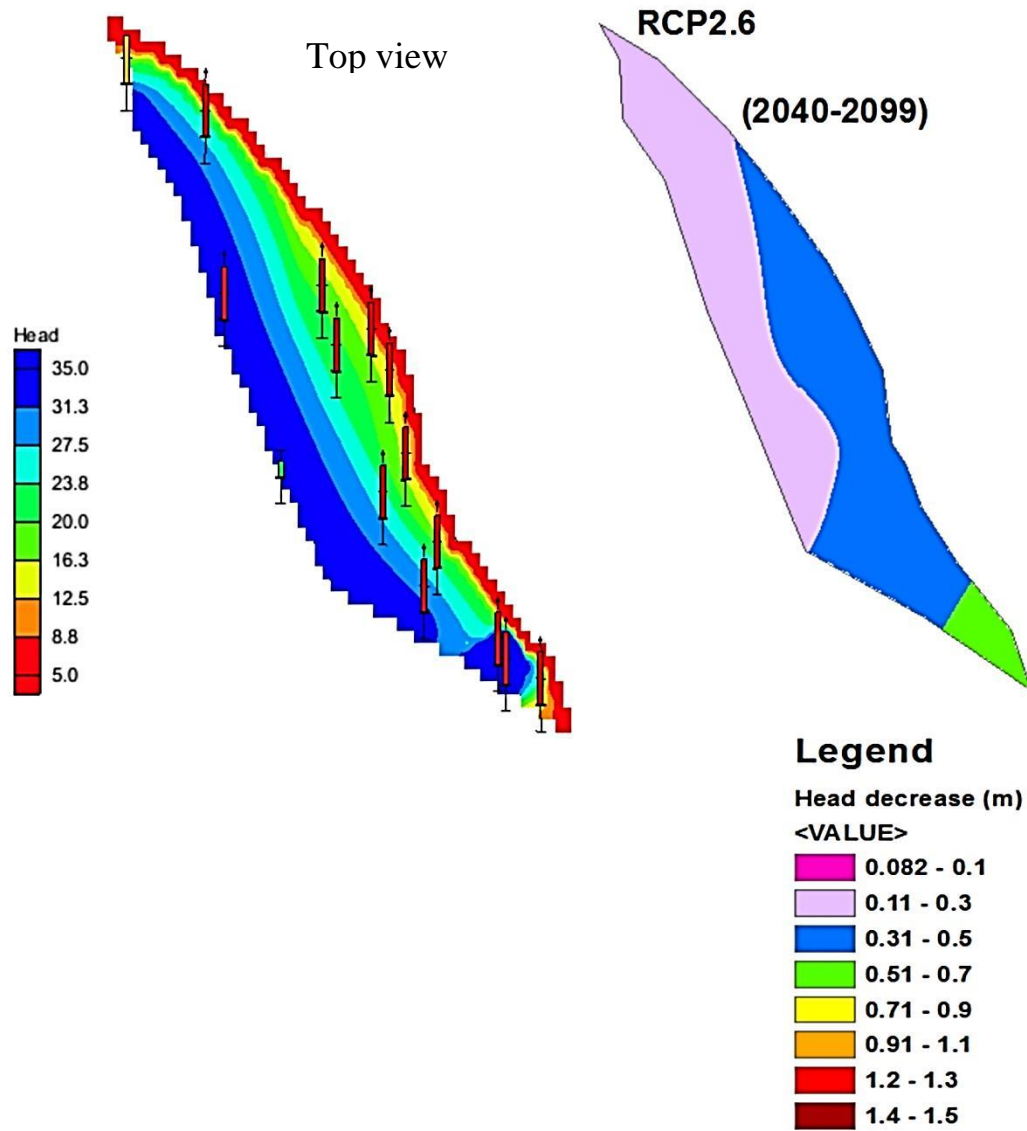
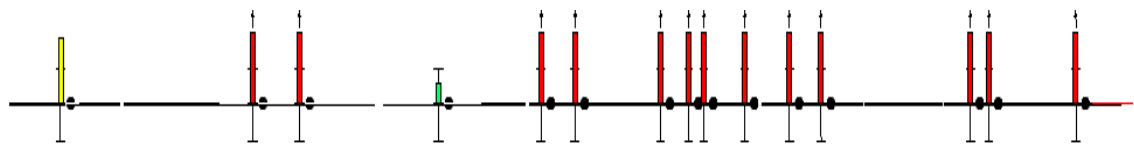


Figure (4- 22): The predicted head distribution for the fourth proposed scenario RCP2.6 at 2099.

### 4.3.2.5 Fifth scenario

The fifth scenario was RCP4.5 under CanESM2 model which predicted an increase in maximum temperature by about 0.68 °C and a decrease in rainfall by about 17.5% at far future (2099). This change in climate data applied on Dibdibba aquifer to determine groundwater recharge. Table (4-10) showed the flow budget predicted at 2099. The predicted recharge decline by 17.6% when compared with current recharge for the study area. This decrease could be due to decreasing in rainfall and increasing in average temperatures that lead to increase in evaporation that can effects on amount of recharge, also increasing in temperatures may lead to groundwater temperatures in aquifers increase that may also lead to increase evapotranspiration and groundwater salinization which effects on quality of groundwater. Figures (4-23) shows the predicted hydraulic head at 2099. The maximum decline in head when compared with observed values reached more than (1 m) in 12 of obs. Wells. The decreasing of the head reaches between (0.1 to 0.9m) at 2099 when compared with current head.

Table (4- 10): The water budget for the study area (Dibdibba aquifer) under RCP4.5 scenario at 2099.

Sources/Sinks	Flow In m <sup>3</sup> /day	Flow Out m <sup>3</sup> /day
CONSTANT HEAD	39,753.327	-48,312.325
RECHARGE	34,141.423	0.0
Total Source/Sink	48,312.325	-48,312.325
TOTAL FLOW	48,312.325	-48,312.325



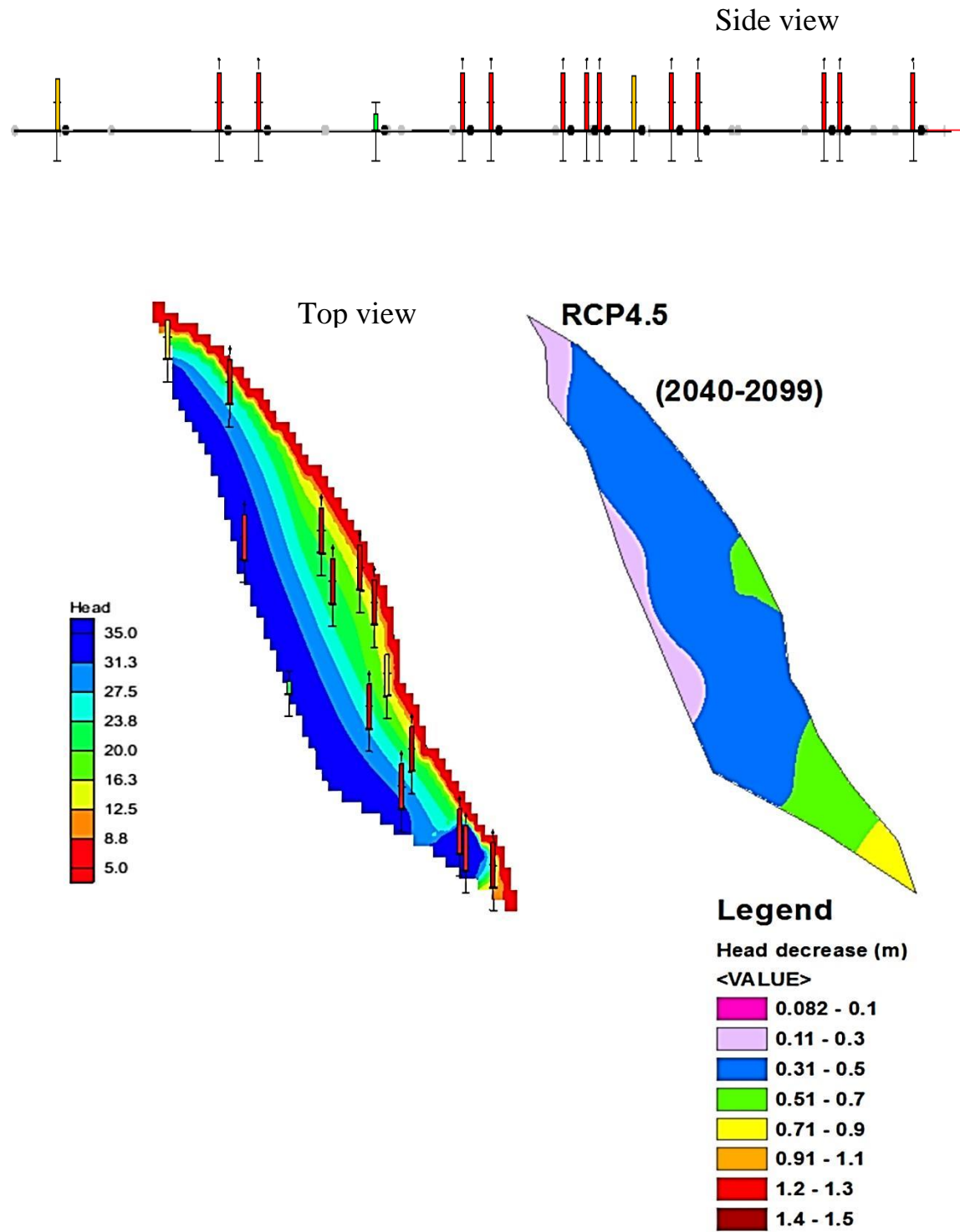


Figure (4- 23): The predicted head distribution for the fifth proposed scenario RCP4.5 at 2099.

#### 4.3.2.6 Sixth scenario

The sixth scenario was RCP8.5 under CanESM2 model which predicted an increase in maximum temperature by about 1.07 °C and a decrease in rainfall by about 21.3% at far future (2099). This change in climate data applied on Dibdibba aquifer to determine groundwater recharge. Table (4-11) showed the flow budget predicted at 2099 .The predicted recharge decline by 25.3% when compared with current recharge for the study area. This decrease could be due to decreasing in rainfall and increasing in average temperatures that lead to increase in evaporation that can effects on amount of recharge, also increasing in temperatures may lead to groundwater temperatures in aquifers increase that may also lead to increase evapotranspiration and groundwater salinization which effects on quality of groundwater. Figures (4-24) shows the predicted hydraulic head at 2099. The maximum decline in head when compared with observed values reached more than (1 m) in 11 of obs. Wells. The decreasing of the head reaches between (0.3 to 1.3m) at 2099 when compared with current head. RCP8.5 expected a greatest decrease in head because this scenario predicted a greatest increase in temperature and greatest decrease in rainfall at 2099.

Table (4- 11): The water budget for the study area (Dibdibba aquifer) under RCP8.5 scenario at 2099.

Sources/Sinks	Flow In m <sup>3</sup> /day	Flow Out m <sup>3</sup> /day
CONSTANT HEAD	40,683.660	-47,209.328
RECHARGE	30,925.888	0.0
Total Source/Sink	47,209.306	-47,209.328
TOTAL FLOW	47,209.306	-47,209.328

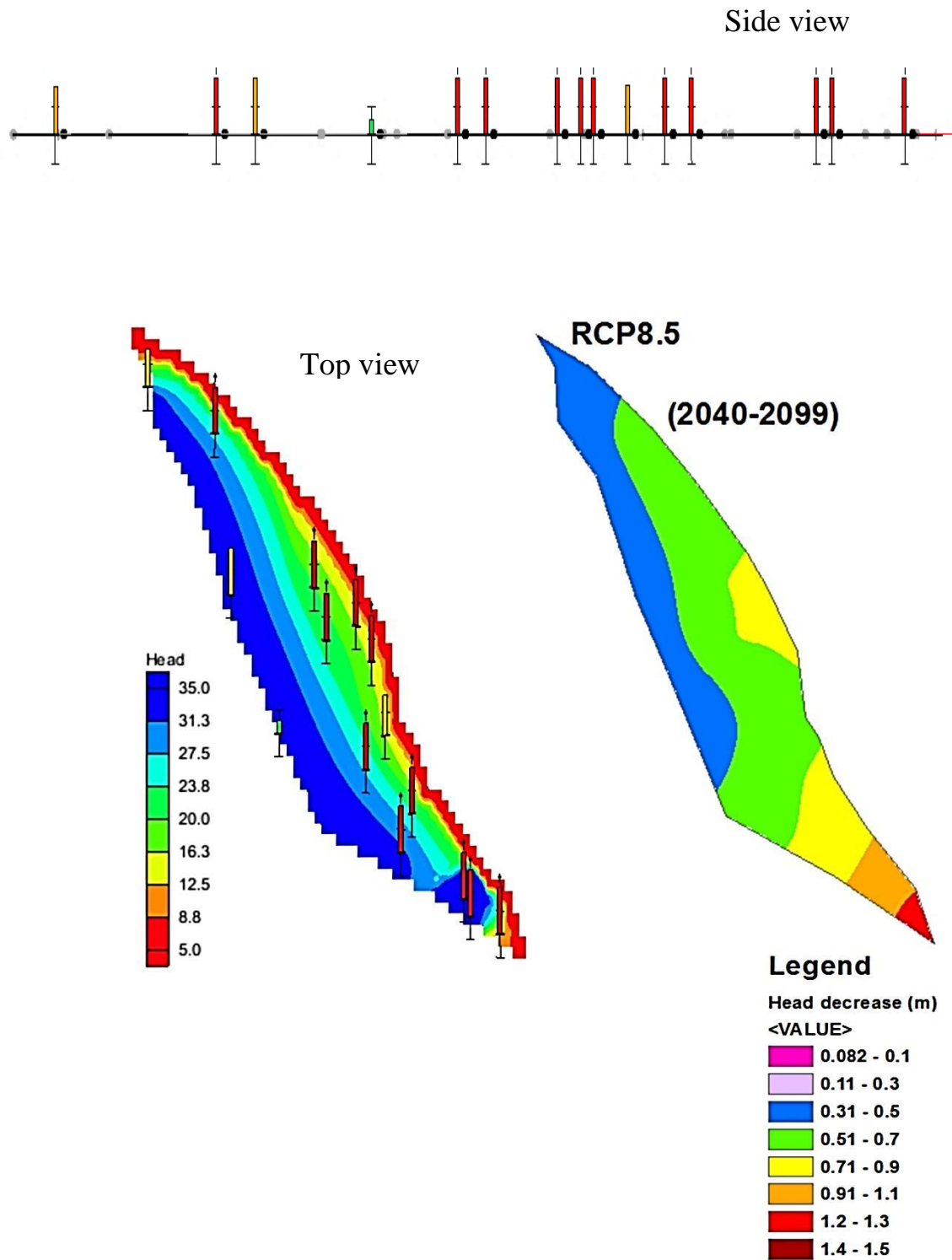


Figure (4- 24): The predicted head distribution for the sixth proposed scenario RCP8.5 at 2099.

The results of six scenarios can be summaries as shown in table (4-12 and 4-13) below:

Table (4-12): Analysis of groundwater recharge under different scenarios of climate change at near future (2040).

Near future (2040)				
scenarios	Increase in Temperature (°C)	Decrease in rainfall%	Decrease in Recharge%	Recharge (mm)/yr.
RCP2.6	0.5	6.3%	6.4%	12.8
RCP4.5	0.7	10.3%	10%	12.36
RCP8.5	0.65	23.8%	27.6%	9.94

This table shows changes of the groundwater recharge for the near future (2040), where the annual recharge will be about 9 mm to 13 mm in the Dibdibba aquifer. The greatest decrease in the recharge of groundwater is found under RCP8.5 scenario of about 27.6% where the recharge will be about 9.94 mm/yr. because this scenario predicted a greatest increase in the temperature and a greatest decrease in rainfall among all other scenarios that lead to increase in evaporation that can effects on amount of recharge. The lowest decrease in the groundwater recharge is found under RCP2.6 scenario of about 6.4 % where the recharge will be about 12.8 mm/yr. because this scenario predicted smallest increase in temperature and rainfall which effects on the amount of recharge.

Table (4-13): Analysis of groundwater recharge under different scenarios of climate change at far future (2099).

Far future (2099)				
scenarios	Increase in Temperature (°C)	Decrease in rainfall%	Decrease in Recharge%	Recharge (mm)/yr.
RCP2.6	0.5	13.8%	13.6%	11.86
RCP4.5	0.68	17.5%	17.6%	11.3
RCP8.5	1.07	21.3%	25.3%	10.26

This table shows changes of the groundwater recharge for the far future (2099), where the annual recharge will be about 10.3 mm to 11.8 mm in the Dibdibba aquifer. The greatest decrease in the recharge of groundwater is found under RCP8.5 scenario of about 25.3% where the recharge will be about 10.3 mm/yr. because this scenario predicted greatest increase in temperature and a greatest decrease in rainfall among all other scenarios that lead to increase in evaporation that can effects on amount of recharge. The lowest decrease in the groundwater recharge is found under RCP2.6 scenario approximately 13.6% where the recharge will be about 11.86 mm/yr. because this scenario predicted smallest increase in temperature and rainfall which effects on the amount of recharge.

## Chapter Five

# CONCLUSIONS AND RECOMMENDATIONS

### 5.1 Introduction

This research was conducted to study the effect of climate change on major climate data (rainfall, and temperature) for the next 20 and 79 years. The expected climate data can be applied on the study area by using GMS model to estimate the groundwater recharge.

### 5.2 Conclusions

The conclusions depended on the results can be summarized below:

1. The calibration of the SDSM model was very good where the validation results show that mean error (ME) for CanESM2 model are very close to zero (0.0027 to 0.0106). The coefficient of determination ( $R^2$ ) for CanESM2 model was (0.877 to 0.905).
2. The temperature increases between (0.5°C to 0.7°C) (for maximum temperature) and between (0.2°C to 0.4°C) (for minimum temperature) for near future (2040).
3. The temperature increases between (0.5°C to 1.07°C) (for maximum temperature) and between (0.2°C to 0.7°C) (for minimum temperature) for far future (2099).
4. The scenario RCP8.5 was predicted the greatest increase in the average annual maximum and minimum temperature by about 32.7°C (for maximum temperature) and 18.5°C (for minimum temperature) for near future (2040).

5. The scenario RCP8.5 was predicted the greatest increase in the average annual maximum and minimum temperature by about 33°C (for maximum temperature) and 18.8°C (for minimum temperature) for far future (2099).
6. The scenario RCP2.6 was predicted the smallest increase in the average annual maximum and minimum temperature by about 32.4°C (for maximum temperature) and 18.3°C (for minimum temperature) for both near and far future (2040 and 2099).
7. For rainfall, (CanESM2) model under (RCP2.6, RCP4.5 and RCP8.5 scenario) expected a decrease in the annual rainfall rates by approximately 6.3%, 10.3% and 23.8%, respectively for near future (2020 -2040).
8. For rainfall, (CanESM2) model under (RCP2.6, RCP4.5 and RCP8.5 scenario) expected a decrease in the annual rainfall rates by approximately 13.8%, 17.5% and 21.3%, respectively for far future (2040 -2099).
9. The correlation between the observed and computed piezometric heads in GMS model was excellent ( $R^2$  was 0.99). In addition, the validation results show that the mean error (ME) was close to zero (-0.2), and there is a relatively value of MAE, and RMSE.
10. The model of the study area is sensitive to both recharge and hydraulic conductivity parameters. But the recharge parameter has more significant effect on the model than hydraulic conductivity parameters.
11. For near future (2040), the first three predictand scenarios of the groundwater recharge show recharge was declined by 6.4 %, 10%, and 27.6%, under RCP2.6, RCP4.5, and RCP8.5 scenarios, respectively.

12. For far future (2099), the last three predictand scenarios of the groundwater recharge show that the recharge was decline by 13.6 %, 17.6%, and 25.3%, under scenarios RCP2.6, RCP4.5, and RCP8.5 respectively.
13. The greatest decrease of groundwater recharge is obtained under scenario RCP8.5 for both near and far future (2040 and 2099).

### **5.3 Recommendations**

1. Making artificial recharge plans in order to increase the charging of groundwater.
2. Establishing rainwater harvesting projects in order to use rainwater in the recharge of groundwater.
3. Reducing the greenhouse gas emissions and transforming its energy to clean energy in order to decrease the effects of climate change during the coming period.
4. Planting trees (afforestation) in order to minimize the global warming.

### **5.4 Recommendations for future studies**

1. Using another models to analysis the climate change to predict future climate data.
2. Taking another case study in the region.
3. Studying the effect of COVID 19 virus on climate change.



## References

- ABBASNIA, M., TAVOUSHI, T. & KHOSRAVI, M. J. A.-P. J. O. A. S. 2016. Assessment of future changes in the maximum temperature at selected stations in Iran based on HADCM3 and CGCM3 models. 52, 371-377.
- ABBASPOUR, K. C., FARAMARZI, M., GHASEMI, S. S. & YANG, H. J. W. R. R. 2009. Assessing the impact of climate change on water resources in Iran. 45.
- AIDI, Z. & HASSANI, A. 2013. Groundwater modeling of Khash aquifer and predicting effect of artificial-recharge project on the groundwater level.
- AL-FATLAWI, A. N. J. E. J. O. A. S. 2011. The application of the mathematical model (MODFLOW) to simulate the behavior of groundwater flow in Umm Er Radhuma unconfined aquifer. 3, 1-16.
- AL-HASSOUN, S. A., MOHAMMAD, T. A. J. P. J. S. & TECHNOL 2011. Prediction of water table in an alluvial aquifer using modflow. 19, 45-55.
- AL-KHARABSHEH, A. J. J. O. A. E. 2000. Ground-water modelling and long-term management of the Azraq basin as an example of arid area conditions (Jordan). 44, 143-153.
- AL-KUBAISI, Q. Y., AL-ABADI, A. M & .AL-GHANIMY, M. A. J. I. J. O. S. 2018. Mapping groundwater quality Index for irrigation in the Dibdibba aquifer at Karbala-Najaf plateau, central of Iraq. 1636-1652.
- AL-MUQDADI, S. W. & MERKEL, B. J. J. I. J. O. G. 2012. Interpretation of groundwater flow into fractured aquifer. 3, 357-364.
- AL-MUSSAWI, W. H. J. J. O. K. U. 2008. Kriging of Groundwater Level-A Case Study of Dibdiba Aquifer in Area of Karballa-Najaf. 6, 170-182.
- AL-MUSSAWY, W. & KHALAF, R. J. P. D. T. 2013. Optimum management models for groundwater use in Karbala desert area.
- Al-Tae T. M. and Al- Sadiq A. A., 2003, "A considerable model for determining groundwater movement trends and estimating quantities in the Sulayfani plain, north of the Mosul Dam lake", Journal of Damascus University, Vol.20, 2nd Issue, (in Arabic).
- ANDERSON, M., WOESSNER, W. & HUNT, R. J. A. P. I., SAN DIEGO, CA. JOURNAL OF HYDROLOGY 1992. Applied groundwater modeling: Simulation of flow and advective transport. 140, 393-395.
- ANDERSON, M. P., WOESSNER, W. W & .HUNT, R. J. 2015. *Applied groundwater modeling: simulation of flow and advective transport*, Academic press.

- BROUYÈRE, S., CARABIN, G. & DASSARGUES, A. J. H. J. 2004. Climate change impacts on groundwater resources: modelled deficits in a chalky aquifer, Geer basin, Belgium. 12, 123-134.
- DOHERTY, J. E., HUNT, R. J. & TONKIN, M. J. J. U. G. S. S. I. R. 2010. Approaches to highly parameterized inversion: A guide to using PEST for model-parameter and predictive-uncertainty analysis. 5211, 71.
- EVANS, J. P. J. C. C. 2009. 21st century climate change in the Middle East. 92, 417-432.
- Environmental Modeling Research Laboratory (EMRL) of Brigham Young University (2000): Groundwater Modeling System (GMS 10.1), Tutorial Manual. ([www.aquaveo.com/software/gms](http://www.aquaveo.com/software/gms))
- FLATO, G., MAROTZKE, J., ABIODUN, B., BRACONNOT, P., CHOU, S. C., COLLINS, W., COX, P., DRIOUECH, F., EMORI, S. & EYRING, V. 2014. Evaluation of climate models. *Climate change 2013 :the physical science basis. Contribution of Working Group I to the Fifth Assessment Report of the Intergovernmental Panel on Climate Change*. Cambridge University Press.
- GURWIN, J. & LUBCZYNSKI, M. J. H. J. 2005. Modeling of complex multi-aquifer systems for groundwater resources evaluation—Swidnica study case (Poland). 13, 627-639.
- HASHEMI, H., UVO, C. B., BERNDTSSON, R. J. H. & SCIENCES, E. S. 2015. Coupled modeling approach to assess climate change impacts on groundwater recharge and adaptation in arid areas. 19, 4165-4181.
- Hussain N. M., 2008, "Simulation of Flow of Groundwater in Karbala City", M.Sc. Thesis, College of Engineering, University of Babylon, Iraq.
- Hassan, W.H., 2020. Climate Change Impact on Groundwater Recharge of Umm ER Raduma Unconfined Aquifer Western Desert, Iraq. *International Journal of Hydrology Science and Technology*, 10(4):392-412, DOI: 10.1504/IJHST.2020.10021823.
- Hassan Janabi. 2013,Climate Change Impact on Iraqi Water and Agriculture Sectors,Iraqieconomists.net.10,08.
- Intergovernmental Panel on Climate Change (IPCC) (2007) *Climate Change: The Physical Science Basis, Contribution of Working Group I to the Fourth Assessment, Report of the Intergovernmental Panel on Climate Change*, Cambridge University Press. Cambridge, UK.
- KAHSAY, K. D., PINGALE, S. M. & HATIYE, S. D. J. G. F. S. D. 2018. Impact of climate change on groundwater recharge and base flow in the sub-catchment of Tekeze basin, Ethiopia. 6, 121-133.

- KAREEM, H. 2018. *Study of water resources by using 3D groundwater modelling in Al-Najaf region, Iraq*. Cardiff University.
- KRESIC, N. 2006. *Hydrogeology and groundwater modeling*, CRC press.
- KRESIC, N. & MIKSZEWSKI, A. 2012. *Hydrogeological conceptual site models: data analysis and visualization*, CRC press.
- LEMKE, P., REN, J., ALLEY, R., ALLISON, I., CARRASCO, J., FLATO, G., FUJII, Y., KASER, G., MOTE, P. & THOMAS, R. J. C. U. P. U., CAMBRIDGE 2007. Observations: changes in snow, ice and frozen ground, climate change 2007: The physical science basis .Contribution of working group I to the fourth assessment report of the intergovernmental panel on climate change. 337-383.
- LIU, H.-H. J. J. O. H. 2011. Impact of climate change on groundwater recharge in dry areas: An ecohydrology approach. 407, 175-183.
- MARNANI, S. A., CHITSAZAN, M., MIRZAEI, Y. & JAHANDIDEH, B. J. A. J. O. G. 2010. Groundwater Resources Management in Various Scenarios Using Numerical Model. 1.
- MCDONALD, M. G. & HARBAUGH, A. W. 1988. *A modular three-dimensional finite-difference ground-water flow model*, US Geological Survey.
- OSMAN, Y., ABDELLATIF, M., AL-ANSARI, N., KNUTSSON, S. & JAWAD, S. J. J. O. E. H. 2017. Climate change and future precipitation in an arid environment of the MIDDLE EAST: CASE study of Iraq. 25.
- OUDE ESSINK, G., VAN BAAREN, E. S. & DE LOUW, P. G. J. W. R. R. 2010. Effects of climate change on coastal groundwater systems: A modeling study in the Netherlands. 46.
- PARRY, M. L., CANZIANI, O. F., PALUTIKOF, J. P., VAN DER LINDEN, P. J. & HANSON, C. E. J. C. U.-V. P., CAMBRIDGE, UK 2007. IPCC, 2007: climate change 2007: impacts, adaptation and vulnerability. Contribution of working group II to the fourth assessment report of the intergovernmental panel on climate change.
- PATHAK, H., AGGARWAL, P. K. & SINGH, S. J. I. A. R. .I., NEW DELHI 2012. Climate change impact, adaptation and mitigation in agriculture: methodology for assessment and applications. 1-302.
- RAMADHAN, A. A., ALI, M. H. & AL-KUBAISY, R. K. J. I. J. O. S. 2013. Evaluation of groundwater recharge in arid and semiarid regions (case study of Dibdiba formation in Karballa-Najaf plateau). 54, 902-910.

- SAMPER, J., LI, Y. & PISANI, B. J. E. E. S. 2015. An evaluation of climate change impacts on groundwater flow in the Plana de La Galera and Tortosa alluvial aquifers (Spain). 73, 2595-2608.
- SANSOM, J., RENWICK, J. A. J. J. O. A. M. & CLIMATOLOGY 2007. Climate change scenarios for New Zealand rainfall. 46, 573-590.
- ŞEN, Z. 2015. *Applied drought modeling, prediction, and mitigation*, Elsevier.
- SHAHID, S., ALAMGIR, M., WANG, X.-J. & ESLAMIAN, S. 2017. Climate change impacts on and adaptation to groundwater. *Handbook of Drought and Water Scarcity*. CRC Press.
- SHAHID, S., WANG, X.-J., RAHMAN, M. M., HASAN, R., HARUN, S. B. & SHAMSUDIN, S. J. J. O. T. G. S. O. I. 2015. Spatial assessment of groundwater over-exploitation in northwestern districts of Bangladesh. 85, 463-470.
- SOLOMON, S., MANNING, M., MARQUIS, M. & QIN, D. 2007. *Climate change 2007-the physical science basis: Working group I contribution to the fourth assessment report of the IPCC*, Cambridge university press.
- SURINAIDU, L., BACON, C., PAVELIC, P. J. H. & SCIENCES, E. S. 2013. Agricultural groundwater management in the Upper Bhima Basin, India: current status and future scenarios. 17, 507-517.
- SZÉKELY, F., SENAY, Y., AL-RASHED, M., AL-SUMAIT, A. & AL-AWADI, E. J. J. O. H. 2000. Computer simulation of the hydraulic impact of water well fields in Kuwait. 235, 205-220.
- WAYNE, G. J. S. S. 2013. The beginner's guide to representative concentration pathways. 25.
- White, F., 2009, "Fluid mechanics", Sixth Edition. New York: McGrawHill
- WILBY, R. L., DAWSON, C., BARROW, E. J. C. I. & PROGRAMME, A. R. 2007. SDSM 4.2—A decision support tool for the assessment of regional climate change impacts (User Manual.)
- WILBY, R. L., DAWSON, C. W., BARROW, E. M. J. E. M. & SOFTWARE 2002. SDSM—a decision support tool for the assessment of regional climate change impacts. 17, 145-157.
- WILBY, R. L. & DAWSON, C. W. J. I. J. O. C. 2013. The statistical downscaling model: insights from one decade of application. 33, 1707-1719.

## الخلاصة

تعتبر المياه الجوفية في العراق موردا مائيا بديلا ، خاصة بالنسبة للمناطق البعيدة عن المياه السطحية. المياه الجوفية تتأثر بالعديد من العوامل منها التغير المناخي، أنشطة الأبناس الصناعية والتحضر غير المخطط له والتصنيع. تتناول هذه الدراسة تطوير نموذج لتوليد بيانات مناخية مستقبلية من أجل تقدير التغذية المستقبلية للمياه الجوفية. تم اختيار حوض الدببة وهي طبقة للمياه الجوفية غير المحصورة في مدينة كربلاء ، العراق كدراسة حالة. حيث تعتمد على تغذية الأمطار التي ترتبط بالتغيرات في درجات الحرارة و الأمطار. تم استخدام البيانات التاريخية للفترة 1979-2018 للتنبؤ بالبيانات المناخية للفترة المستقبلية 2040 و 2099 باستخدام نموذج المناخ العالمي (GCMs) CanESM2 ، بناءً على سيناريوهات الانبعاثات الثلاثة RCP2.6 و RCP4.5 و RCP8.5 بواسطة استخدام برنامج نموذج المصغر الإحصائي SDSM. تلك البيانات تم تقسيمها إلى مجموعتين: تم استخدام البيانات من 1979 إلى 2000 لعملية المعايرة وبناء النموذج المصغر ، بينما أستخدمت البيانات للفترة من 2001 إلى 2018 للتحقق من صحة النماذج. حيث أعطت نتائج معايرة برنامج SDSM قيمة لمعامل التحديد  $R^2$  تراوحت من 0.877 إلى 0.905. بعد التحقق من قدرة نموذج المصغر الإحصائي (SDSM) على توليد بيانات المناخ على أساس الفترة من 1979 إلى 2018. يتم توليد بيانات المناخ (الحرارة والأمطار) للسنوات القادمة (2040 و 2099). بعد ذلك ، تم إنشاء نموذج لنمذجة المياه الجوفية (GMS) من أجل تقييم تغذية المياه الجوفية تحت بيانات المناخ في المستقبل. تشير النتائج إلى أن درجة الحرارة متوقع ان تزداد بين 0.5 إلى 0.7 درجة مئوية للفترة المستقبلية قريبة المدى 2040 و تزداد بين 0.5 إلى 1.07 درجة مئوية للفترة المستقبلية بعيدة المدى 2099. ومتوقع ان يقل هطول الأمطار بنسبة 6.3 % و 10.3 % و 23.8 % على المدى القريب (2040)، وينقص بنسبة 13.8 % و 17.5 % و 21.3 % على المدى البعيد (2099) لسيناريوهات RCP2.6 و RCP4.5 و RCP8.5 ، على التوالي. تم اختيار ستة سيناريوهات متوقعة لتغذية المياه الجوفية كانت مختارة لكل سيناريو من البيانات المناخية للفترتين (2040 و 2099) بعد معايرة النموذج كانت قيمة ال  $R^2$  تساوي 0.99 للحالة المستقرة. حيث أظهرت النتائج بأن تغذية المياه الجوفية تقل بنسبة 6.4 % و 10 % و 27.6 % للفترة المستقبلية قريبة المدى (2040) و تقل بنسبة 13.6 % ، 17.6 % و 25.3 % للفترة المستقبلية بعيدة المدى (2099) مقارنة بسنة (2018) تحت سيناريوهات RCP2.6 و RCP4.5 و RCP8.5 على التوالي.



جمهورية العراق  
وزارة التعليم العالي والبحث العلمي  
جامعة كربلاء  
كلية الهندسة  
قسم الهندسة المدنية

## تأثير التغير المناخي على تغذية المياه الجوفية في حوض الدببة, العراق

الرسالة مقدمة إلى  
قسم الهندسة المدنية / كلية الهندسة في جامعة كربلاء كجزء من متطلبات نيل  
درجة الماجستير في علوم الهندسة المدنية

من قبل  
**فرقان سعد هاشم**  
(بكلوريوس في علوم الهندسة المدنية 2017 )

بإشراف  
الاستاذ الدكتور  
**واقد حميد حسن**

أيلول (2020)

محرم (1442)